Studies on the Mechanism of Direct Arylation of Pyridine *N*-oxides: Evidence for the Essential Involvement of Acetate from the $Pd(OAc)_2$ Pre-Catalyst at the C-H Bond Cleaving Step

By

Ho-Yan Sun

B. Sc., University of Ottawa, 2008

A thesis submitted to the Faculty of Graduate and Postdoctoral Studies
In partial fulfillment of the requirements for the
Master of Science (M. Sc.) degree in chemistry

Candidate	Supervisor	Co-Supervisor
Ho-Yan Sun	Keith Fagnou	Louis Barriault

Ottawa-Carleton Chemistry Institute
Faculty of Science
University of Ottawa

Acknowledgements

First and foremost, I must thank Prof. Keith Fagnou, to whom this thesis is dedicated, for his many years of guidance and support. I am so grateful for having had the opportunity to work under the supervision of such an incredible researcher and mentor. I can't thank you enough for taking such good care of me and the rest of the group. I miss you dearly and will always cherish the memories of all the fun times the group spent with you.

To all my lab mates, past and present, thank you for being such a fantastic bunch to work with. Although I would never admit it outside of these acknowledgements, I enjoyed and will sorely miss the Fagnou Group's crude and oftentimes inappropriate (boys, I'm talking to you!) humour. Dave and Ben, thank you so much for taking care of the group during difficult times. Sophie, you're one of the best listeners I know - thanks for always lending an ear. Nicdas – please never change! I love your hilarious one-liners that seem to come ever so naturally to you. Your enthusiasm is refreshing and an inspiration. Derek, it has been a pleasure sharing a fumehood bay with you. I'll strangely miss having your stuff slowly but surely migrate over onto my bench. Malcolm and Olivier, I'm glad the bucca boys have been reunited in California. I look forward to hearing of your future escapades. To Tom, Christina, Lina and Marieke, best of luck in the years to come. I know you guys will be great! LC, thanks for being the one to show me how awesome chemistry is and for always being there to help me out. Finally David, for all your support and your incredible friendship, "thank you" simply isn't enough. I also need to thank Dr. Serge Gorelsky for running all the computational experiments discussed in this thesis and of course Prof. Louis Barriault for having been so patient, supportive and generous with his time.

Last, but certainly not least, I cannot have done this without the endless support of my family. Goxish, you're the best sister in the entire world. I love you to bits. Mom and Dad, thank you for understanding me and for your love and encouragement. The next one is for you!

Abstract

Detailed mechanistic studies on the palladium-catalyzed direct arylation of pyridine *N*-oxides are presented. The order of each reaction component is determined to provide a general mechanistic picture. The C-H bond cleaving step is examined in further detail through computational studies, and the calculated results are in support of an inner-sphere concerted metallation-deprotonation (CMD) pathway. Competition experiments were conducted using *N*-oxides of varying electronic characters, and results revealed an enhancement of rate when using a more electron-deficient species which is in support of a CMD transition state. The effect of base on reaction rate was also examined and it was found that a carboxylate base was required for the reaction to proceed. This led to the conclusion that $Pd(OAc)_2$ plays a pivotal role in the reaction mechanism as more than merely a pre-catalyst, but as a source of acetate base required for the C-H bond cleavage step.

Table of Contents

Acknowledgements ii
Abstract iii
List of Abbreviations v
List of Figures vii
List of Schemes viii
List of Tables ix
Chapter 1 – Biaryl Synthesis Via Methods in Direct Arylation 1
1.1 Direct Arylation of Electron-Rich Arenes 2
1.2 Direct Arylation of Electron-Poor Arenes 8
1.3 Direct Arylation of Simple Arenes 11
1.4 Proposed Mechanisms of Direct Arylation 15
1.5 Project Overview 21
Chapter 2 – Mechanistic Evaluation of the Pd-Catalyzed Direct Arylation of Pyridine N-Oxides 22
2.1 Kinetics 22
2.2 Computational Analysis 27
2.3 Base Effects 39
2.4 Summary of Mechanistic Data & Revised Catalytic Cycle 44
2.5 Towards the Development of Improved Reaction Conditions 46
Chapter 3 – Conclusions 49
Chapter 4 – Supporting Information 50
General Methods 50
Kinetics Experiments 53
Kinetic Isotope Effect Experiments 62
Measurement of Rate at Varying Temperatures (Construction of Arrhenius Plot) 63
Regioselectivity with 3-Substituted Pyridine N-oxides 69
One-Pot Competitions Between 4-Substituted Pyridine N-oxides 70
Hammett Study 70
Stoichiometric Reactions Using 1 77
Base Effects - Rate Measurements 79
Stoichiometric Reactions using 2 83
Kinetic Experiment Using $Pd(OPiv)_2$ 85
Section Claims 86

List of Abbreviations

Ac	acetyl
Ad	adamantyl
Ar	aryl
Bu	butyl
Cy	cyclohexyl
CMD	concerted metallation-deprotonation
DCM	dichloromethane
DDQ	2,3-dichloro-5,6-dicyano-1,4-benzoquinone
DFT	density functional theory
DG	directing group
DMA	*N,N*-dimethylaminopyridine
Et	ethyl
Equiv	equivalents
HPLC	high performance liquid chromatography
HRMS	high resolution mass spectrometry
h	hours
Hz	hertz
IR	infrared
kcal	kilocalories
KIE	kinetic isotope effect
L	ligand
m	*meta*
M	molar
“M”	a metal species
Me	methyl

Mes	mesityl
mol	mole
NMP	*N*-methylpyrrolidone
NMR	nuclear magnetic resonance
Piv	pivalyl
Ph	phenyl
RT	room temperature
S_EAr	electrophilic aromatic substitution
^tBu	tertiary butyl
TMEDA	tetramethylethylenediamine

List of Figures

Figure 1. Scope of the direct arylation of indoles using diaryl iodonium salts..... 6
Figure 2. Scope of azine and azole *N*-oxide direct arylation. 11
Figure 3. Log plot of the initial rate dependence on the concentration of a) 5-bromo-*m*-xylene, b) 4-nitropyridine *N*-oxide, c) $Pd(^tBu_3)_2$, d) P^tBu_3. 26
Figure 4. Inner- and outer-sphere mechanisms for the concerted metallation-deprotonation process..... 30
Figure 5. Arrhenius plot constructed for the coupling of 4-nitropyridine *N*-oxide. 34
Figure 6. Free energy of activation ($\Delta G^{\ddagger}_{298K}$, kcal•mol-1 in toluene) for the three possible sites of arylation via the inner- and outer-sphere mechanisms. 35
Figure 7. Computational and experimental results for competition experiments between pyridine *N*-oxides of different electronics. 38
Figure 8. Hammett plot for the direct arylation of C4-substituted pyridine *N*-oxides..... 38
Figure 9. Dependence of rate on the identity of the base used. 41
Figure 10. Comparison of reaction rates using $Pd(OPiv)_2$ and $Pd(P^tBu_3)_2$ as catalysts. 41
Figure 11. Initial rate of a reaction run with a catalytic amount of 2..... 43

List of Schemes

Scheme 1. The evolution of cross-coupling methods with representative examples. 2
Scheme 2. Sames' C2-arylation of indoles by Rh catalysis. 4
Scheme 3. Control of regioselectivity in indole arylation by choice of counterion. 5
Scheme 4. General Strategy for the use of an *N*-oxide in pyridine arylation and functionalization. 10
Scheme 5. Anion-accelerated intramolecular direct arylation. 12
Scheme 6. Palladium-catalyzed direct arylation using iodonium salts. 13
Scheme 7. Directing group mediated direct *ortho*-arylation of anilides. 14
Scheme 8. The four possible mechanisms of palladium-catalyzed direct arylation. 17
Scheme 9. KIE experiment for indolizine arylation. 18
Scheme 10. General mechanism for the palladium-catalyzed direct arylation of simple arenes. 23
Scheme 11. Free energy diagram (Δ*G*‡298K, kcal•mol-1 in toluene) for the relevant intermediates, transition states, and products in the oxidative insertion pathway. 28
Scheme 12. Free energy diagram (Δ*G*‡298K, kcal•mol-1 in toluene) for the relevant intermediates, transition states, and products in the Heck-type pathway. 29
Scheme 13. Free energy diagram (Δ*G*‡298K, kcal•mol-1 in toluene) for the relevant intermediates, transitions states, and products in the inner- and outer-sphere CMD pathways using bicarbonate as the base. 31
Scheme 14. Free energy diagram (Δ*G*‡298K, kcal•mol-1 in toluene) for the relevant intermediates, transitions states, and products in the inner- and outer-sphere CMD pathways using acetate as the base. 32
Scheme 15. Relevant intermediates, transition states, and products in the SEAr pathway. 33
Scheme 16. Stoichiometric reactivity of complex 2. 42
Scheme 17. Revised catalytic cycle for the direct arylation of pyridine *N*-oxides *via* a CMD transition state. 45

List of Tables

Table 1. Scope of electron-rich heterocycle arylation using aryl chlorides. 7
Table 2. Experimental and computational results for the regioselectivity in the direct arylation of C3-substituted pyridine *N*-oxides. 36
Table 3. Yields of a stoichiometric reaction between 1 and 4-nitropyridine *N*-oxide using different bases..... 39
Table 4. Optimization of reaction conditions for 4-picoline *N*-oxide arylation. 47

Chapter 1 – Biaryl Synthesis Via Methods in Direct Arylation

The formation of carbon-carbon bonds *via* direct arylation has undergone significant advances in recent years with efforts focused toward expanding substrate scope and novel catalyst development.[1] In light of these studies, direct arylation of aryl halides has become an attractive alternative to the use of stoichiometric organometallic reagents in the preparation of biaryl compounds. Many groups have been successful in developing a range of methods allowing for the coupling of electron-rich,[2] -neutral[3] and –poor[4] arenes (Scheme 1).

---

[1] For comprehensive reviews on direct arylations, see: (a) Ackermann, L.; Vicente, R.; Kapdi, A. R. *Angew. Chem. Int. Ed.* **2009**, *48*, 9792. (b) Campeau, L.-C.; Stuart, D. R.; Fagnou, K. *Aldrichimica Acta* **2007**, *40*, 35. (c) Alberico, D.; Scott, M. E.; Lautens, M. *Chem. Rev.* **2007**, *107*, 174. (d) *Modern Arylation Methods*, (Ed. :Ackermann, L.) Wiley-VCH, **2009**.

[2] (a) Park, C.-H.; Ryabova, V.; Seregin, I. V.; Sromek, A. W.; Gevorgyan, V. *Org. Lett*. **2004**, *6*, 1159. (b) Lane, B. S.; Brown, M. A.; Sames, D. *J. Am. Chem. Soc.* **2005**, *127*, 8050. (c) Chuprakov, S.; Chernyak, N.; Dudnik, A. S.; Gevorgyan, V. *Org. Lett.* **2007**, *9*, 2333.

[3] Lafrance, M.; Rowley, C. N.; Woo, T. K.; Fagnou, K. *J. Am. Chem. Soc.* **2006**, *128*, 8754.

[4] (a) Campeau, L.-C.; Rousseaux, S.; Fagnou, K. *J. Am. Chem. Soc.* **2005**, *127*, 18021. (b) Campeau, L.-C.; Stuart, D. R.; Leclerc, J.-P.; Bertrand-Laperle, M.; Villemure, E.; Sun, H.-Y.; Lasserre, S.; Guimond, N.; Lecavallier, M.; Fagnou, K. *J. Am. Chem. Soc.* **2009**, *131*, 3291.

Scheme 1. The evolution of cross-coupling methods with representative examples.

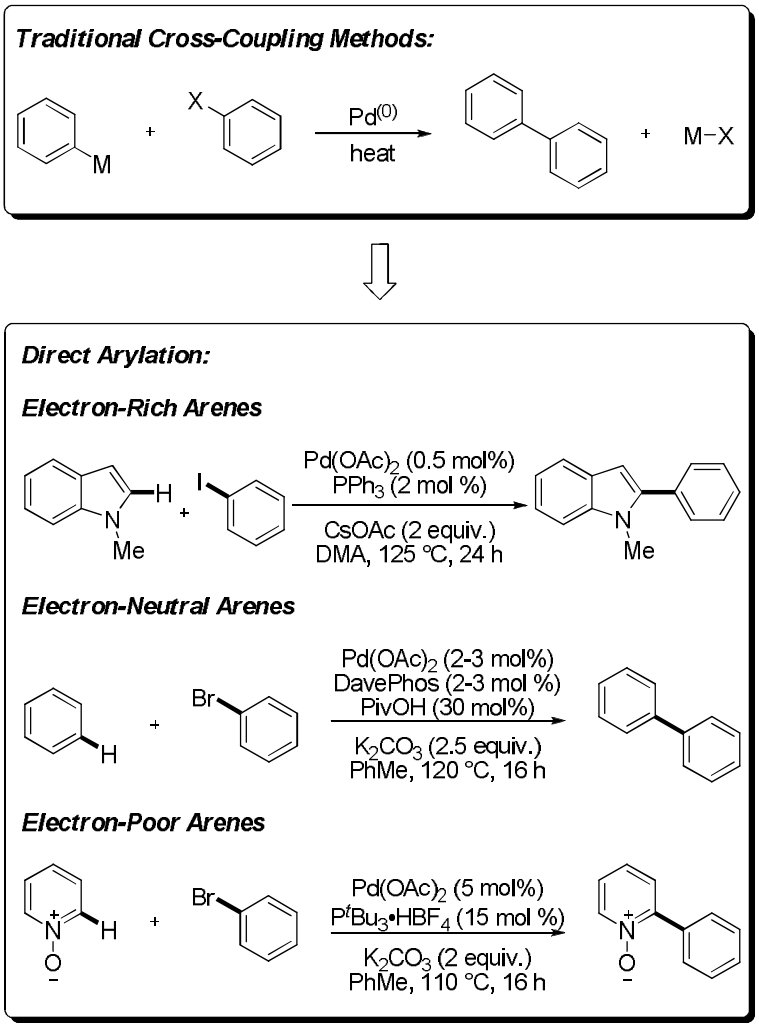

1.1 Direct Arylation of Electron-Rich Arenes

Among the first examples of direct arylation of heterocycles was Ohta's arylation of *N*-alkyl indoles (1), reported in 1989.[5] Arylation at both the C2 and C3 positions was possible, depending on the identity of the substituent on the indole nitrogen. The

[5] Akita, Y.; Itagaki, Y.; Takizawa, S.; Ohta, A. *Chem. Pharm. Bull.* **1989**, *37*, 1477.

reaction required high catalyst loading (15 mol%) as well as extremely high temperatures.

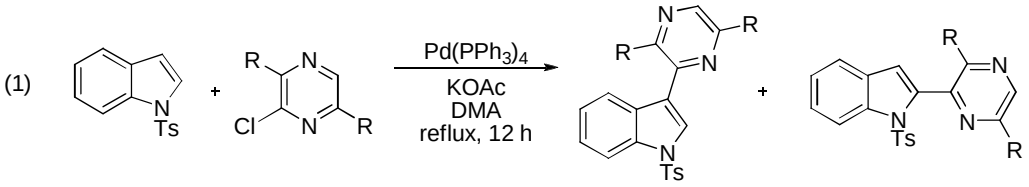

Since then, efforts have been aimed towards achieving reactivity under milder conditions as well as to broaden substrate scope. In 2005, Sames reported a Rh-catalyzed C2-arylation of indoles (Scheme 2).[6] This reaction features a selective targeting of C-H bonds while in the presence of the more reactive N-H functionality to give the C2-arylated product. The process is proposed to proceed through a $Rh^{(III)}$ complex **1** formed *in situ* by insertion of an aryl iodide into the Rh catalyst. The authors validate **1** as a reaction intermediate by demonstrating that **1** is a catalytically competent species. This arylrhodium (III) intermediate could then bind and metallate the indole to afford the diarylrhodium (III) species **3** which would then reductively eliminate to give the product and regenerate the rhodium (I) catalyst.

[6] Wang, X.; Lane, B. S.; Sames, D. *J. Am. Chem. Soc.* **2005**, *127*, 4996.

Scheme 2. Sames' C2-arylation of indoles by Rh catalysis.

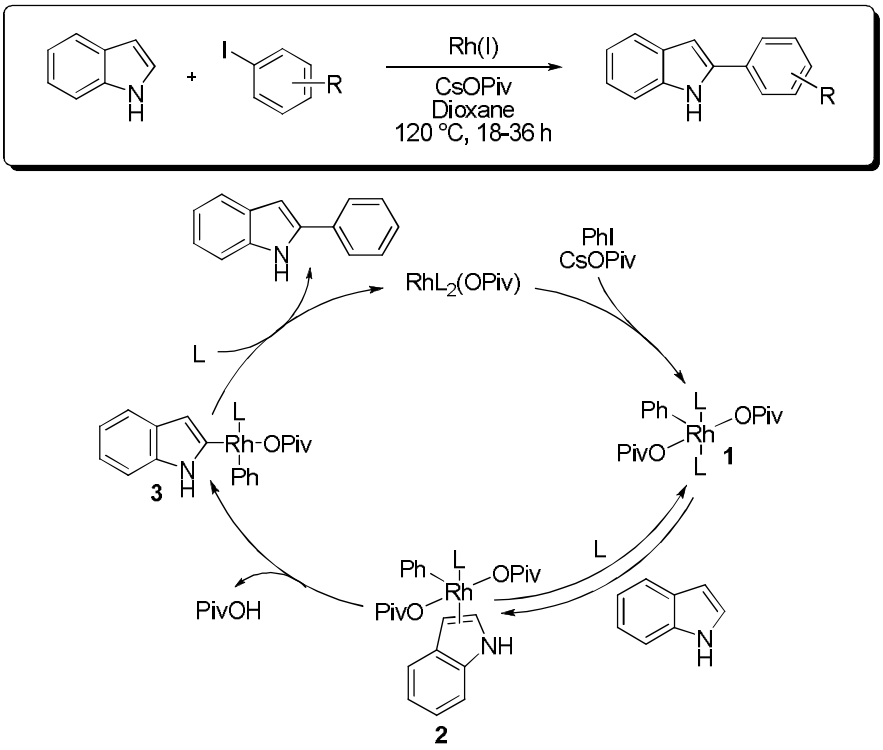

While CsOPiv was found to play a crucial role in obtaining useful yields, the initial rate was not affected by this reagent. Although no further study was performed on the C-H metallation step of the catalytic cycle, the authors suggested that the pivalate was assisting in the C-H bond cleaving step as an internal base.

The Sames group has also developed palladium-catalyzed indole arylation reactions that were compatible with a wide range of *N*-substituted indoles.[7] These reactions were typically selective for the C2 position of the indole, but it was found that a careful choice in the counterion of the base would allow for selective arylation at either the C2 or the C3 positions (Scheme 3). This selectivity was proposed to arise from a migration of the palladium during the metallation event.

---

[7] Touré, B. B.; Lane, B. S.; Sames, D. *Org. Lett.* **2006**, *8*, 1979.

Scheme 3. Control of regioselectivity in indole arylation by choice of counterion.

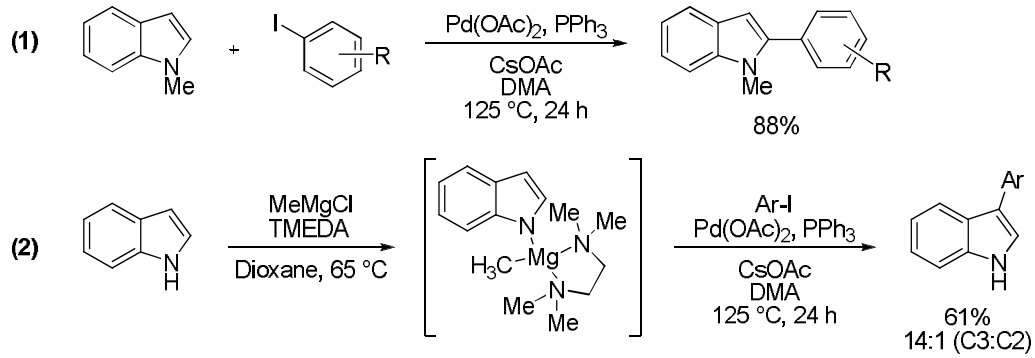

An alternative method of arylating selectively at the C2 position of indole was developed by Sanford and co-workers in which a $Pd^{(II)}/Pd^{(IV)}$ catalytic manifold was used in place of the $Pd^{(0)}/Pd^{(II)}$ system.[8] It was reasoned that the limitations of previous indole arylation systems, including the need for high temperatures, were a direct consequence of the $Pd^{(0)}/Pd^{(II)}$ mechanism. This mechanism was thought to proceed via a rate-limiting electrophilic indole palladation by an electron-rich palladium-aryl species. It was thus believed that the rate of this palladation step could be improved by using a more electron-deficient $Pd^{(II)}$ catalyst. Under this concept, Sanford *et al.* were able to selectively arylate at the C2 position of indoles under extremely mild conditions using aryl iodonium salts and $Pd(OAc)_2$ as the catalyst (Figure 1). This system was able to extend to cover a broad range of substrates, including free (NH)-indoles and pyrroles.

[8] Deprez, N. R.; Kalyani, D.; Krause, A.; Sanford, M. S. *J. Am. Chem. Soc.* **2006**, *128*, 4972.

Figure 1. Scope of the direct arylation of indoles using diaryl iodonium salts.

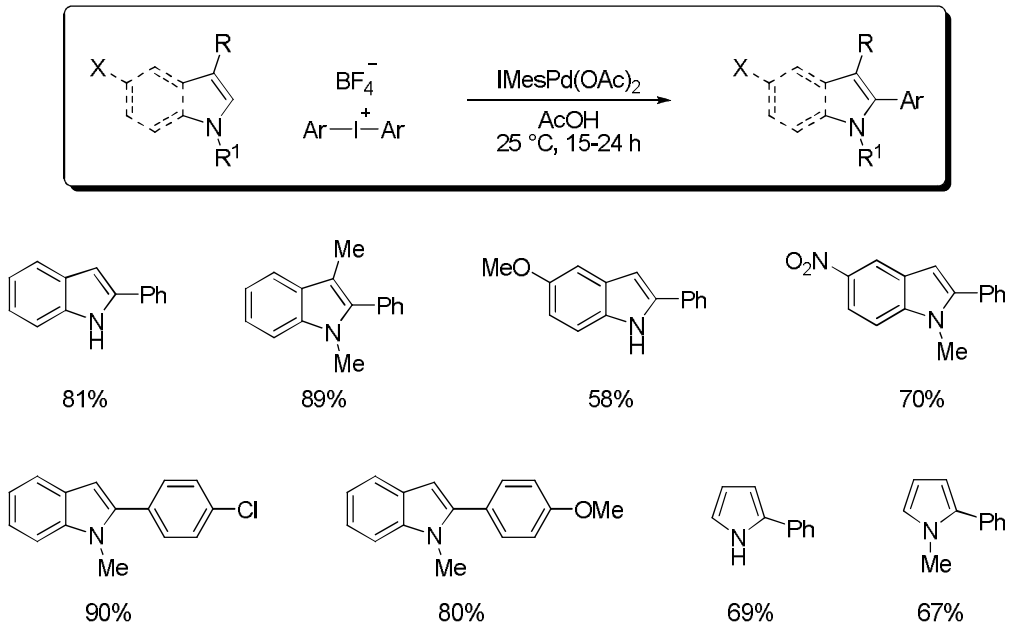

In 2007, a general method for electron-rich heterocycle arylation was reported by Daugulis.[9] Using electron-rich and sterically encumbered alkylphosphines in combination with $Pd(OAc)_2$, a remarkably broad scope of electron-rich arenes could be arylated, including thiophenes, oxazoles, and caffeine (Table 1). An advantage to this method was its use of aryl chlorides as the coupling partner, instead of the more expensive aryl bromides and iodides which were the more frequently used reagents in previously reported methods. Electron-rich, electron-poor, and heteroaryl chlorides can all be used, although as expected, the electron-poor aryl chlorides were the most reactive.

[9] Chiong, H. A.; Daugulis, O. *Org. Lett.* **2007**, *9*, 1449.

Table 1. Scope of electron-rich heterocycle arylation using aryl chlorides.

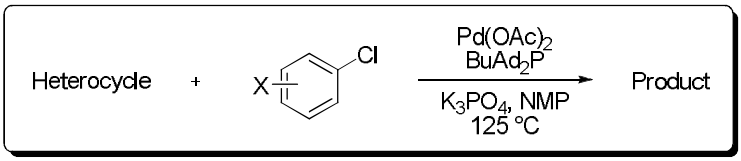

Entry	Heterocycle	X	Product	Yield
1	Thiophene	3-NHAc	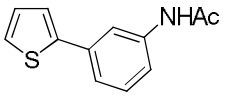	54%
2	Benzothiophene	H	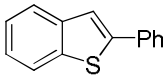	63%
3	Benzofuran	H	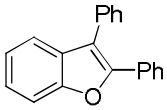	68%
4	Benzoxazole	3-CO_2Et	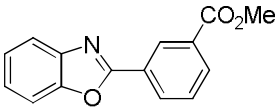	84%
5	Benzothiazole	4-CF_3	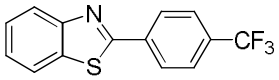	82%
6	Butylimidazole	H	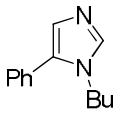	52%
7	Caffeine	2-OMe	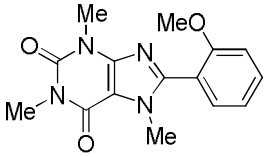	71%

At the time, Fagnou and co-workers had been involved in the development of palladium-catalyzed direct arylation reaction with electron-deficient arenes (*vide infra*). In these processes, both experimental and computational data has pointed towards the

involvement of a concerted metallation-deprotonation (CMD) pathway.[3,10] A strong agreement between computational predictions and experimentally observed outcomes led to the speculation that this mode of reaction might also occur with electron-rich aromatics which are more commonly proposed to proceed through the electrophilic aromatic substitution (S_EAr) pathway. This prompted the use of "CMD conditions" for the coupling of π-excessive aromatics, which led to the establishment of reaction conditions which are applicable to a wide range of coupling partners (2).[11] Of note is the use of a sub-stoichiometric amount of pivalic acid, an additive which has demonstrated its utility in accelerating direct arylation in other systems.[12,13]

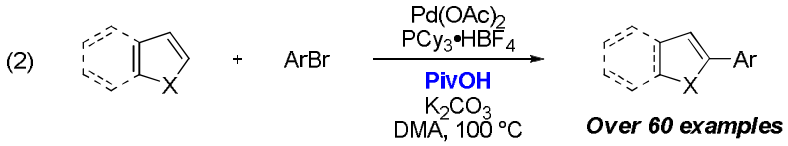

1.2 Direct Arylation of Electron-Poor Arenes

Compared to their electron-rich counterparts, reports on the direct arylation of electron-deficient arenes has been relatively scarce. In 2000, Sasson and co-workers used a Pd/C, zinc and water catalyst system in conjunction with chlorobenzene and pyridine to prepare 2-phenylpyridine (3).[14] This remains, to our knowledge, the only

---

[10] (a) Davies, D. L.; Donald, S. M. A.; Macgregor, S. A. *J. Am. Chem. Soc.* **2005**, *127*, 16754. (b) Garcia-Cuadrado, D.; Braga, A. A. C.; Maseras, F.; Echavarren, A. M. *J. Am. Chem. Soc.* **2006**, *128*, 1066. (c) Garcia-Cuadrado, D.; de Mendoza, P.; Braga, A. A. C.; Maseras, F.; Echavarren, A. M. *J. Am. Chem. Soc.* **2007**, *129*, 6880. (d) Pascual, S.; de Mendoza, P.; Braga, A. A. C.; Maseras, F.; Echavarren, A. M. *Tetrahedron*, **2008**, *64*, 6021. (e) Ackermann, L.; Vincent, R.; Althammer, A. *Org. Lett.* **2008**, *10*, 2299.
[11] Liégault, B.; Lapointe, D.; Caron, L.; Vlassova, A.; Fagnou, K. *J. Org. Chem.* **2009**, *74*, 1826.
[12] Caron, L.; Campeau, L.-C.; Fagnou, K. *Org. Lett.* **2008**, *10*, 4533-4536.
[13] Lafrance, M.; Fagnou, K. *J. Am. Chem. Soc.* **2006**, *128*, 16496.
[14] Mukhopadhyay, S.; Rothenberg, G.; Gitis, D.; Baidossi, M.; Ponde, D. E.; Sasson, Y. *J. Chem. Soc. Perkin Trans. 2* **2000**, 1809.

example of a Pd-catalyzed direct arylation of an azine, without pre-activation, with an aryl halide.[15]

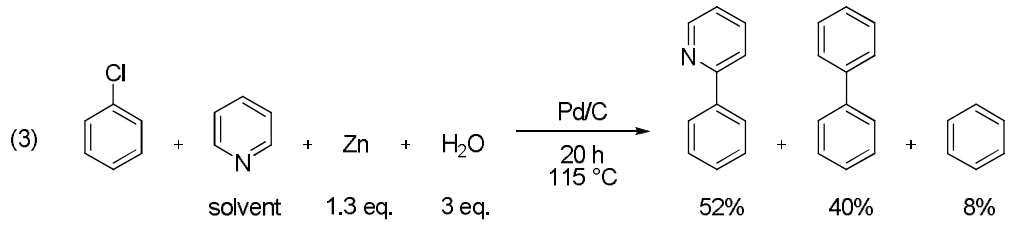

Since then, the Fagnou group has focussed on the applicability of azine *N*-oxides as useful scaffolds for direct arylation. Although still requiring an activation step, the overall process of arylating an azine is achieved in fewer steps as both the installation of a halide or an organometallic on the azine typically proceeds through an *N*-oxide species (Scheme 4). As such, improved efficiency would be achieved if the *N*-oxide itself could be used in the cross-coupling process. Furthermore, the *N*-oxide moiety may also be imagined to prevent unproductive binding of the Pd onto the nitrogen lone pairs to instead favour π-binding interactions which can lead to the desired metallation of the azine ring.

[15] For an example of regioselective azine direct arylation without substrate pre-activation catalyzed by Rh(I) see: Berman, A. M.; Lewis, J. C.; Bergman, R. G.; Ellman, J. A. *J. Am. Chem. Soc.* **2008**, *130*, 14926.

Scheme 4. General Strategy for the use of an *N*-oxide in pyridine arylation and functionalization.

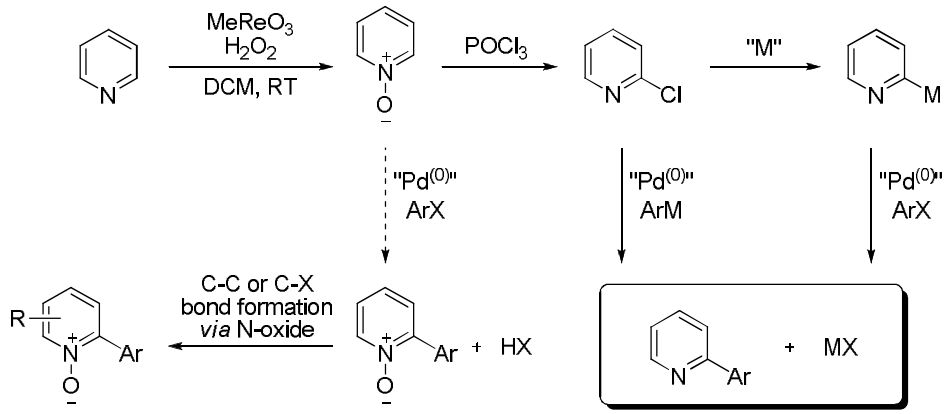

Since their first report on the direct arylation of pyridine *N*-oxides in 2005, the Fagnou group has developed a range of methods for the direct arylation of various azine and azole *N*-oxides (Figure 2).[4,16] The conditions for these processes all involve the use of $Pd(OAc)_2$ as the source of Pd catalyst as well as electron-rich alkylphosphine ligands and stoichiometric amounts of carbonate base. In some cases, sub-stoichiometric amounts of PivOH is also added.

[16] Leclerc, J.-P.; Fagnou, K. *Angew. Chem. Int. Ed.* **2006**, *45*, 7781.

Figure 2. Scope of azine and azole *N*-oxide direct arylation.

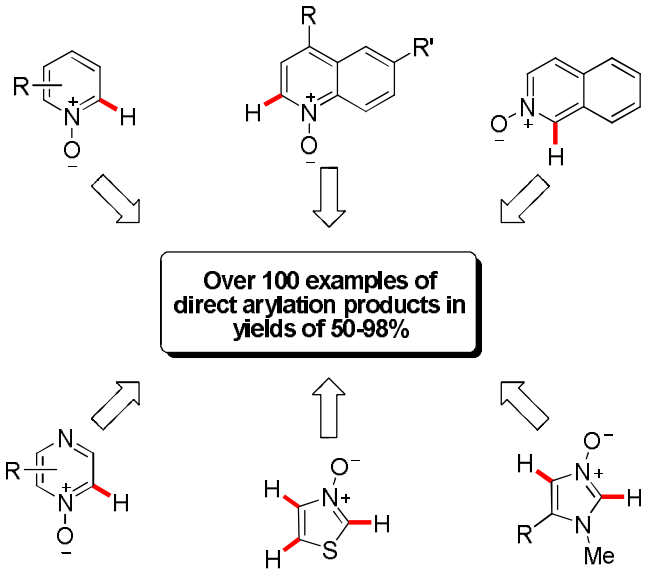

1.3 Direct Arylation of Simple Arenes

Simple arenes are much less reactive than heteroarenes in direct arylation – a characteristic which is often attributed to their diminished nucleophilicity, however many examples of both intra- and intermolecular direct arylation reactions have appeared in the literature. An early example of intramolecular direct arylation was reported by Ames and co-workers as a side reaction which was observed while attempting a Heck reaction using bromocinnolines, where the direct arylation of a phenyl group to give a five membered ring was observed (4).[17]

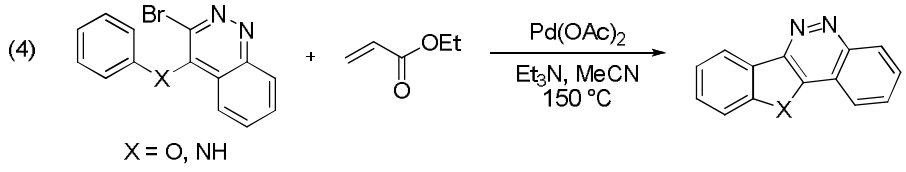

[17] Ames, D. E.; Bull, B. *Tetrahedron* **1982**, *38*, 383.

The scope of this reaction allowed for the formation of a variety of five-membered benzofurans, however the formation of benzopyrans could only be formed in approximately 40% yield.[18]

Rawal and co-workers overcame the reduced nucleophilicity of simple arenes by using a phenol functionality, which when depronated would generate an enolate, thus generating a much more reactive coupling partner.[19] Employing this strategy, they were able to successfully perform an intramolecular coupling of phenols with aryl halides (Scheme 5). The reaction was performed in DMA using $Pd(PPh_3)_4$ and ^tBuOK as the base to deprotonate the phenol. The process was believed to proceed via an oxidative addition of palladium to the aryl halide followed by a nucleophilic attack of the phenolate on the electrophilic palladium. Following reductive elimination, the cyclized product would be formed.

Scheme 5. Anion-accelerated intramolecular direct arylation.

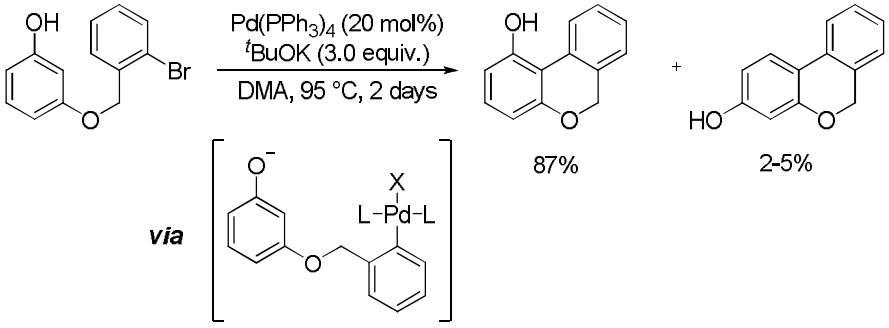

The possibility of a benzyne intermediate was excluded based on the observation that using a weaker base, K_2CO_3 which is unlikely to produce benzyne under the reaction conditions, the same results were obtained as when ^tBuOK was used. Furthermore, when ^tBuOK was used with no palladium catalyst, formation of product was not observed.

---

[18] Ames, D. E.; Opalko, A.; *Tetrahedron* **1984**, *40*, 1919.
[19] Hennings, D. D.; Iwasa, S.; Rawal, V. H.; *J. Org. Chem.* **1997**, *62*, 2.

In 2005, Sanford *et al.* reported a palladium-catalyzed intermolecular direct arylation of simple arenes using substrates which had nitrogen containing directing groups and iodine(III) reagent $[Ph_2I]BF_4$ (Scheme 6).[20] The reaction proceeds in good yield with a variety of arenes as well as with benzylic substrates. A diverse selection of heterocycles including pyridines, quinolines, pyrrolidinones and oxazolidinones are tolerated as effective directing groups.

Scheme 6. Palladium-catalyzed direct arylation using iodonium salts.

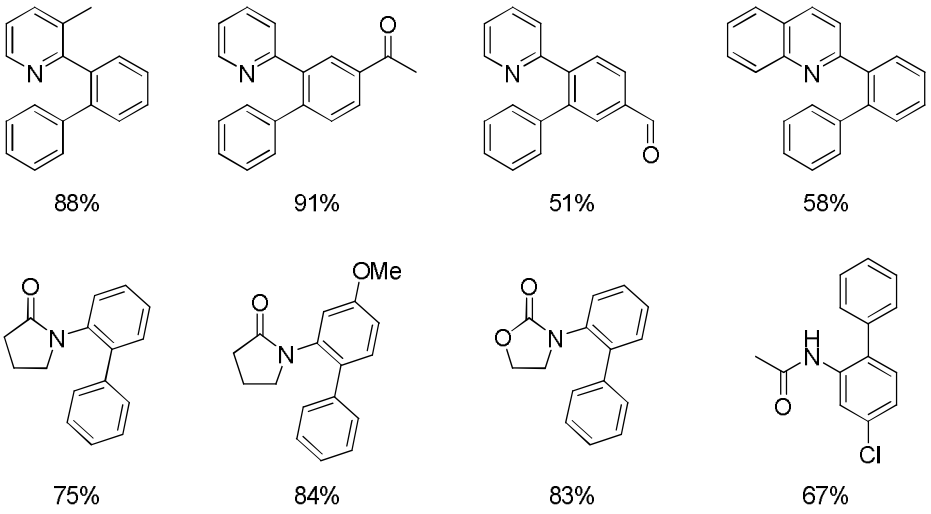

Substrates containing a *meta* substituted arene would react to form a single detectable isomer regardless of the electronic nature of the substituent, leading to the speculation that the process is predominantly sterically controlled.

[20] Kalyani, D.; Deprez, N.R; Desai, L.V.; Sanford, M. S. *J. Am. Chem. Soc.* **2005**, *127*, 7330.

This strategy of employing the use of directing groups for intermolecular direct arylations was also utilized by other groups including Daugulis and co-workers who developed a palladium-catalyzed arylation of anilides containing *ortho*-directing groups.[21] Using $Pd(OAc)_2$ as the source of Pd catalyst along with a combination of aryl iodides and AgOAc and trifluoroacetic acid as the solvent, they were successful in catalytically arylating anilides in good yield (Scheme 7). In most cases, diarylation occured at the positions *ortho* to the directing group with the exception of *meta* substituted substrates, in which case monoarylation occured at the most sterically accessible position. A number of anilides could be arylated using this method, although pivaloyl derivatives proved to be the best substrates. Acetamides were also found to be compatible, however due to the sterically more accessible nature of the acetyl group, *N*-arylation becomes a competing side reaction.

Scheme 7. Directing group mediated direct *ortho*-arylation of anilides.

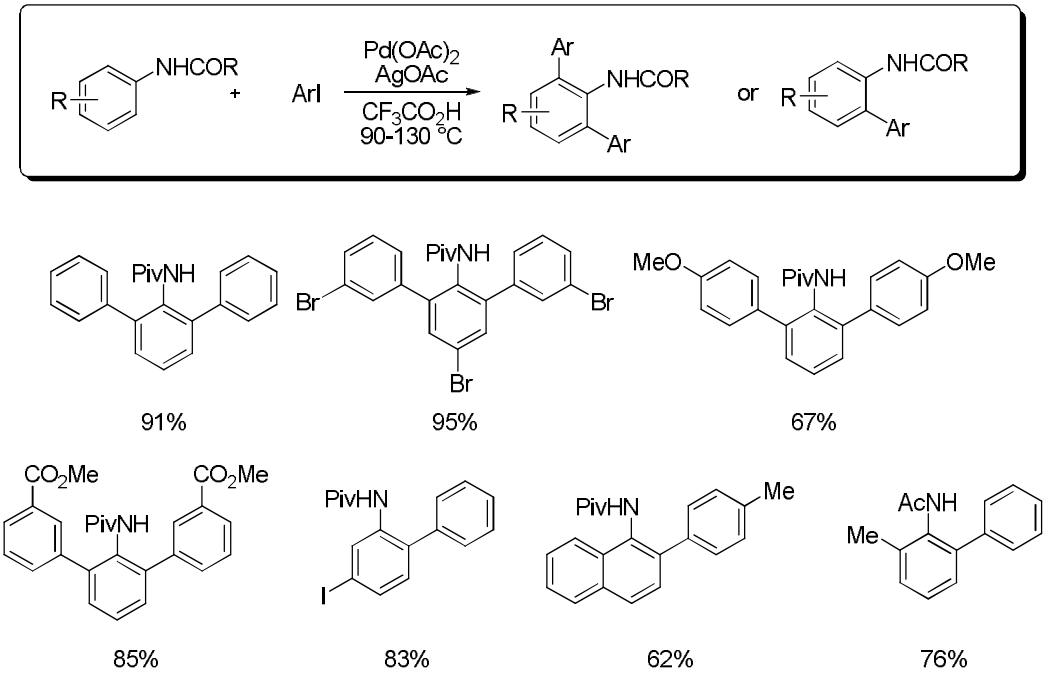

[21] Zaitsev, V. G.; Daugulis, O. *Angew. Chem. Int. Ed.* **2005**, *44*, 4046.

While pursuing mechanistic insight on the direct arylation process (*vide infra*), the Fagnou group chose to examine the direct arylation of pentafluorobenzene since this substrate would not be able to react *via* a S_EAr-type process. It was found that excellent results could be obtained by reacting a nearly equimolar ratio of 4-bromotoluene and pentafluorobenzene using $Pd(OAc)_2$ and the HBF_4 salt of di-*tert*-butylmethylphosphine in conjunction with K_2CO_3 in DMA at 120 °C (5).[3] Under these conditions, the reaction exhibits a broad scope in both the aryl halide and the polyfluoroarene components. Both electron donating and withdrawing groups are compatible on the aryl halide while tetrafluoro-, trifluoro- and some di-fluorobenzenes can be arylated.

(5)

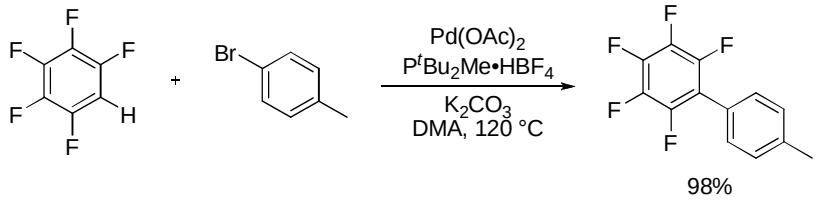

98%

The discovery that even fluorobenzene could be arylated (albeit in lower yield) prompted the initiative to expand the scope of arenes to more challenging simple arenes. Fagnou and Lafrance developed a palladium/pivalic acid co-catalyst system which exhibited unprecedented reactivity in direct arylation, including the arylation of a completely unactivated arene, benzene.[13]

1.4 Proposed Mechanisms of Direct Arylation

While many synthetically useful direct arylation methods exist, the development of novel catalysts which show increased reactivity at lower temperatures and catalyst loadings still remain a challenge. A better mechanistic understanding of direct arylation is crucial to the development of new catalysts as there are relatively few of these

studies published to date in the literature.[2,10bc,22,23,24] Such studies would be useful when developing new reactions, allowing for improvements to be made to existing reaction conditions and in the development of specially designed catalysts to reveal the necessary reactivity for an even broader range of direct C-H bond transformations in organic synthesis.

Of the studies directed towards elucidating the mechanism of palladium-catalyzed direct arylation processes, computational studies have been prominently featured while little experimental evidence in support of the various proposals have been brought forth. Electrophilic, nucleophilic, and electron-neutral palladium aryl species have all been suggested to interact with aromatic substrates of varying electronic characters. Moreover, few if any of these studies deal with the relationship between pre-catalyst and active catalyst. Studies of this kind have been crucial for the development of very active catalysts in other palladium-catalyzed processes.

The most discussed mechanisms of direct arylation are the carbopalladation or Heck-type pathway,[23] the oxidative insertion pathway,[25,26,27] electrophilic palladation or electrophilic aromatic substitution (S_EAr) pathway,[2,22] and the concerted metallation-deprotonation (CMD) pathway (Scheme 8).[3,10b,c,24]

---

[22] (a) Pivsa-Art, S.; Satoh, T.; Kawamura, Y.; Miura, M.; Nomura, B. *Bull. Chem. Soc. Jpn*. **1998**, *71*, 467. (b) Yanagisawa, S.; Sudo, T.; Noyori, R.; Itami, K. *J. Am. Chem. Soc*. **2006**, *128*, 11748.
[23] (a) McClure, M. S.; Glover, B.; McSorley, E.; Millar, A.; Osterhout, M. H; Roschanger, F. *Org. Lett.* **2001**, *3*, 1677. (b) Glover, B.; Harvey, K. A.; Liu, B.; Sharp, M. J.; Tymoschenko, M. F. *Org. Lett.* **2003**, *5*, 301. (c) Li, W.; Nelson, D. P.; Jensen, M. S.; Hoerrner, R. S.; Javadi, G. J.; Cai. D.; Larsen, R. D. *Org. Lett.* **2003**, *5*, 4835. (d) Wang, J.-X.; McCubbin, J. A.; Jin, M.; Laufer, R. S.; Mao, Y.; Crew, A. P.; Mulvihill, M. J.; Snieckus, V. *Org. Lett.* **2008**, *10*, 2923. and references therein.
[24] Gorelsky, S. I.; Lapointe, D.; Fagnou, K. *J. Am. Chem. Soc.* **2008**, *130*, 10848.
[25] Okazawa, T.; Satoh, T.; Miura, M.; Nomura, M. *J. Am. Chem. Soc.* **2002**, *124*, 5286.
[26] Campo, M. A.; Huang, Q.; Yao, T.; Tian, Q.; Larock, R. C. *J. Am. Chem. Soc.* **2003**, *125*, 11506.
[27] Capito, E.; Brown, J. M.; Ricci, A. *Chem. Commun.* **2005**, 1854.

Scheme 8. The four possible mechanisms of palladium-catalyzed direct arylation.

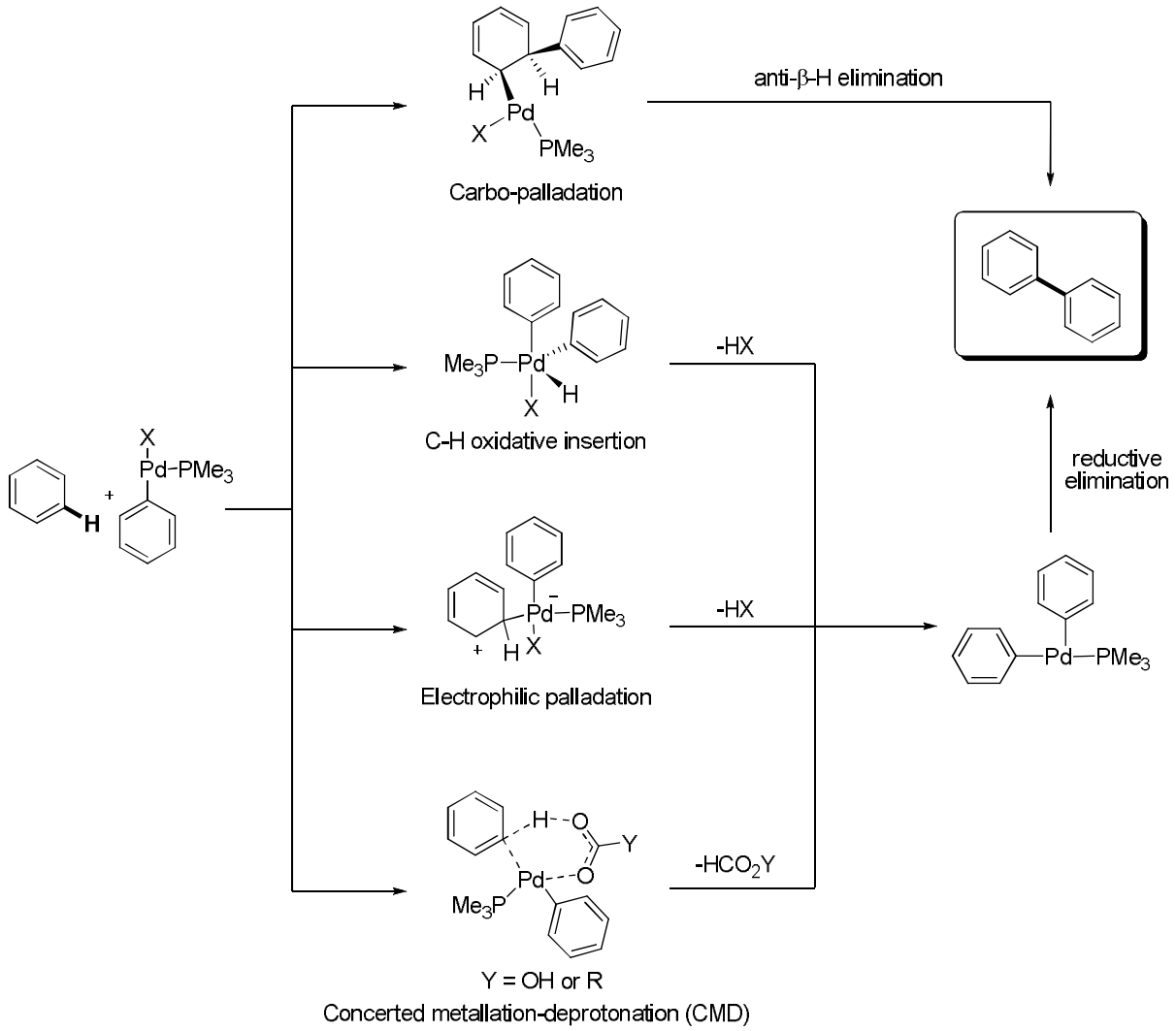

The Heck-type (carbo-palladation) pathway is characterized by *syn*-addition of a palladium-carbon bond across a double bond of the aromatic coupling partner. While *anti*-β-hydride elimination is a high energy process, the formation of a π-allyl species is often proposed, which could then isomerize to allow for a lower energy *syn*-β-hydride elimination.[23a]

Less described in the literature involves the oxidative addition of a $Pd^{(II)}$ species to a $Pd^{(IV)}$ species through an insertion into a C-H bond of an aromatic coupling partner. A

double reductive elimination would then afford the biaryl product as well as regenerate the catalytically active $Pd^{(0)}$ species.

To date, the most commonly suggested hypothesis for the mechanism of direct arylation is electrophilic palladation. An electrophilic palladation or electrophilic aromatic substitution (S_EAr) type process would involve a rate-determining nucleophilic attack by the arene on an electrophilic $Pd^{(II)}$-aryl species followed by rapid deprotonation of the resulting Wheland intermediate. Subsequent reductive elimination of the biaryl from $Pd^{(II)}$ would form the desired carbon-carbon bond as well as regenerate the active catalyst. This type of reaction profile is governed by the nucleophilicity of the aromatic coupling partner. Originally proposed for the arylation of electron-rich heteroaromatics, this has since been referenced numerous times for other direct arylation reactions.[2,22,28]

In 2004, Gevorgyan and co-workers reported a palladium-catalyzed arylation of indolizines for which they proposed an S_EAr pathway.[2a] This conclusion was drawn mostly from the observation of a lack of a kinetic isotope effect (KIE) for the reaction (Scheme 9).

Scheme 9. KIE experiment for indolizine arylation.

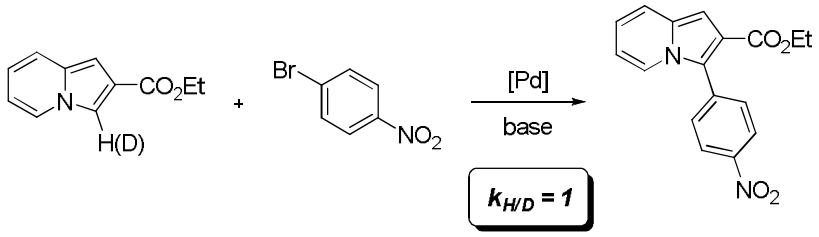

In addition to KIE studies, competition experiments (6) were run between indolizine (**4a**), 2-methylindolizine (**4b**), and 2-carboethoxyindolizine (**4c**). The relative rates of the arylation of **4a**:**4b**:**4c** was found to be 1.00:0.97:0.66. The observation that the indolizine

[28] Zhao, X.; Yeung, C. S.; Dong, V. M. *J. Am. Chem. Soc.* **2010**, *132*, 5837.

substituted with the electron-withdrawing carboethoxy group reacted the most slowly was interpreted as evidence in favour of an S_EAr mechanism. The slight discrepancy between **4a** and **4b** was attributed to the steric bulk of the methyl group in **4b** lowering the rate of the reaction.

(6) 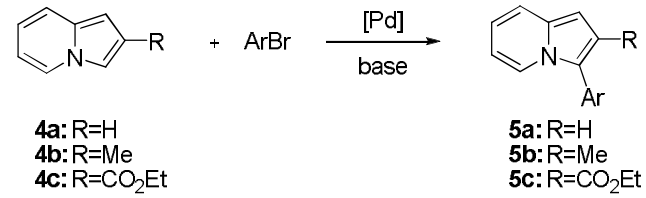

4a: R=H
4b: R=Me
4c: R=CO_2Et

5a: R=H
5b: R=Me
5c: R=CO_2Et

Similarly, in 2005 Sames *et al.* reported a mechanistic rational for the observed selectivity in their palladium catalyzed C2 and C3 arylaton of indoles.[2b] Sames reported a secondary KIE at the C3 position of indole for the process, while no significant KIE at the C2 position was observed. The secondary KIE at the C3 position was rationalized by a mechanism involving electrophilic aromatic substitution at the C3 position followed by a palladium migration to the C2 position. Sames also performed a Hammett study using various 6-substituted 1-methylindoles. A ρ-value of -0.71 was observed, which was consistent with a transition state bearing an arene with a positive character – a feature commonly assiciated with an S_EAr-type mechanism.

The Fagnou group, as well as others, have found computationally that for simple or electron-deficient aromatics, a CMD pathway is the lowest energy process which was consistent with experimental observations.[3,4,10,24,29] In a CMD pathway, the Pd-C bond formation occurs concurrently with the cleavage of the C-H bond of the arene to afford a $Pd^{(II)}$ diaryl species. This is then followed by reductive elimination of the biaryl product, regenerating the active catalyst.

[29] Biswas, B.; Sugimoto, M.; Sakaki, S. *Organometallics* **2000**, *19*, 3895.

This pathway was first proposed by Echavarren for the palladium-catalyzed intramolecular arylation of bromobenzyldiarylmethanes when it was observed that electron-withdrawing substitutents on the aromatic ring facilitates the reaction – a feature that is inconsistent with an S_EAr mechanism.[10b] Intramolecular competition experiments revealed that reaction occurred preferentially at the more electron-deficient arene.[10c] This was particularly well demonstrated by substrates which contained fluorines *ortho* to the arylation site (7). These observations were corroborated by a large intramolecular KIE of 5.0.

(7)

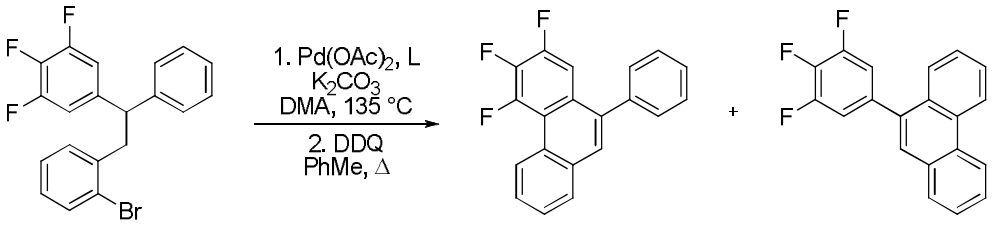

25 : 1

Recently, Fagnou *et al.* reported strong computational evidence which suggested that the CMD pathway is more broadly applicable than originally thought.[24] Not only was the CMD transition state able to accurately predict the reactivity and regioselectivities observed with electron-deficient arenes, but it was able to do so with a range of electron-rich arenes as well. These results pointed towards the possible involvement of a CMD transition state with substrates which were previously thought to react *via* a S_EAr pathway.

1.5 Project Overview

Herein a detailed investigation of the possible modes of C-H bond cleavage in the direct arylation of pyridine *N*-oxides will be described. Coupled with detailed kinetic studies and other key experimental evidence, DFT calculations were performed for the four most proposed mechanisms for direct arylation. Kinetic studies were performed in order to obtain a clearer picture of the overall structure of the catalytic cycle. Stoichiometric studies have also been used to elucidate the true role of base in this transformation and have led to an un-expected and critical role of the acetate ligand on the pre-catalyst in the active catalyst formed in direct aylation. These studies have led to the advancement of a revised catalytic cycle for the direct arylation of pyridine *N*-oxide.

Chapter 2 – Mechanistic Evaluation of the Pd-Catalyzed Direct Arylation of Pyridine N-Oxides

2.1 Kinetics

The generally accepted mechanism for palladium catalyzed direct arylation of aryl halides and simple arenes is shown in Scheme 10. The active $Pd^{(0)}$ catalyst undergoes oxidative insertion into the aryl halide, followed by C-H bond cleavage of the simple arene. Reductive elimination provides the desired biaryl product and regenerates the active $Pd^{(0)}$ catalyst. With the goal of obtaining a more detailed understanding of the catalytic cycle, and more specifically the intimate role of each of the primary reaction components, the order for each reagent in the coupling of 4-nitropyridine *N*-oxide and 5-bromo-*m*-xylene was obtained.[30] Using either $Pd(OAc)_2$ and tri-*tert*-butylphosphonium tetrafluoroborate salt or $Pd(P^tBu_3)_2$ as the catalyst, the concentration of each reaction

[30] The choice of substrate was mainly guided by analytical simplicity as all analyses were performed using ^1H NMR.

component was varied and the progression of the reaction at 110 °C was monitored. The initial time (t_0) of each kinetic run corresponded to the time at which the reaction flask was placed into the oil bath, which was pre-heated to 110 °C. During the course of the reaction, aliquots of the reaction mixture were removed, at which point the *N*-oxide readily precipitated out of solution, thus stopping the reaction. The solvent was then removed and the resulting samples were analyzed by NMR spectroscopy for the formation of product using trimethoxybenzene as an internal standard.

Scheme 10. General mechanism for the palladium-catalyzed direct arylation of simple arenes.

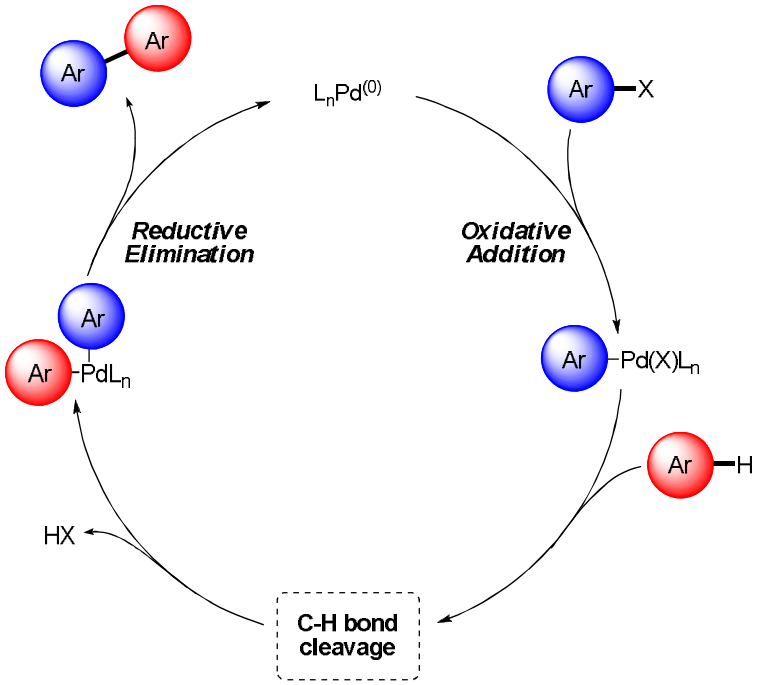

There are several mechanistic scenarios to be considered for the direct arylation of pyridine *N*-oxides. One possible scenario involves oxidative addition as the rate-determining step of the reaction. In this case, one would expect to observe a first-order behaviour in both aryl bromide and palladium catalyst, while zero-order behaviour in pyridine *N*-oxide would be observed. If the CMD step were to be rate determining, two possible scenarios may be anticipated; if the catalyst resting state is at the $Pd^{(0)}$ species, then first-order behaviour in the aryl halide, palladium catalyst and the pyridine *N*-oxide may be expected. However, if the catalyst was saturated as a $Pd^{(II)}$ species

formed after oxidative addition, the aryl-bromide would then be expected to exhibit zero-order behaviour, while first-order behaviour may still be established for both the Pd catalyst and the *N*-oxide. The same observed kinetic consequences could be expected if reductive elimination was the rate-determining step, but these two cases may be distinguished by looking for the presence or absence of a significant kinetic isotope effect at the C2 position of the *N*-oxide (*vide infra*).

The order in 5-bromo-*m*-xylene was determined by plotting the log of the initial rate versus the log of the concentration, using 5 mol% $Pd(OAc)_2$ as the pre-catalyst (Figure 3a). A slope of 0.04 was obtained revealing that varying the concentration of the aryl halide from 0.2 M to 0.6 M has no effect on the reaction rate, thus establishing zero-order behaviour in this system. The zero-order dependence in 5-bromo-*m*-xylene is indicative of a fast oxidative addition in which the palladium catalyst is saturated as a $Pd^{(II)}$-aryl species and thus ruling out the possibility of oxidative insertion being the rate determining step.

The order in 4-nitropyridine *N*-oxide was also determined in a similar manner by varying its concentration from 0.1 M to 0.8 M (Figure 3b). A slope of 1.16 was obtained indicating a first order behaviour in pyridine *N*-oxide. A first-order dependence on pyridine *N*-oxide suggests that a single molecule of the *N*-oxide participates at the transition state of the reaction, which is consistent with arene metallation or reductive elimination being the rate determining step. Reductive elimination was discarded as a possible rate determining step due to the observation of a significant KIE in a side-by-side comparison of rates (k_H/k_D = 3.3) using pyridine *N*-oxide or pyridine *N*-oxide d_5 as the starting azine.[31]

The rate-constant dependence on catalyst concentration was determined by using $Pd(P^tBu_3)_2$ as the catalyst in order to eliminate catalyst pre-activation. PivOH (30 mol%)

[31] For results from a one-pot KIE experiment, please see reference 4a.

was consequently added to account for the acetate that is normally in solution when $Pd(OAc)_2$ is used. The reaction rate was measured over a range of catalyst loadings of $Pd(P^tBu_3)_2$, varying from 1 mol% to 20 mol%. This order was determined with respect to an aryl bromide concentration of 0.3 M and an *N*-oxide concentration of 0.6 M, and a slope of 0.56 was obtained from the kinetic plot (Figure 3c), which is consistent with half-order behaviour in catalyst. This behaviour has been associated with systems in which the catalyst resting state is a dimer, while the active form of the catalyst is a monomer.[32] According to the zero-order dependence on aryl bromide and first-order dependence on the *N*-oxide, the dimeric resting state should be found between the oxidative addition and arene metallation steps.

Finally, the order in ligand was determined, also using 5 mol% of $Pd(P^tBu_3)_2$ as the catalyst. No change in rate was observed over a range of ligand concentrations, from a 1:2 Pd: ligand ratio to a 1:6 ratio (Figure 3d), thus establishing a zero-order behaviour in this system. It has been previously determined that the oxidative addition product of $Pd(P^tBu_3)_2$ into the C-Br bond of an aryl bromide is a T-shaped complex bearing a single phosphine ligand and a free co-ordination site (8)[33] and as such, the arene metallation transition state should have at most one bound phosphine ligand. Additionally, the zero-order dependence on phosphine ligand supports the arene metallation transition-state containing a single phosphine ligand and hence it is unlikely that any dissociation of P^tBu_3 from Pd occurs before the rate-determining step of the reaction.

(8) $Pd(P^tBu_3)_2 + \underset{\text{(excess)}}{PhBr} \xrightarrow{70\ ^\circ C,\ 2.5h} {}^tBu_3P-\overset{\overset{Ph}{|}}{Pd}-Br$

[32] (a) Fairlie, D. P.; Bosnich, B. *Organometallics* **1988**, *7*, 946. (b) Van Strijdonck, G. F. P.; Boele, M. D. K.; Kamer, P. C. J.; de Vries, J. G.; van Leeuwen, P. W. N. M. *Eur. J. Inorg. Chem.* **1999**, 1073. (c) Kina, A.; Hiroshi, I.; Hayashi, T. *J. Am. Chem. Soc.* **2006**, *128*, 3904. (d) Collum, D. B.; McNeil, A. J.; Ramirez, A. *Angew. Chem. Int. Ed.* **2007**, *46*, 3002. (e) Shen, Z.; Dornan, P. K.; Khan, H. A.; Woo, T. K.; Dong, V. M. *J. Am. Chem. Soc.* **2009**, *131*, 1077.

[33] Stambuli, J. P.; Bühl, M.; Hartwig, J. F. *J. Am. Chem. Soc.* **2002**, *124*, 9346.

Figure 3. Log plot of the initial rate dependence on the concentration of a) 5-bromo-*m*-xylene, b) 4-nitropyridine *N*-oxide, c) Pd(^{t}Bu$_3$)$_2$, d) P^{t}Bu$_3$.

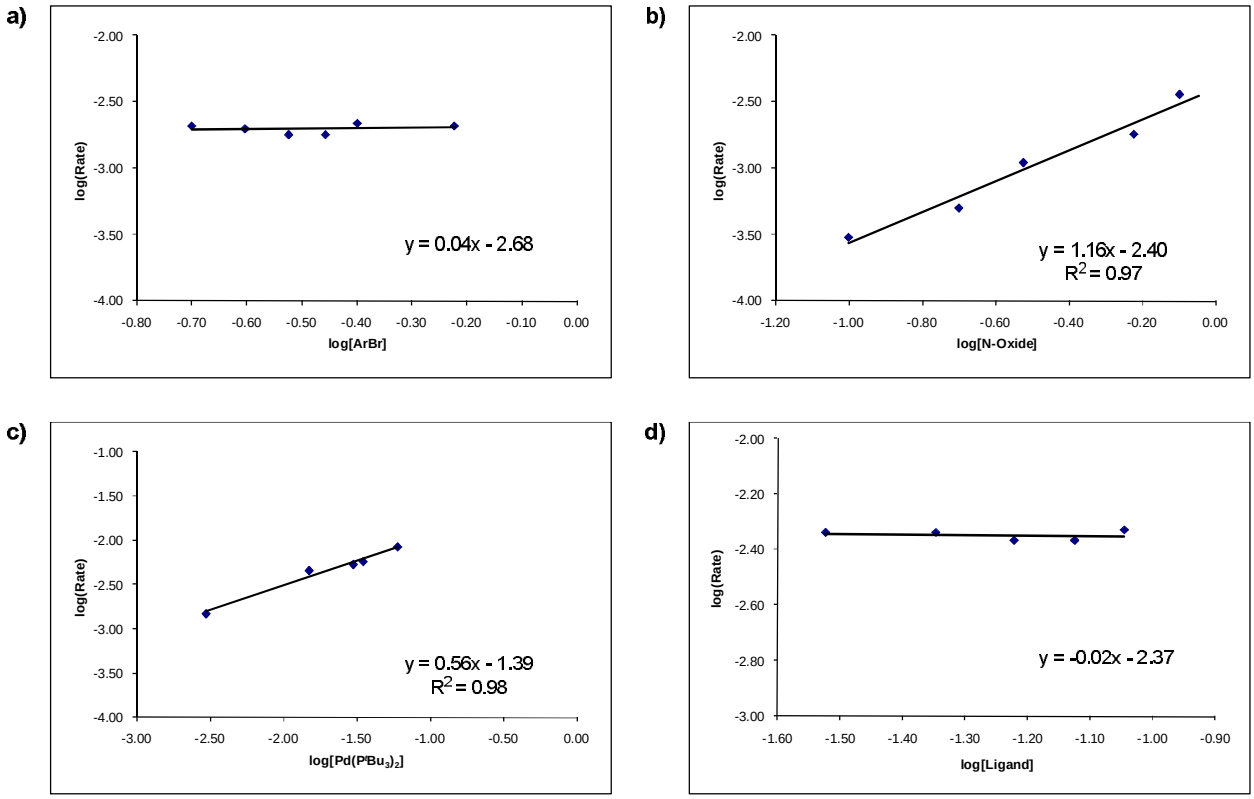

All kinetic evidence obtained was in support of a rate determining C-H bond cleaving step. With a basic understanding of the catalytic cycle in hand, the mechanism of the C-H bond cleavage was investigated in greater detail through both computational and experimental studies.

2.2 Computational Analysis

Quantum chemical[34] density functional theory [35] calculations were used to assist in differentiating amongst the four possible mechanistic scenarios and determining the lowest energy pathway for the C-H bond cleavage step.[36] All computations, were performed at the Hybrid B3LYP level[37] with a TZVP[38] basis set for all atoms except palladium, for which a DZVP[39] basis set was used. The ligand (either PMe^tBu_2 or P^tBu_3) in the reaction was approximated with PMe_3 in all computations in order to reduce computational time. This is a commonly used technique and was not expected to change the qualitative findings of the calculations. Energy diagrams show the relative Gibbs free energies for the various transition states, intermediates and products involved in each of the potential mechanisms. Calculations were performed in both the gas phase and with a solvent correction for toluene.[40] The initial structures for all calculations are pyridine *N*-oxide **A** and a palladium(II) species **(B, F, or F')** coordinated by one PMe_3 ligand after oxidative insertion into the C-Br bond of bromobenzene. In the case of species **F** the bromide has been replaced by a bicarbonate anion while species **F'** contains an acetate anion in place of bromide. The relative geometry between the aryl group and the other anionic ligand is denoted as *trans* where the *cis* isomer is only marginally higher in energy.

Among the processes examined, the C-H oxidative insertion pathway (Scheme 11) was found to be the highest in energy, thus making it an unlikely candidate as the acting mechanism of the reaction. This pathway was found to proceed through transition state

---

[34] Ziegler, T.; Autschbach, J. *Chem. Rev.* **2005**, *105*, 2695.
[35] (a) Hohenburg, P.; Kohn, W. *Phys. Rev. B* **1964,** *136*, 864. (b) Kohn, W.; Sham, L. *J. Phys. Rev. A* **1965**, *140*, 1133.
[36] All computational calculations were performed by Dr. S. I. Gorelsky.
[37] Lee, C.; Yang, W.; Parr, R. G. *Phys. Rev. B.* **1988**, *37*, 785.
[38] Schafer, A.; Huber, C.; Ahlrichs, R. *J. Chem. Phys.* **1994**, *100*, 5829.
[39] Godbout, N.; Salahub, D. R.; Andzelm, J.; Wimmer, E. *Can. J. Chem.* **1992**, *70*, 560.
[40] Foresman, J. B.; Keith, T. A.; Wiberg, K. B.; Snoonian, J.; Frisch, M. J. *J. Phys. Chem.* **1996**, *100*, 16098.

C having an energy of 56.6 kcal/mol and the resulting pentacoordinate $Pd^{(IV)}$ intermediate **D** has an energy of 51.7 kcal/mol. Reductive elimination of HBr gives the common intermediate **E** having an energy of 28.5 kcal/mol. The Heck-type pathway (Scheme 12) is only slightly lower in energy than the C-H oxidative insertion pathway having a transition state **G** with an energy of 53.4 kcal/mol, though this results in an intermediate **H** with a relatively low lying energy of 16.6 kcal/mol (Scheme 11). The required *anti*-β-hydride elimination however, would be a difficult and unlikely process which further disqualifies it as a possible pathway.

Scheme 11. Free energy diagram ($\Delta G^{\ddagger}_{298K}$, kcal•mol^{-1} in toluene) for the relevant intermediates, transition states, and products in the oxidative insertion pathway.

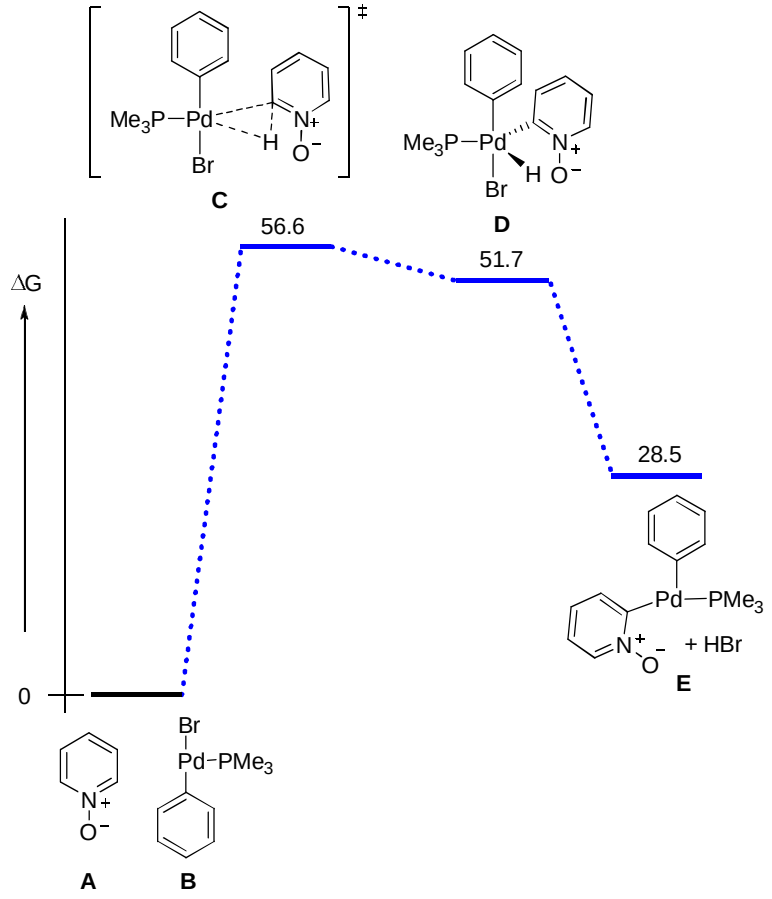

Scheme 12. Free energy diagram ($\Delta G^{\ddagger}_{298K}$, kcal•mol^{-1} in toluene) for the relevant intermediates, transition states, and products in the Heck-type pathway.

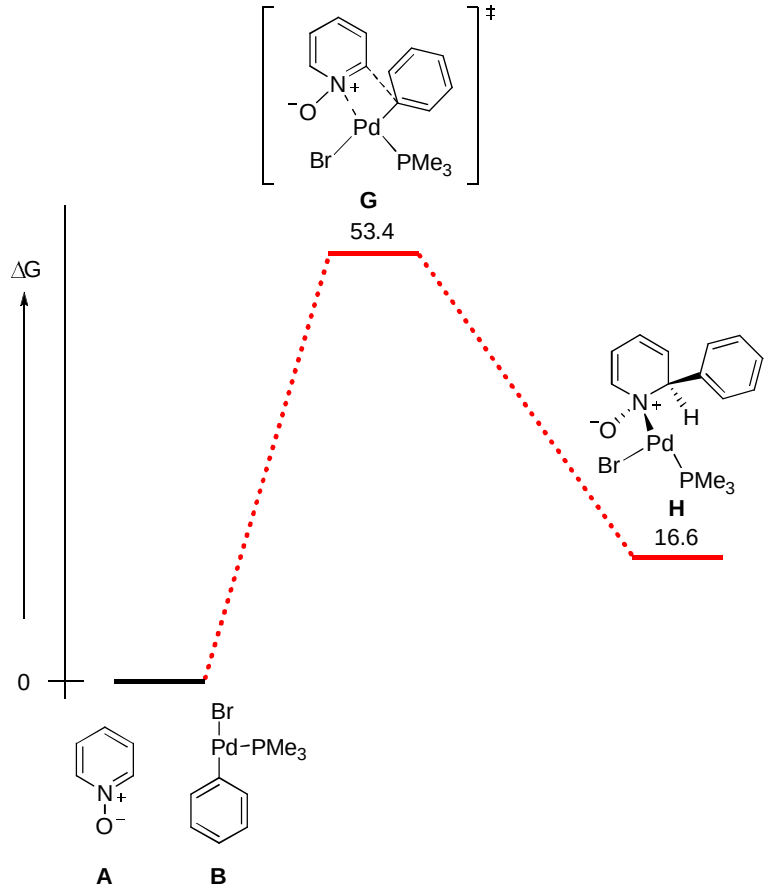

When investigating the CMD pathway two variants must be considered: an inner sphere mechanism and an outer sphere mechanism (Figure 4).[3,10b,c,d] An inner sphere mechanism is characterized by an internal base coordinated to palladium participating in the CMD process. This base can be either the halide from the aryl halide or a carbonate/carboxylate anion from a ligand exchange on palladium. Differentiated from this is the outer-sphere mechanism in which the deprotonation is performed by an external base (a carbonate or carboxylate anion).

Figure 4. Inner- and outer-sphere mechanisms for the concerted metallation-deprotonation process.

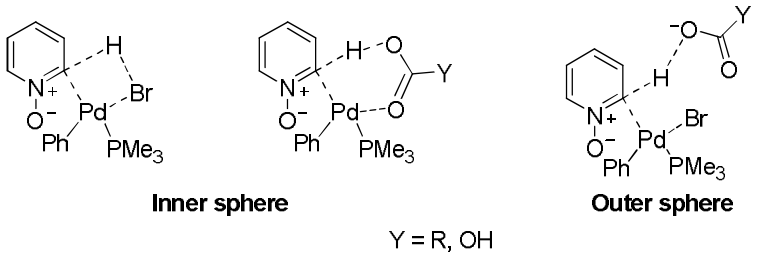

Both CMD variants were found to be substantially lower in energy than the alternate pathways (Scheme 13 & Scheme 14). Starting with species **B** and carbonate as the external base, the outer sphere mechanism had a transition state **L**, with an energy of 40.3 kcal/mol and the inner sphere mechanism starting from **F** as the $Pd^{(II)}$ species, had a transition state **J** with an energy of 32.4 kcal/mol. The inner sphere mechanism with bromide as the base was found to have no thermodynamic barrier and arrives at the product **E** (36.8 kcal/mol) with subsequent loss of HBr (Scheme 13). This pathway led to higher energy products than if carbonate was used as the base, and thus it was discarded. Calculations were also performed using acetate as the base. The relative energies of the transition states reflected those found when bicarbonate was used as the base, although the absolute values were found to be slightly lower (Scheme 14).

Scheme 13. Free energy diagram ($\Delta G^{\ddagger}_{298K}$, kcal•mol^{-1} in toluene) for the relevant intermediates, transitions states, and products in the inner- and outer-sphere CMD pathways using bicarbonate as the base.

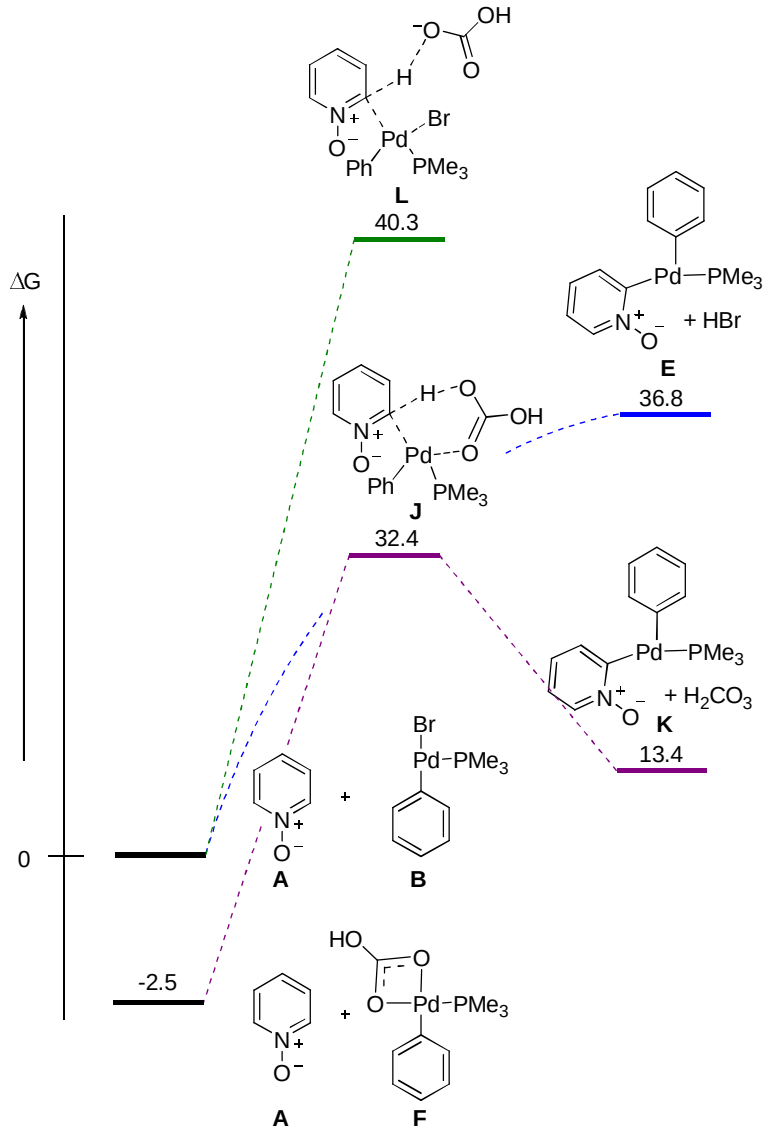

Scheme 14. Free energy diagram ($\Delta G^{\ddagger}_{298K}$, kcal•mol^{-1} in toluene) for the relevant intermediates, transitions states, and products in the inner- and outer-sphere CMD pathways using acetate as the base.

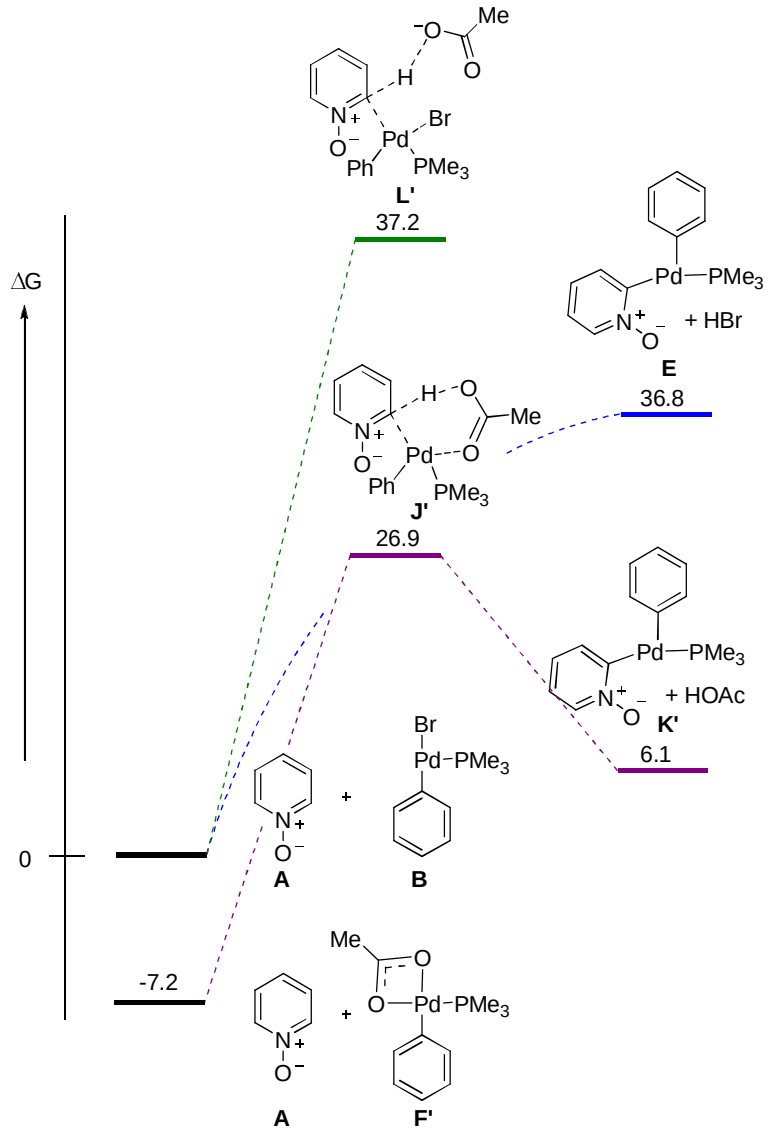

Efforts were made to locate the transition state energy leading to the Wheland intermediate in an S_EAr type pathway (Scheme 15) starting with **F** as the initial $Pd^{(II)}$ species. However, only the intermediate **I** (18.9 kcal/mol), a η^2 π-complex having no cationic character on the aromatic ring, could be located. Departing from intermediate **I** this reaction pathway converges with that of the inner-sphere CMD pathway at transition state **J** (34.9 kcal/mol). Formation of the carbon-palladium bond and loss of H_2CO_3

yields products **K** (15.9 kcal/mol). The possibility of an S_EAr mechanism was thus discarded on the basis that no Wheland intermediate or complex containing arene cationic character could be located computationally.

Scheme 15. Relevant intermediates, transition states, and products in the S_EAr pathway.

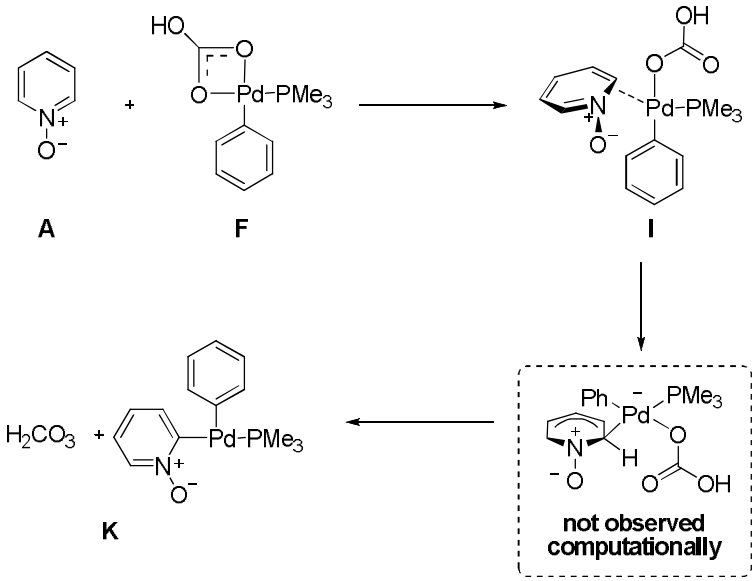

From these results, the inner sphere CMD mechanism was determined to be the most likely pathway for the C-H bond cleavage step in direct arylation. Computational results were also correlated to experimental findings to further support the proposal for a CMD mechanism. An Arrhenius plot was constructed for the coupling between 4-nitropyridine *N*-oxide and 5-bromo-*m*-xylene (Figure 5) and the Arrhenius energy of activation was determined to be 18.5 kcal/mol. This value is in good agreement with the calculated $\Delta E^{\ddagger}$ of 17.6 kcal/mol (at 298 K, in toluene), suggesting that the inner-sphere CMD pathway is an energetically viable process.

Figure 5. Arrhenius plot constructed for the coupling of 4-nitropyridine *N*-oxide.

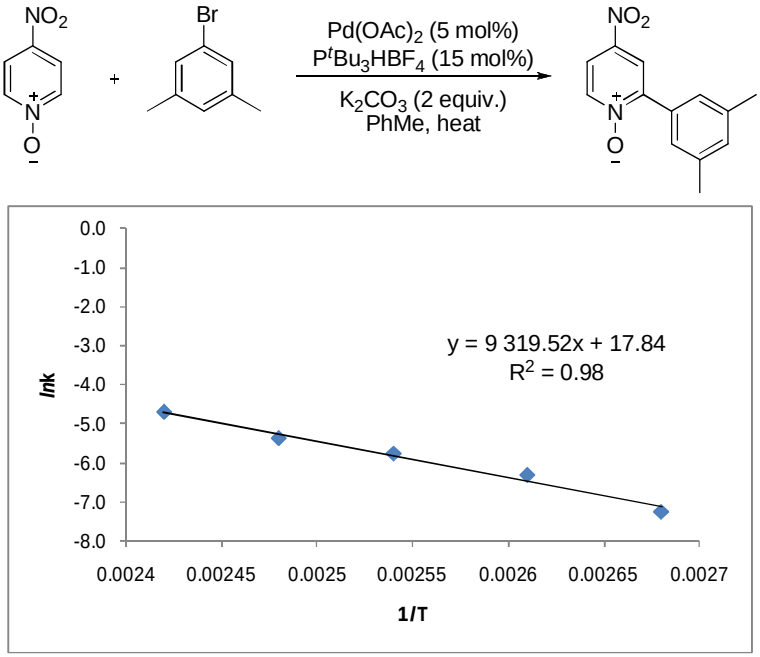

The regioselectivity of the reaction was also examined and proved to be particularly illustrative. Computationally, the energies for arylation to take place at each position on pyridine *N*-oxide ring were calculated for the inner- and outer-sphere mechanisms using both carbonate and acetate as the acting base (Figure 6). In both cases, the inner-sphere mechanism was predicted to arylate preferentially at the C2 position, followed by C4 and with arylation at the C3 position being the highest in energy, while the outer-sphere mechanism was predicted to have the opposite selectivity, favouring arylation at the C4 position while arylation at the C2 position was highest energy process. Pyridine *N*-oxide is known to be amphoteric, acting as both a nucleophile and an electrophile.[41] The *N*-oxide moiety also imparts an increased acidity of the C-H bonds at positions 2 and 4 on the pyridine ring.[42] While our initial hypothesis was that an increased acidity of the C-H bond was a necessary component for the CMD mechanism, recent

[41] (a) Andersson, H.; Almqvist, F.; Olsson, R. *Org. Lett.* **2007**, *9,* 1335. (b) Taylor Jr., E. C. Crovetti, A. J. *Organic Syntheses*, *Coll. Vol. 4*, p.654 (**1963**); *Vol. 36*, p.53 (**1956**).
[42] (a) Paudler, W. W.; Humphrey, S. A. *J. Org. Chem.* **1970**, *35*, 3467. (b) Kreuger, S. A.; Paudler, W. W. *J. Org. Chem.* **1972**, *37*, 4188.

computational results from our group have shown that a more important factor is electropositive character at the position *ortho* to the nitrogen in the aromatic ring (as present at the C2 position of pyridine *N*-oxide).[24] Experimentally, the regiochemical outcome for the direct arylation of pyridine *N*-oxide is such that only arylation at the C2 position is observed, which is in agreement with calculated predictions for the inner sphere mechanism.

Figure 6. Free energy of activation ($\Delta G^{\ddagger}_{298K}$, kcal mol^{-1} in toluene) for the three possible sites of arylation via the inner- and outer-sphere mechanisms.

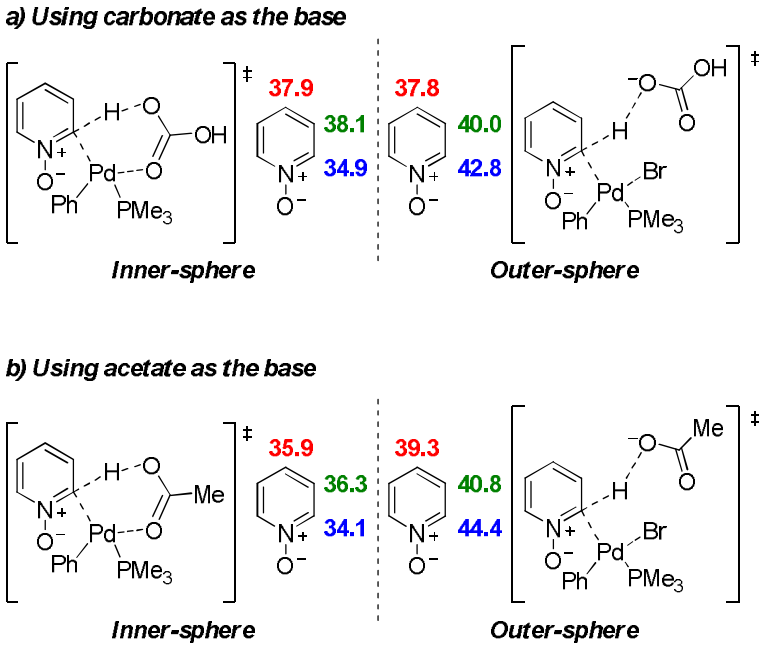

The inner-sphere CMD mechanism also accurately predicts the regioselective outcome for substituted pyridine *N*-oxides (Table 2).[43] When pyridine *N*-oxides bearing a phenyl or methylester substituent at the C3 position are used, the regioselectivity is sterically controlled and arylation takes place preferentially at the C6 position, suggesting that a steric bias for the less hindered site is controlling the regiochemical

[43] Regioselectivity experiments using 3-substituted pyridine *N*-oxides performed by Louis-Charles Campeau.

outcome of the reaction. A smaller C3 substituent, such as a methoxy group, results in non-selective arylation when P^{t}Bu$_3$ is used as the ligand, which is in agreement with a steric argument for the selectivities observed, while selectivity for the C2 position is observed when the smaller P^{t}Bu$_2$Me is used. This apparent ligand effect has been observed with other pyridine *N*-oxide and aryl halide substrates,[4b,44,45] and along with the observed zero-order in ligand during kinetic experiments, it is also in agreement with the phosphine ligand being present on the metal at the CMD step. The regioselectivity is also inversed to the C2 position when a C3 electron-withdrawing substituent, such as a nitro, cyano, or fluoro group, is present. The electron-withdrawing substituent could impart an electropositive character to the C2 position of the *N*-oxide through resonance and inductive effects, thus stabilizing the developing negative charge of the CMD transition state which involves the development of a negative charge at the C2 position. In all cases, the elaborated DFT model accurately predicts regiochemistry.

Table 2. Experimental and computational results for the regioselectivity in the direct arylation of C3-substituted pyridine *N*-oxides.

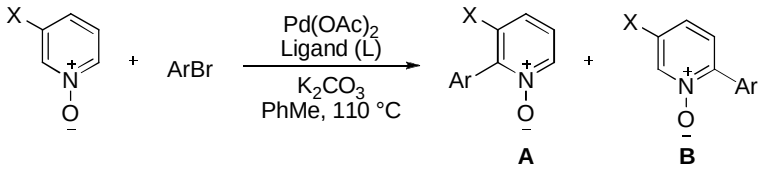

Entry	X=	Calculated A:B (L=PMe$_3$)	Experimental A:B (L=P^{t}Bu$_3$)	Experimental A:B (L=P^{t}Bu$_2$Me)
1	Ph	1:11	1:10	-
2	CO_2Me	1:4	1:7	-
3	OMe	6:1	1:1	5:1
4	NO_2	9:1	4:1	6:1
5	CN	4:1	10:1	15:1
6	F	76:1	25:1	-

[44] Schipper, D. J.; El-Salfiti, M.; Whipp, C. J.; Fagnou, K. *Tetrahedron* **2009**, 4977.
[45] The regioselectivities for 3-fluoro and 3-phenylpyridine *N*-oxide have also been reproduced stoichiometrically using **2**. See supporting information.

Additionally, one-pot competition experiments[46] and computational predictions of relative rates under a CMD mechanism were performed (Figure 7) and it was found that the experimental values correlated well with those which were calculated. It was seen that in all cases, the aryl bromide reacted most readily with the more electron-deficient arene, which is contrary to what would be expected if S_EAr was the acting mechanism. The greater reaction rate of the methoxy-substituted *N*-oxide over the methyl-substituted *N*-oxide is due to the σ-withdrawing effect of the methoxy substituent to the *meta* position of the arene, which is also reflected in the positive σ_{meta} value of a methoxy substituent. The results of these competition experiments are also in agreement with the obtained Hammett plot, which provides a side-by-side comparison of the different *N*-oxides' reaction rates (Figure 8). In the past, Hammett studies conducted for direct arylation reactions have generally resulted in negative ρ values, and this observation was commonly used as the main argument in support of an S_EAr mechanism for direct arylation.[2ab] The obtained Hammett plot shows a positive correlation, giving a ρ value of +1.53. The positive ρ value suggests the enhancement of rate with increasing electron-withdrawing ability of the substituent located at the C4 position of the *N*-oxide, which is in support of the CMD pathway. An electron-withdrawing substituent would be expected to stabilize the development of a negative charge at the CMD transition state, and thus lower the energy of the process.

[46] One-pot competition experiments performed by David R. Stuart.

Figure 7. Computational and experimental results for competition experiments between pyridine *N*-oxides of different electronics.

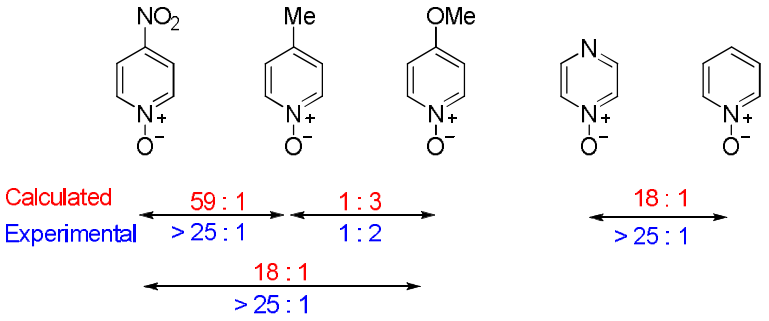

Figure 8. Hammett plot for the direct arylation of C4-substituted pyridine *N*-oxides.

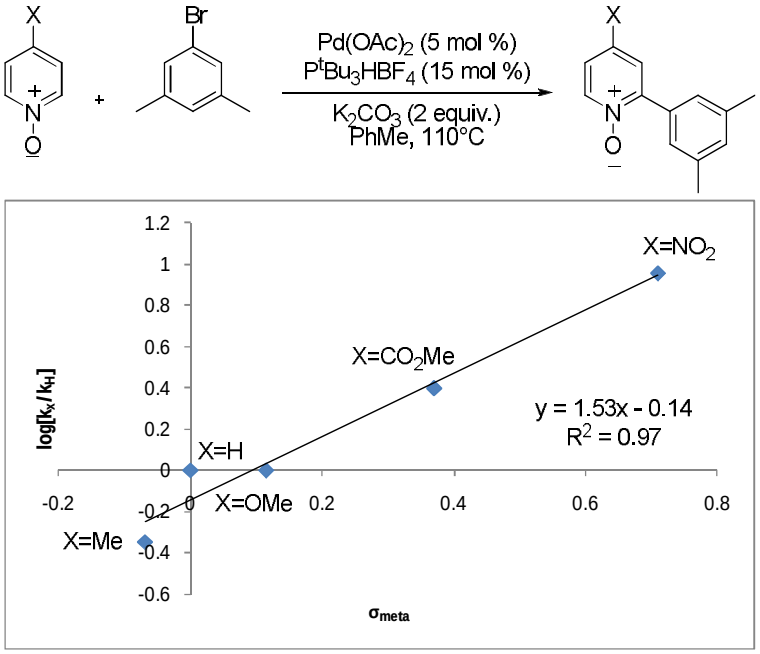

2.3 Base Effects

Further experiments were performed to examine the nature of the base in the CMD process. The three coordinate arylpalladium halide complex **1** (Table 3), a possible intermediate in the catalytic cycle, was synthesized according to a procedure reported by Hartwig *et al.*[33] and was stoichiometrically reacted with 4-nitropyridine *N*-oxide in the presence of K_2CO_3 and/or KOPiv as a base. Reactivity was found to depend heavily on the presence of pivalate base in the reaction mixture. While no product is observed in the absence of any base, surprisingly low reactivity was observed when using K_2CO_3 (Table 3, entries 1-2). However, in the presence of pivalate, with or without K_2CO_3, the desired coupling product is obtained in approximately 30% yield (Table 3, entries 3-4).

Table 3. Yields of a stoichiometric reaction between 1 and 4-nitropyridine *N*-oxide using different bases.

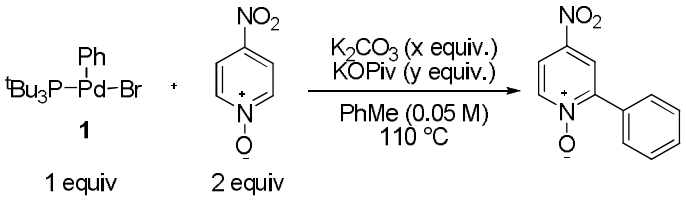

Entry	K_2CO_3	KOPiv	NMR Yield (%)
1	none	none	0
2	10 equiv	none	5
3	none	10 equiv	29
4	10 equiv	10 equiv	31

The reaction rate was also found to depend heavily on the identity of the base present in the reaction mixture. Kinetic experiments were run using $Pd(P^tBu_3)_2$ as the catalyst in order to eliminate catalyst pre-activation as a potentially significant factor when measuring reaction rates. The rate of the reaction was observed to be slow when only one of K_2CO_3 or KOPiv was used, but when a combination of excess K_2CO_3 with a sub-stoichiometric amount of PivOH was used, the reaction rate increased

approximately six-fold and was comparable to that of a reaction run under the standard reported conditions (Figure 9). The poor reactivity of a system using only KOPiv as the base may be attributed to the eventual build-up of PivOH in the reaction mixture, which could result in the proto-demetallation of a palladium aryl organometallic, generating reduced arene and catalytically inactive $Pd^{(II)}$. This unwanted side-reaction would lead to the consumption of the starting material and an overall decreased yield and reaction rate. Using K_2CO_3 with a catalytic amount of PivOH would allow for the prevention of the build-up of acid by allowing the PivOH that is formed to be deprotonated by the K_2CO_3, thus re-generating the pivalate anion required for another turn of the catalytic cycle. When using $Pd(OAc)_2$ as the catalyst however, no pivalate additive was required to achieve good reactivity. Furthermore, when $Pd(OPiv)_2$ was used in place of $Pd(OAc)_2$ as the palladium pre-catalyst, an activation period of approximately 20 minutes was observed. Once the formation of product began, however, the rate of the reaction paralleled that of the reaction run with K_2CO_3 and catalytic PivOH (Figure 10). which alludes to a secondary role for $Pd(OAc)_2$. While $Pd(OAc)_2$ has always been considered to serve only as a pre-catalyst, these results are indicative of its ability to act as a source of soluble carboxylate base to perform the deprotonation at the CMD step.[47]

[47] To test this hypothesis, the rate of a reaction using a catalytic amount of KOAc was measured, but was found to be quite slow, likely due to the insolubility of KOAc in the toluene.

Figure 9. Dependence of rate on the identity of the base used.

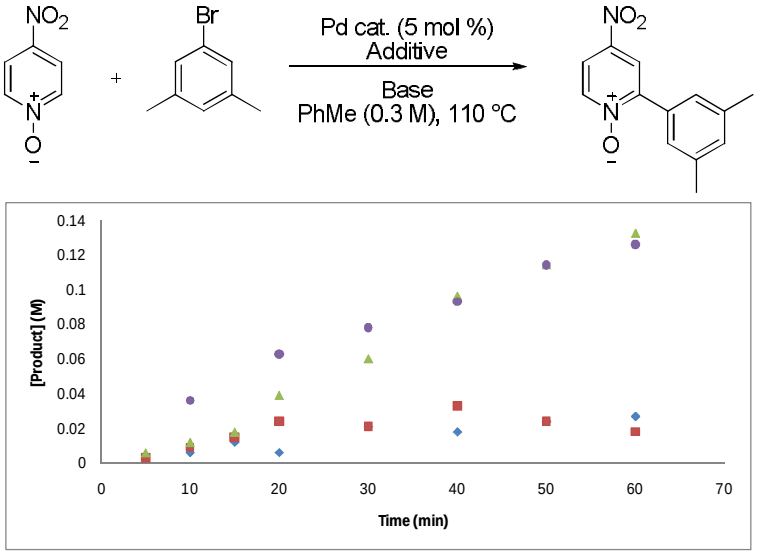

Conditions: (♦) $Pd(P^tBu_3)_2$, 2 equiv. K_2CO_3; (■) 5 mol% $Pd(P^tBu_3)_2$, 2 equiv. KOPiv; (▲) $Pd(P^tBu_3)_2$, 2 equiv. K_2CO_3, 30 mol% PivOH; (●) $Pd(OAc)_2$, 15 mol% P^tBu_3•HBF_4, 2 equiv. K_2CO_3.

Figure 10. Comparison of reaction rates using $Pd(OPiv)_2$ and $Pd(P^tBu_3)_2$ as catalysts.

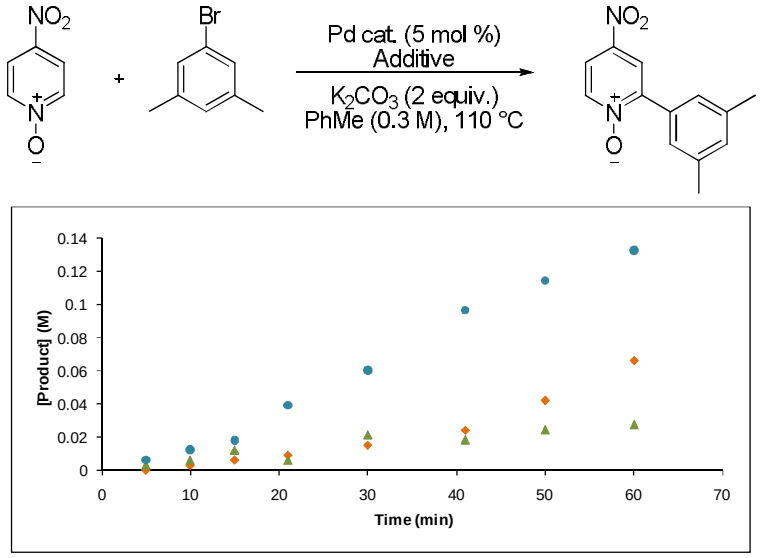

Conditions: (▲) $Pd(P^tBu_3)_2$, (●) $Pd(P^tBu_3)_2$, 30 mol% PivOH, (♦) $Pd(OPiv)_2$, 15 mol% P^tBu_3·HBF_4.

To probe this hypothesis, the aryl palladium acetate complex **2** was synthesized[48] and reacted stoichiometrically with 4-nitropyridine *N*-oxide in the presence and absence of K_2CO_3. The conditions used were chosen to mimic the conditions used in the catalytic reaction. The obtained yield in both cases were identical, revealing little dependence of the stoichiometric reaction on the presence of K_2CO_3 (Scheme 16). The yields of these stoichiometric reactions are also comparable to that of the analogous catalytic reaction.[49] These stoichiometric studies show that **2** is a likely intermediate in the catalytic cycle. Furthermore, the observed identical yields between the reactions run with and without K_2CO_3 are in support of acetate, and not carbonate, performing the necessary deprotonation at the CMD step.

Scheme 16. Stoichiometric reactivity of complex **2**.

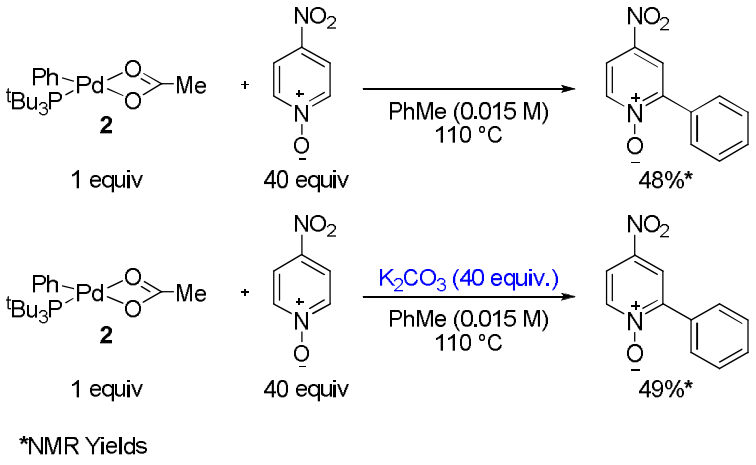

The participation of **2** in the catalytic cycle is further supported by its ability to act as a competent catalyst as well as by the similarity in initial rates between a reaction run with catalytic $Pd(P^tBu_3)_2$ with PivOH and one run with a catalytic amount of **2** (Figure 11). A catalytic amount of KOPiv (5 mol%) was added to the reaction run with **2** as the catalyst

[48] Barrios-Landeros, F. *Oxidative Addition of Haloarenes by Pd(0) Complexes of Bulky Alkyl Phosphines: Synthesis of Intermediates and Mechanistic Studies*. Diss. Yale University, 2007.
[49] Conditions: Bromobenzene (1 equiv.), 4-nitropyridine *N*-oxide (2 equiv.), $Pd(OAc)_2$ (5 mol%), P^tBu_3•HBF_4 (15 mol%), K_2CO_3 (2 equiv.), PhMe, 110 °C, 16 h. NMR yield: 62%.

in order to mimic the ratio of Pd to carboxylate base that is present when $Pd(OAc)_2$ is used as the catalyst.

Figure 11. Initial rate of a reaction run with a catalytic amount of **2**.

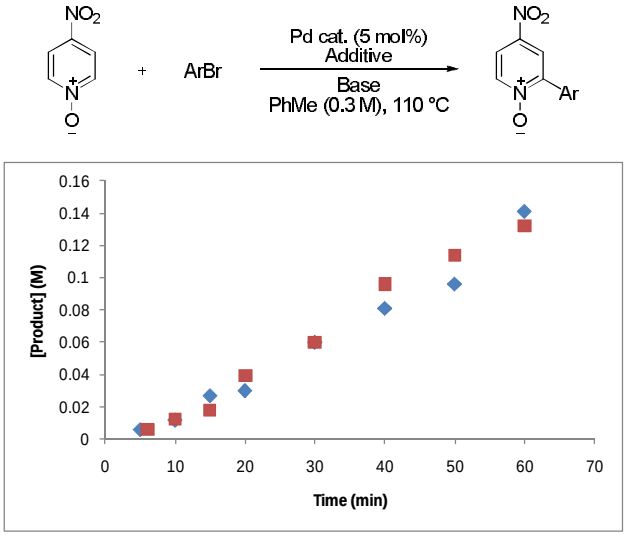

Conditions: (♦) **2**, 2 equiv. K_2CO_3, 5 mol% KOPiv; (■) $Pd(P^tBu_3)_2$, 2 equiv. K_2CO_3, 30 mol% PivOH.

2.4 Summary of Mechanistic Data & Revised Catalytic Cycle

Given the mechanistic insight we obtained from the results of the computational studies as well as the various experiments performed, it was possible to propose a revised catalytic cycle for the direct arylation of pyridine *N*-oxides (Scheme 17). The results from the kinetic experiments suggest a fast oxidative addition of the aryl halide into a $Pd^{(0)}$ species after which the catalyst is saturated as a $Pd^{(II)}$ species. According to the observed half-order dependence on catalyst concentration, this $Pd^{(II)}$ species could possibly exist as an inactive dimer which is in equilibrium with the less favoured active monomeric form of the catalyst.[50] Stoichiometric studies using different palladium complexes have pointed to the involvement of an acetate at the transition state as the deprotonating agent. The reaction likely proceeds via a κ^2-bound acetate on the palladium metal **2** from which the pyridine *N*-oxide can displace one of the acetate oxygens and co-ordinate to the metal centre.[51] The reaction is then proposed to proceed through a 6-membered inner-sphere CMD transition state, generating the palladium biaryl species which goes on to the reductive elimination step to give product and regenerate the $Pd^{(0)}$ catalyst. The acetic acid generated in this process is likely deprotonated by the carbonate base in the reaction mixture, which regenerates the acetate required for another turnover of the catalytic cycle.

[50] Efforts to isolate and characterize the dimeric resting state of the catalyst were unfruitful. However, as both the Pd-Br (**1**) and Pd-OAc (**2**) are known to be monomeric, we suspect the involvement of pyridine *N*-oxide in the dimeric form.

[51] It is likely that the initial coordination of pyridine *N*-oxide occurs via oxygen. For references on *O*-bound Pd complexes, see: Cho, S. H.; Hwang, S. J.; Chang, S. *J. Am. Chem. Soc.* **2008**, *130*, 9254.

Scheme 17. Revised catalytic cycle for the direct arylation of pyridine *N*-oxides *via* a CMD transition state.

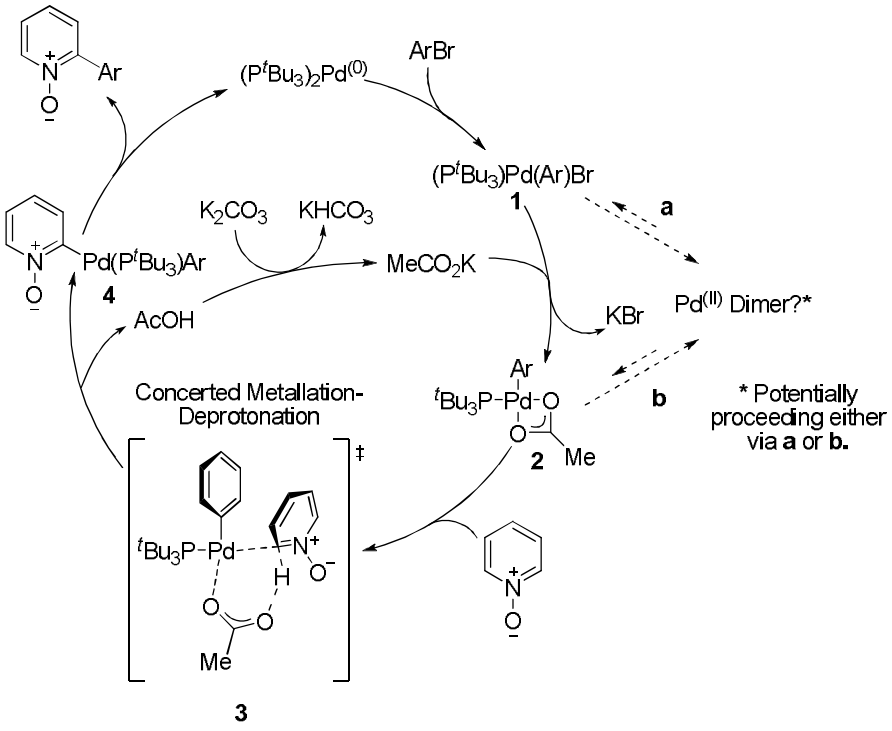

2.5 Towards the Development of Improved Reaction Conditions

There are several limitations associated with direct arylation reactions including harsh conditions (typically heating to 110 °C),[4,23b,52,53] and high catalyst loadings (typically 5 mol%).[2c,4,23b,52,54,55] The presence of an induction period of up to one hour in some cases has also been noted for these processes. This phenomenon has been attributed to the need for an *in situ* reduction of the $Pd(OAc)_2$ pre-catalyst to $Pd^{(0)}$. Unfortunately, use of other readily available $Pd^{(0)}$ pre-catalysts fail to eliminated this induction period. Through an in-depth mechanistic evaluation of this process, it was determined that the acetate ligands associated with the $Pd(OAc)_2$ pre-catalyst play an essential role in the reaction. Building on this observation, efforts were directed towards developing improved reactions conditions which would address these current limitations of direct arylation.

This optimization was directed towards achieving a much lower catalyst loading than in the existing reaction conditions (5 mol%). All yields were obtained as NMR yields using trimethoxybenzene as the internal standard. Based on our previous observation that the acetate ligands on the $Pd(OAc)_2$ pre-catalyst likely plays an important role at the C-H bond cleaving step. It was also determined through kinetic analysis that this C-H bond cleaving step is likely the rate determining step. Given these observations, it was reasoned that using a more soluble source of carboxylate base could facilitate this step.

The reaction optimization was performed using 4-picoline *N*-oxide as the substrate. Equation 9 shows the reference conditions which were used.

---

[52] Lazareva, A.; Daugulis, O. *Org. Lett.* **2006**, *8*, 5211.
[53] Roger, J.; Pozgan, F.; Doucet, H. *J. Org. Chem.* **2009**, *74*, 1179.
[54] Lebrasseaur, N.; Larrosa, I. *J. Am. Chem. Soc.* **2008**, *130*, 2926.
[55] Verrier, C.; Martin, T.; Hoarau, C.; Marsais, F. *J. Org. Chem.* **2008**, *73*, 7383.

(9)

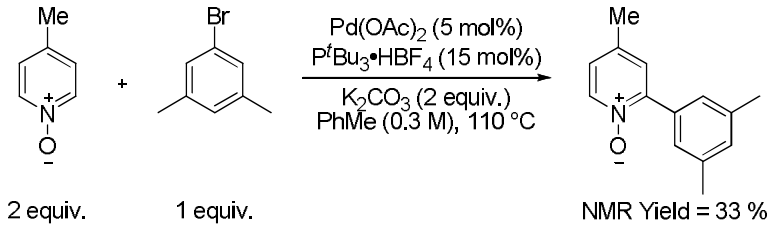

It was found that when the catalyst loading was dropped to 1 mol%, only 12% product was formed (Table 4, entry 2). However, when 10 mol% of CsOPiv (a soluble carboxylate base in toluene) was added, it was found that the yield was greatly improved to 63% (Table 4, entry 3). It was also found that lowering the amount of CsOPiv to 2 mol% had little effect on yield (Table 4, entry 4 & 5). In the instance where CsOPiv was used, K_2CO_3 was replaced by Cs_2CO_3 in order to keep the counter ion in the reaction mixture consistent.

Table 4. Optimization of reaction conditions for 4-picoline *N*-oxide arylation.

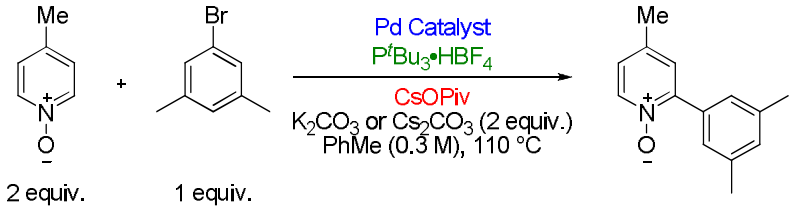

Entry	Pd Catalyst	Pd Catalyst (mol%)	P^tBu_3•HBF_4 (mol %)	CsOPiv (mol %)	NMR Yield (%)
1	$Pd(OAc)_2$	5	15	-	33
2	$Pd(OAc)_2$	1	3	-	12
3	$Pd(OAc)_2$	1	3	10	63
4	$Pd(OAc)_2$	1	3	5	64
5	$Pd(OAc)_2$	1	3	2	64
6	$Pd(OAc)_2$	0.5	1.5	2	50
7	**$Pd(P^tBu_3)_2$**	**0.5**	**-**	**2**	**91**

Dropping catalyst loading further to 0.5 mol% lowered product yield to 50% (Table 4, entry 6). At this point, it was hypothesized that the dilute concentrations in $Pd(OAc)_2$ and $P^tBu_3 \bullet HBF_4$ was hindering catalyst activation and thus lowering the overall yield of the reaction. As a result, the reaction was attempted using the pre-formed $Pd(P^tBu_3)_2$ to eliminate the need for catalyst pre-activation. It was found that using only 0.5 mol% of $Pd(P^tBu_3)_2$, a yield of 91% could be achieved (Table 4, entry 7).

These initial results were very encouraging and these new reaction conditions should be more completely evaluated with other challenging substrates such as pyrimidines and some azoles which still exhibit low direct arylation reactivity, even under the best literature conditions to date.

Chapter 3 – Conclusions

In conclusion, the mechanism of direct arylation of pyridine *N*-oxides has been examined through kinetic and computational analysis. The data obtained from these studies allowed for the proposal of a revised catalytic cycle which points to CMD being the rate limiting step in the process. The critical role of the base in the CMD process was investigated in further detail in both catalytic and stoichiometric variations of the transformation. The observed dependence of reactivity on the presence of soluble carboxylate indicates that the acetate from the $Pd(OAc)_2$ pre-catalyst is acting as the deprotonating agent at the CMD step. This observation is also in accord with the prevalence of $Pd(OAc)_2$ being used as a pre-catalyst in direct arylation reactions and should be considered in the development of new direct arylation processes. The need for a soluble carboxylate base has been used as a basis for the development of improved reaction conditions for the direct arylation of azine *N*-oxides. It was found that the use of catalytic CsOPiv allowed for a reduction in the amount of required Pd catalyst, from 5 mol% to 1 mol% or less. Improved conversions were also observed by NMR. These new reaction conditions can potentially greatly expand the current scope of direct arylation and should be explored using other challenging substrates.

Chapter 4 – Supporting Information

General Methods

All experiments were carried out under an argon atmosphere unless otherwise stated. ^{1}H and ^{13}C NMR spectra were recorded in $CDCl_3$ solutions on a Bruker AVANCE 400 MHz. High-resolution mass spectra were obtained on a Kratos Concept IIH. Infra-Red analysis was performed with a Bruker EQUINOX 55. HPLC Grade benzene and toluene are dried and purified via MBraun SP Series solvent purification system. Phosphonium salts were either synthesized according to literature procedures[56] or purchased from Strem, stored in a dessicator and used without further purification. Palladium sources were stored in a dessicator and were weighed out to air unless otherwise specified. All other reagents and solvents were used as is from commercial sources. Characterization data is provided for all new compounds, unless noted below, all other compounds have been reported in the literature or are commercially available.

[56] Netherton, M. R.; Fu, G. C. *Org. Lett.* **2001**, *3*, 4295.

General Procedure (A) for the Direct Arylation of Pyridine *N*-Oxides using Aryl Bromides

Pyridine *N*-oxide (3 equiv.), K_2CO_3 (2 equiv.) P^tBu_3•HBF_4 (15 mol%), $Pd(OAc)_2$ (5 mol%) were weighed into a 100 mL flask equipped with a teflon stir bar. The flask was fitted with a reflux condenser and the reaction vessel was then evacuated and refilled with argon (repeat 3 times). A solution of 5-bromo-*m*-xylene (1 equiv.) in toluene (0.3 M with respect to aryl bromide) was purged with argon (10-15 min) and added to the reaction flask. The flask was placed in an oil bath and heated to 110 °C with constant stirring. The reaction was allowed to heat at 110 °C overnight after which the flask was removed from the oil bath and allowed to cool to room temperature. The reaction was then filtered through celite (washing with CH_2Cl_2) and the filtrate was concentrated under reduced pressure then loaded onto a short silica gel column for chromatography.

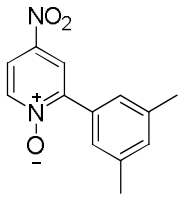

2-(3,5-dimethylphenyl)-4-nitropyridine 1-oxide

^{1}H NMR (400 MHz, $CDCl_3$, 293 K): 8.36 (1H, d, *J*= 7.2 Hz), 8.26 (1H, d, *J*= 3.2 Hz), 8.02 (1H, dd, *J*= 3.2, 7.2 Hz), 7.39 (2H, s), 7.16 (1H, s), 2.40 (6H, s)**.**

^{13}C NMR (100 MHz, $CDCl_3$, 293 K): 150.8, 142.0, 141.3, 138.4, 132.5, 130.6, 126.7, 121.6, 118.3, 21.4.

HRMS: Calculated for $C_{13}H_{12}N_2O_3$ (M+): 244.0848; Found: 244.0846

IR (ν_{max}/cm^{-1}): 3106, 3085, 3055, 2917, 2859, 1520, 1341, 1278.

m.p.: 174-175 °C

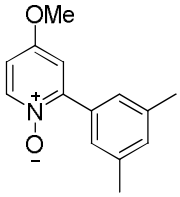

2-(3,5-dimethylphenyl)-4-methoxypyridine 1-oxide

^{1}H NMR (400 MHz, $CDCl_3$, 293 K): 8.24 (1H, d, *J*= 7.3 Hz), 7.38 (2H, s), 7.09 (1H, s), 6.89 (1H, d, *J*= 3.5 Hz), 6.78 (1H, dd, *J*= 3.5, 7.3 Hz), 3.87 (3H, s), 2.37 (6H, s).

^{13}C NMR (100 MHz, $CDCl_3$, 293 K): 157.7, 150.4, 141.2, 137.9, 132.7, 131.4, 126.9, 112.4, 110.8, 50.1, 21.3.

HRMS: Calculated for $C_{14}H_{15}NO_2$ (M+): 229.1103; Found: 229.1097

IR (ν_{max}/cm^{-1}): 3021, 2956, 2920, 2859, 1626, 1602, 1475, 1193.

m.p.: 113-117 °C

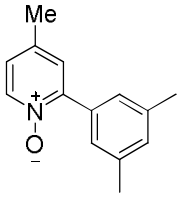

2-(3,5-dimethylphenyl)-4-methylpyridine 1-oxide

^{1}H NMR (400 MHz, $CDCl_3$, 293 K): 8.19 (1H, d, *J*= 6.6 Hz), 7.35 (2H, s), 7.16 (1H, d, *J*= 2.6 Hz), 7.05 (1H, s), 6.99 (1H, dd, *J*= 2.6, 6.7 Hz), 2.35 (6H, s), 2.34 (3H, s).

^{13}C NMR (100 MHz, $CDCl_3$, 293 K): 148.9, 139.8, 137.8, 137.0, 132.7, 131.2, 128.0, 126.9, 125.1, 21.4, 20.3.

HRMS: Calculated for $C_{14}H_{15}NO$ (M+): 213.1154; Found: 213.1167

IR (ν_{max}/cm^{-1}): 2918, 2860, 1601, 1470, 1226.

m.p.: 118-124 °C

Kinetics Experiments

General Procedure (B) for Kinetic Measurements

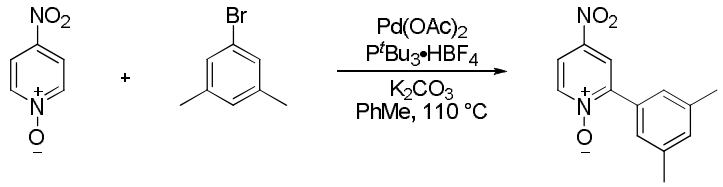

4-Nitropyridine *N*-oxide, K_2CO_3, P^tBu_3•HBF_4, $Pd(OAc)_2$, and trimethoxybenzene as an internal standard were weighed into a two-necked 100 mL flask equipped with a teflon stir bar. The flask was fitted with a reflux condenser and the second neck was sealed with a rubber septum. The reaction vessel was then evacuated and refilled with argon (repeat 3 times). A solution of 5-bromo-*m*-xylene in toluene was purged with argon (10-15 min) and added to the reaction flask. The flask was placed in an oil bath pre-heated to 110 °C with constant stirring. Aliquots were taken at 5 to 10 min time intervals, unless otherwise stated. Upon removal of an aliquot, remaining *N*-oxide precipitated out of solution as a pale-yellow solid. The vial containing the aliquot was concentrated on the vacuum pump and analyzed by NMR for the formation of product.

Representative crude NMR Spectrum for Kinetic Measurements

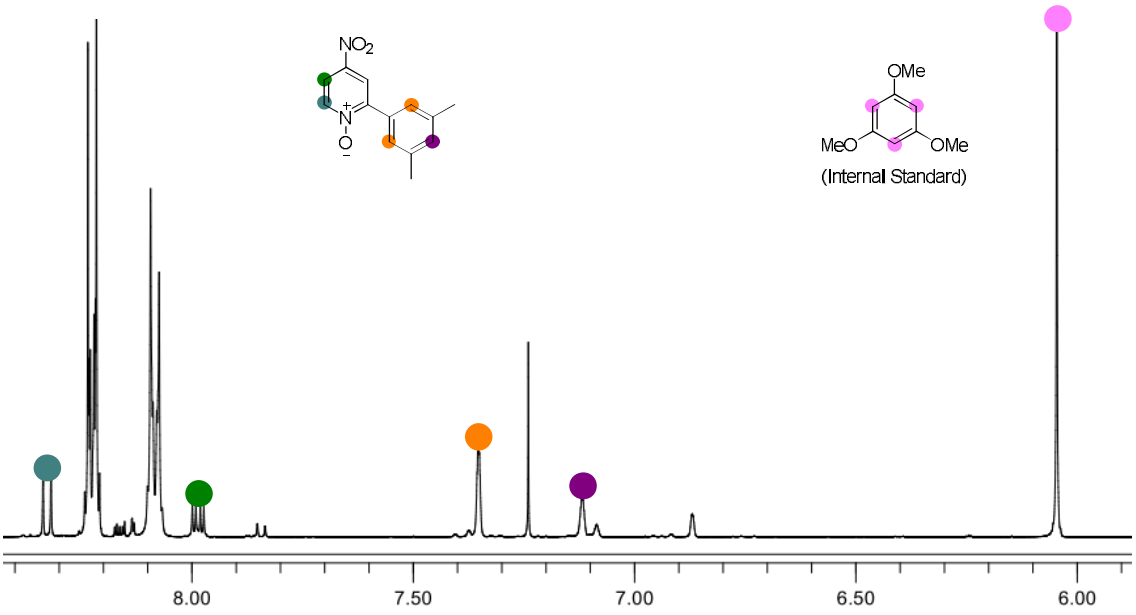

Order in 5-bromo-*m*-xylene

Following General Procedure B, 4-nitropyridine *N*-oxide (0.153 g, 1.09 mmol), K_2CO_3 (0.151 g, 1.09 mmol), P^tBu_3•HBF_4 (0.024 g, 0.081 mmol), $Pd(OAc)_2$ (0.006 g, 0.027 mmol), and trimethoxybenzene (0.091 g, 0.54 mmol) as an internal standard were weighed into a two-necked 100mL flask equipped with a teflon stir bar. The flask was fitted with a reflux condenser and the second neck was sealed with a rubber septum. The reaction vessel was then evacuated and refilled with argon (repeat 3 times). A solution of 5-bromo-*m*-xylene in toluene (0.20 M, 0.25 M, 0.30 M, 0.35 M, 0.40 M, or 0.60 M) was purged with argon (10-15 min) and added to the reaction flask. The flask was placed in an oil bath pre-heated to 110 °C with constant stirring. Aliquots were taken at 5 to 10 minute time intervals. Upon removal of an aliquot, remaining *N*-oxide precipitated out of solution as a pale-yellow solid. The vial containing the aliquot was concentrated on the vacuum pump and analyzed by NMR for the formation of product.

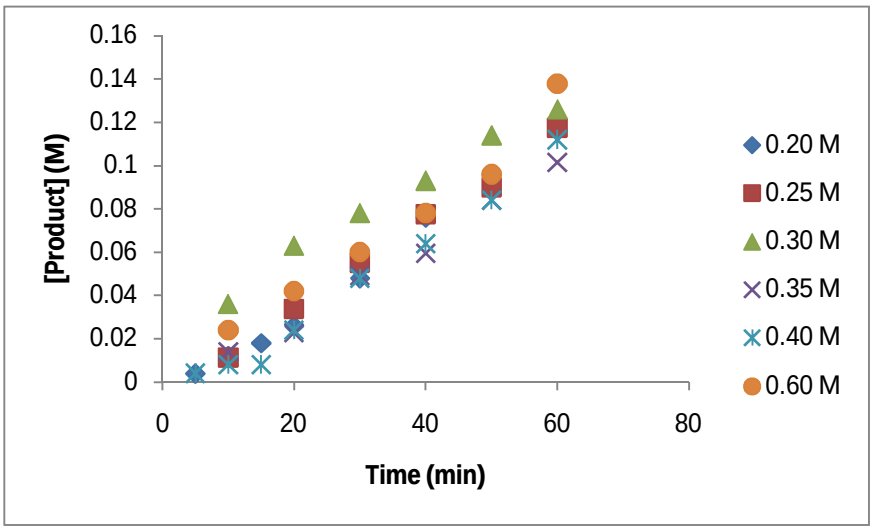

[ArBr] (M)	Time (min)	NMR Yield (%)	[Product] (M)	V_0
0.20	5	2	0.004	0.0021
	10	6	0.012	
	15	9	0.018	
	20	13	0.026	
	30	24	0.048	
	40	38	0.076	
	50	48	0.096	
	60	58	0.116	
0.25	10	5	0.011	0.0020
	20	14	0.034	
	30	22	0.055	
	40	31	0.078	
	50	36	0.090	
	60	47	0.118	
0.30	10	12	0.036	0.0018
	20	21	0.063	
	30	26	0.078	
	40	31	0.093	
	50	38	0.114	

	60	42	0.126	
0.35	10	4	0.014	0.0019
	20	7	0.023	
	30	14	0.049	
	40	17	0.060	
	50	24	0.084	
	60	29	0.102	
0.40	5	1	0.004	0.0022
	10	2	0.008	
	15	2	0.008	
	20	6	0.024	
	30	12	0.048	
	40	16	0.064	
	50	21	0.084	
	60	28	0.112	
0.60	10	4	0.024	0.0021
	20	7	0.042	
	30	10	0.060	
	40	13	0.078	
	50	16	0.096	
	60	23	0.138	

Order in 4-nitropyridine *N*-oxide

Following General Procedure B, 4-nitropyridine *N*-oxide (0.10 M, 0.20 M, 0.30 M, 0.60 M, or 0.80 M), K_2CO_3 (0.1506 g, 1.09 mmol), P^tBu_3•HBF_4 (0.024 g, 0.081 mmol), $Pd(OAc)_2$ (0.006 g, 0.027 mmol), and trimethoxybenzene (0.091 g, 0.54 mmol) as an internal standard were weighed into a two-necked 100 mL flask equipped with a teflon stir bar. The flask was fitted with a reflux condenser and the second neck was sealed with a rubber septum. The reaction vessel was then evacuated and refilled with argon (repeat 3 times). A solution of 5-bromo-*m*-xylene (0.100 g, 0.54 mmol) in toluene (1.80

mL) was purged with argon (10-15 min) and added to the reaction flask. The flask was placed in an oil bath pre-heated to 110 °C with constant stirring. Aliquots were taken at 5 to 10 minute time intervals. Upon removal of an aliquot, remaining *N*-oxide precipitated out of solution as a pale-yellow solid. The vial containing the aliquot was concentrated on the vacuum pump and analyzed by NMR for the formation of product.

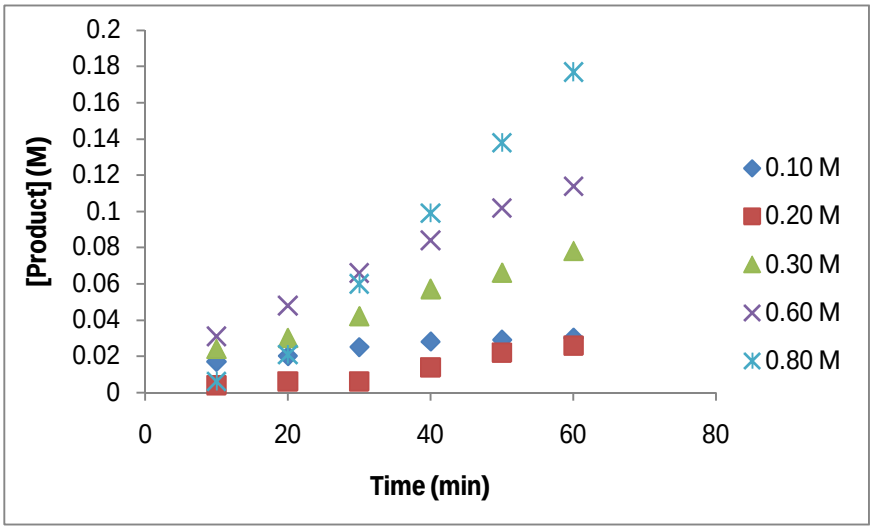

[*N*-Oxide] (M)	Time (min)	NMR Yield (%)	[Product] (M)	V_0
0.10	10	17	0.017	0.0003
	20	20	0.020	
	30	25	0.025	
	40	28	0.028	
	50	29	0.029	
	60	30	0.030	
0.20	10	2	0.004	0.0005
	20	3	0.006	
	30	3	0.006	
	40	7	0.014	
	50	11	0.022	
	60	13	0.026	
0.30	10	8	0.024	0.0011

	20	10	0.030	
	30	14	0.042	
	40	19	0.057	
	50	22	0.066	
	60	26	0.078	
0.60	10	12	0.036	0.0018
	20	21	0.063	
	30	26	0.078	
	40	31	0.093	
	50	38	0.114	
	60	42	0.126	
0.80	10	2	0.006	0.0036
	20	7	0.021	
	30	20	0.060	
	40	33	0.099	
	50	46	0.138	
	60	59	0.177	

Order in $Pd(P^tBu_3)_2$

Following General Procedure B, 4-nitropyridine *N*-oxide (0.153 g, 1.09 mmol), K_2CO_3 (0.151 g, 1.09 mmol), PivOH (0.016 g, 0.16 mmol) and trimethoxybenzene (0.091 g, 0.54 mmol) as an internal standard were weighed into a two-necked 100 mL flask equipped with a teflon stir bar. The flask was fitted with a reflux condenser and the second neck was sealed with a rubber septum. The reaction vessel was then evacuated and refilled with argon (repeat 3 times) then brought into a gloxebox where $Pd(P^tBu_3)_2$ (0.003 M, 0.015 M, 0.030 M, 0.035 M, or 0.060 M) was weighed into the flask. The reaction vessel was then taken out of the glovebox. A solution of 5-bromo-*m*-xylene (0.100 g, 0.54 mmol) in toluene (1.80 mL) was purged with argon (10-15 min) and added to the reaction flask. The flask was placed in an oil bath pre-heated to 110 °C with constant stirring. Aliquots were taken at 5 to 10 minute time intervals. Upon

removal of an aliquot, remaining *N*-oxide precipitated out of solution as a pale-yellow solid. The vial containing the aliquot was concentrated on the vacuum pump and analyzed by NMR for the formation of product.

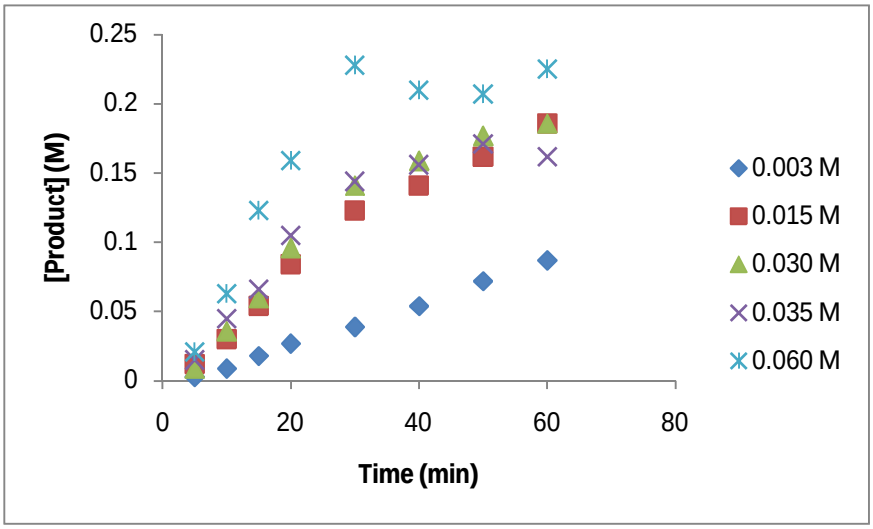

[Pd(P^tBu_3)$_2$] (M)	Time (min)	NMR Yield (%)	[Product] (M)	V_0
0.003	5	1	0.003	0.0015
	10	3	0.009	
	15	6	0.018	
	20	9	0.027	
	30	13	0.039	
	40	18	0.054	
	50	24	0.072	
	60	29	0.087	
0.015	5	4	0.012	0.0046
	10	10	0.030	
	15	18	0.054	
	20	28	0.084	
	30	41	0.123	
	40	47	0.141	
	50	54	0.162	

	60	62	0.186	
0.030	5	3	0.009	0.0054
	10	12	0.036	
	15	20	0.060	
	20	32	0.096	
	30	47	0.141	
	40	53	0.159	
	50	59	0.177	
	60	62	0.186	
0.035	5	5	0.015	0.0058
	10	15	0.045	
	15	22	0.066	
	20	35	0.105	
	30	48	0.144	
	40	52	0.156	
	50	57	0.171	
	60	54	0.162	
0.060	5	7	0.021	0.0085
	10	21	0.063	
	15	41	0.123	
	20	53	0.159	
	30	76	0.228	
	40	70	0.210	
	50	69	0.207	
	60	75	0.225	

Order in P^{t}Bu$_3$

Following General Procedure B, 4-nitropyridine *N*-oxide (0.153 g, 1.09 mmol), K_2CO_3 (0.151 g, 1.09 mmol), P^{t}Bu$_3$•HBF$_4$ (0.003 M, 0.015 M, 0.030 M, 0.035 M, or 0.060 M)** and trimethoxybenzene (0.091 g, 0.54 mmol) as an internal standard were weighed into

a two-necked 100 mL flask equipped with a teflon stir bar. The flask was fitted with a reflux condenser and the second neck was sealed with a rubber septum. The reaction vessel was then evacuated and refilled with argon (repeat 3 times) then brought into a gloxebox where $Pd(P^tBu_3)_2$ (0.014 g, 0.027 mmol) was weighed into the flask. The reaction vessel was then taken out of the glovebox. A solution of 5-bromo-*m*-xylene (0.100 g, 0.54 mmol) in toluene (1.80 mL) was purged with argon (10-15 min) and added to the reaction flask. The flask was placed in an oil bath pre-heated to 110 °C with constant stirring. Aliquots were taken at 5 to 10 minute time intervals. Upon removal of an aliquot, remaining *N*-oxide precipitated out of solution as a pale-yellow solid. The vial containing the aliquot was concentrated on the vacuum pump and analyzed by NMR for the formation of product.

** *These concentrations take into account the 5 mol% of P^tBu_3 which will come from $Pd(P^tBu_3)_2$.*

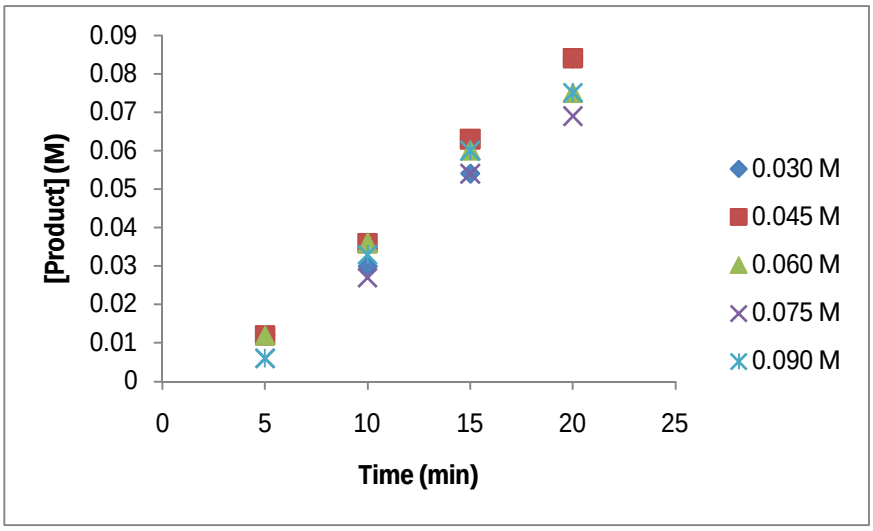

[P^{t}Bu$_3$] (M)	Time (min)	NMR Yield (%)	[Product] (M)	V_0
0.030	5	4	0.012	0.0046
	10	10	0.030	
	15	18	0.054	
	20	28	0.084	
0.045	5	4	0.012	0.0046
	10	12	0.036	
	15	21	0.063	
	20	28	0.084	
0.060	5	4	0.012	0.0043
	10	12	0.036	
	15	20	0.060	
	20	25	0.075	
0.075	5	2	0.006	0.0043
	10	9	0.027	
	15	18	0.054	
	20	23	0.069	
0.090	5	2	0.006	0.0047
	10	11	0.033	
	15	20	0.060	
	20	25	0.075	

Kinetic Isotope Effect Experiments

General Procedure (C) for KIE Experiments

Pyridine *N*-oxide (1.09 mmol), K_2CO_3 (1.09 mmol), P^{t}Bu$_3$•HBF$_4$ (0.081 mmol), $Pd(OAc)_2$ (0.027 mmol), and trimethoxybenzene (0.54 mmol) as an internal standard were weighed into a two-necked 100 mL flask equipped with a teflon stir bar. The flask

was fitted with a reflux condenser and the second neck was sealed with a rubber septum. The reaction vessel was then evacuated and refilled with argon (repeat 3 times). A solution of 5-bromo-*m*-xylene (0.54 mmol) in toluene (1.80 mL) was purged with argon (10-15 min) and added to the reaction flask. The flask was placed in an oil bath pre-heated to 110 °C with constant stirring. Aliquots were taken at the indicated time intervals, unless otherwise stated. Upon removal of an aliquot, remaining *N*-oxide precipitated out of solution as a pale-yellow solid. The vial containing the aliquot was concentrated on the vacuum pump and analyzed by NMR for the formation of product.

For Pyridine *N*-Oxide-d_5

Time (min)	NMR Yield (%)	[Product] (M)
60	2	0.006
120	3	0.009
180	5	0.015
300	7	0.021

Raw data for pyridine N-oxide may be found on pp. 74-75.

Measurement of Rate at Varying Temperatures (Construction of Arrhenius Plot)

4-Nitropyridine *N*-oxide (0.153 g, 1.09 mmol), K_2CO_3 (0.151 g, 1.09 mmol), P^tBu_3•HBF_4 (0.024 g, 0.081 mmol), $Pd(OAc)_2$ (0.006 g, 0.027 mmol), and trimethoxybenzene (0.091 g, 0.54 mmol) as an internal standard were weighed into a two-necked 100 mL flask equipped with a teflon stir bar. The flask was fitted with a reflux condenser and the second neck was sealed with a rubber septum. The reaction vessel was then evacuated and refilled with argon (repeat 3 times). A solution of 5-bromo-*m*-xylene (0.100 g, 0.54 mmol) in toluene (1.80 mL) was purged with argon (10-15 min) and added to the reaction flask. The flask was placed in an oil bath (pre-heated

to 100 °C, 110 °C, 120 °C, 130 °C, or 140 °C) with constant stirring. Aliquots were taken at 5 to 10 minute time intervals. Upon removal of an aliquot, remaining *N*-oxide precipitated out of solution as a pale-yellow solid. The vial containing the aliquot was concentrated on the vacuum pump and analyzed by NMR for the formation of product.

At 100 °C

V_0 = 0.0007 M/min

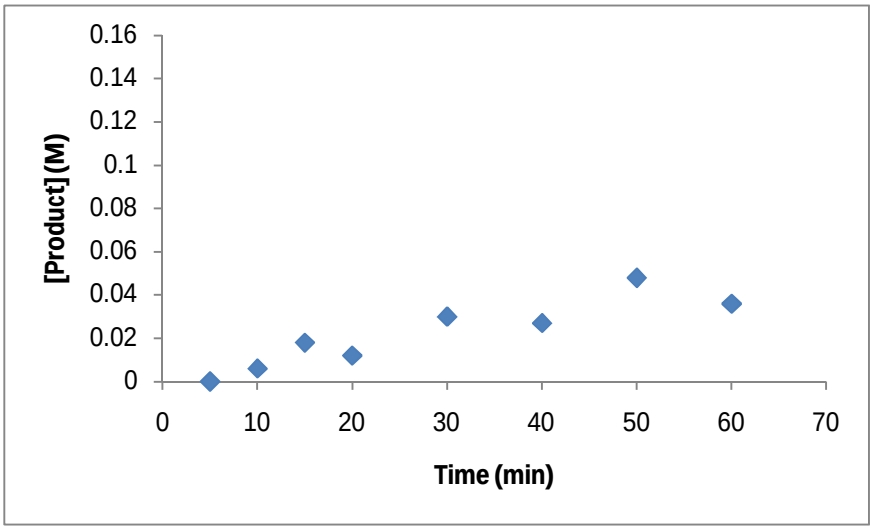

Time (min)	NMR Yield (%)	[Product] (M)
5	0	0.000
10	2	0.006
15	6	0.018
20	4	0.012
30	10	0.030
40	9	0.027
50	16	0.048
60	12	0.036

At 110 °C

V_0 = 0.0018 M/min

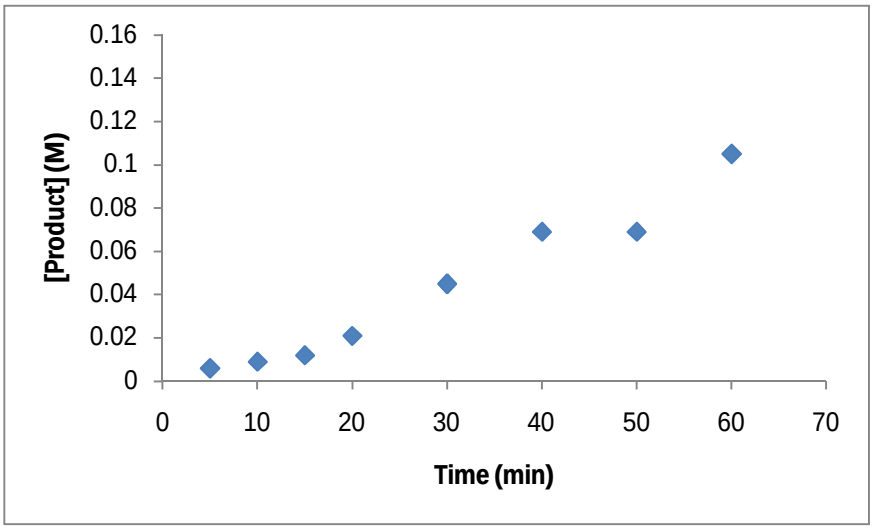

Time (min)	NMR Yield (%)	[Product] (M)
5	2	0.006
10	3	0.009
15	4	0.012
20	7	0.021
30	15	0.045
40	23	0.069
50	23	0.069
60	35	0.105

At 120 °C

V_0 = 0.0031 M/min

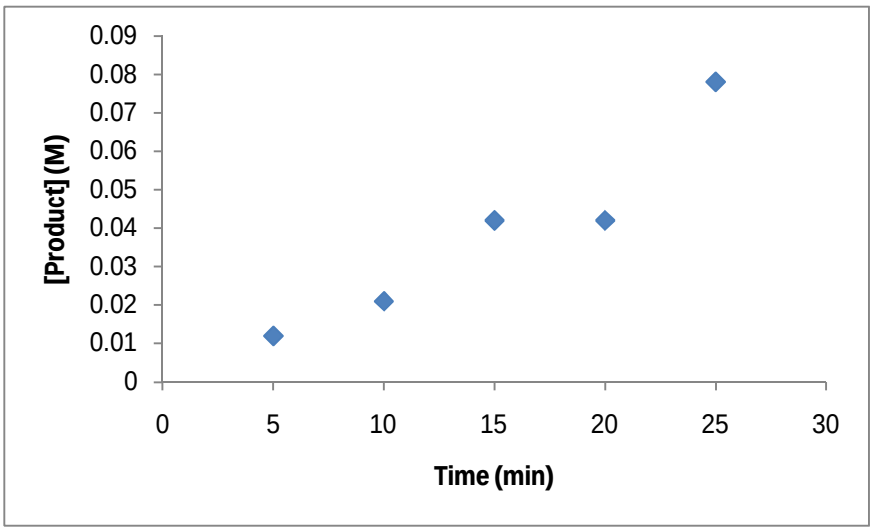

Time (min)	NMR Yield (%)	[Product] (M)
5	4	0.012
10	7	0.021
15	14	0.042
20	14	0.042
25	26	0.078

At 130 °C

V_0 = 0.0046 M/min

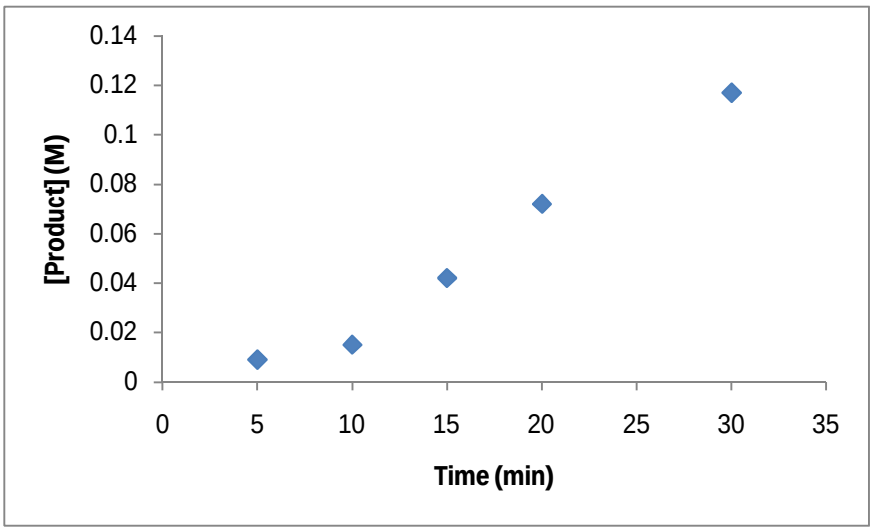

Time (min)	NMR Yield (%)	[Product] (M)
5	3	0.009
10	5	0.015
15	14	0.042
20	24	0.072
30	39	0.117

At 140 °C

V_0 = 0.0090 M/min

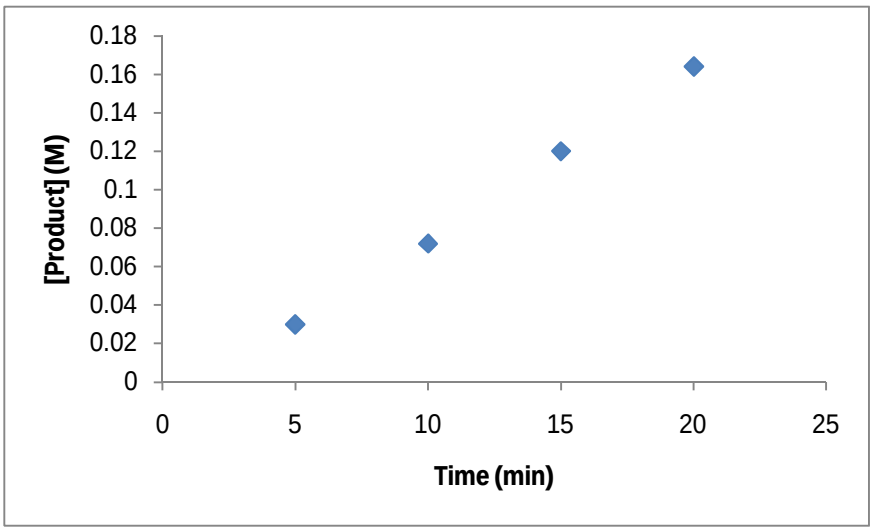

Time (min)	NMR Yield (%)	[Product] (M)
5	10	0.030
10	24	0.072
15	40	0.120
20	54	0.164

Regioselectivity with 3-Substituted Pyridine N-oxides

General Procedure (D) For the Catalytic Process

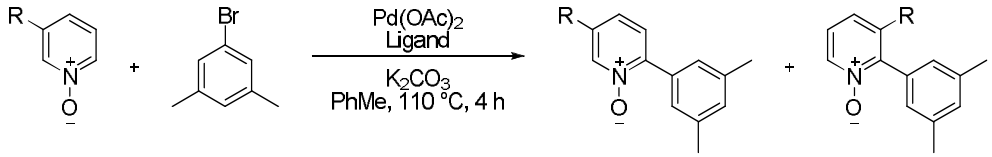

Pyridine *N*-oxide (0.45 mmol), ligand (0.009 mmol), K_2CO_3 (0.225 mmol), and $Pd(OAc)_2$ (0.0075 mmol) were weighed to air and placed in a 10 mL Radley's test-tube. A rubber septum was placed on the test-tube and the vessel was evacuated and purged with argon (repeat 3 times). 5-bromo-*m*-xylene and degassed toluene were then added to the vessel under argon. The reaction was then placed in an oil bath and the heat source was set to 115 °C. The reaction was left to stir overnight (12-18 h) after which it was allowed to cool. 1,3,5-trimethoxybenzene (0.05 mmol) was added and the reaction was diluted with DCM (5 mL). An aliquot was removed for NMR analysis to provide the ratio of products.

General Procedure (E) for the Stoichiometric Process Using 2

Pyridine *N*-oxide (0.49 mmol) and trimethoxybenzene (0.022 mmol) were weighed into a screw-cap vial equipped with a teflon stir bar. The vial was sealed with a cap containing a teflon septum and was then evacuated and refilled with argon (repeat 3 times). The vial was brought into the glovebox where toluene (1.0 mL) was added to the reaction vial and the vial was placed into an aluminum heating block pre-heated to 110 °C with stirring for 20 min. In the glovebox, **2** (0.022 mmol) was weighed into a screw-cap vial equipped with a stir bar. Toluene (0.5 mL) was added to the vial and the solution was placed on a stirring plate until **2** was completely dissolved. Using a syringe, the solution of **2** in toluene was added dropwise to the stirring hot solution of pyridine *N*-oxide and trimethoxybenzene in toluene. The mixture was heated at 110 °C with stirring for 30 min. An aliquot was taken and concentrated on the vacuum pump and analyzed by NMR to provide the ratio of products.

One-Pot Competitions Between 4-Substituted Pyridine N-oxides

General Procedure (F)

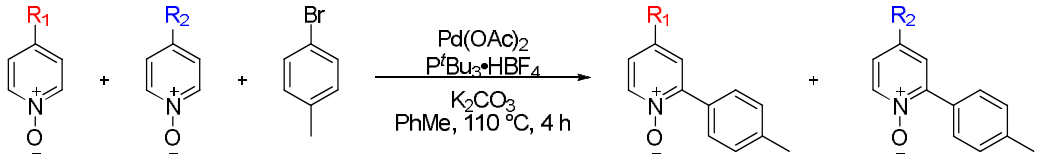

The two competing pyridine *N*-oxide substrates (1.22 mmol each), K_2CO_3 (0.39 mmol), P^tBu_3•HBF_4 (0.018 mmol), and $Pd(OAc)_2$ (0.015 mmol) were weighed into a screw-cap vial with a teflon septum and equipped with a teflon stir bar. The reaction vessel was then evacuated and refilled with argon (repeat 3 times). A solution of 4-bromotoluene (0.3 mmol) in toluene (2 mL) was purged with argon (10-15 min) and added to the reaction flask. The flask was placed in an aluminum heating block pre-heated to 110 °C with constant stirring. The reaction mixture was allowed to heat and stir for 4 hours, after which a crude NMR was taken to measure the ratio between the two products formed.

Hammett Study

General Procedure (G) for a Rate Measurement

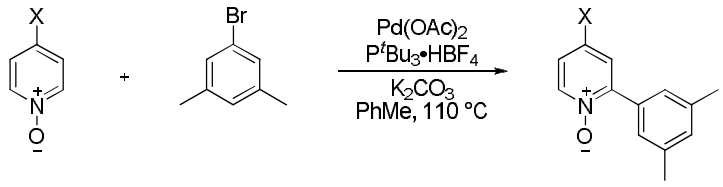

4-Substituted pyridine *N*-oxide (0.60 M), K_2CO_3 (0.151 g, 1.09 mmol), P^tBu_3•HBF_4 (0.024g, 0.081 mmol), $Pd(OAc)_2$ (0.006 g, 0.027 mmol), and trimethoxybenzene (0.091 g, 0.54 mmol) as an internal standard were weighed into a two-necked 100 mL flask equipped with a teflon stir bar. The flask was fitted with a reflux condenser and the

second neck was sealed with a rubber septum. The reaction vessel was then evacuated and refilled with argon (repeat 3 times). A solution of 5-bromo-*m*-xylene (0.100 g, 0.54 mmol) in toluene (1.80 mL) was purged with argon (10-15 min) and added to the reaction flask. The flask was placed in an oil bath pre-heated to 110 °C with constant stirring. Aliquots were taken at time intervals as indicated in the data tables below. Upon removal of an aliquot, remaining *N*-oxide precipitated out of solution as a pale-yellow solid. The vial containing the aliquot was concentrated on the vacuum pump and analyzed by NMR for the formation of product.

Using pyridine *N*-oxide[57]

V_0 = 0.0002 M/min

k_X/k_H = 1.00

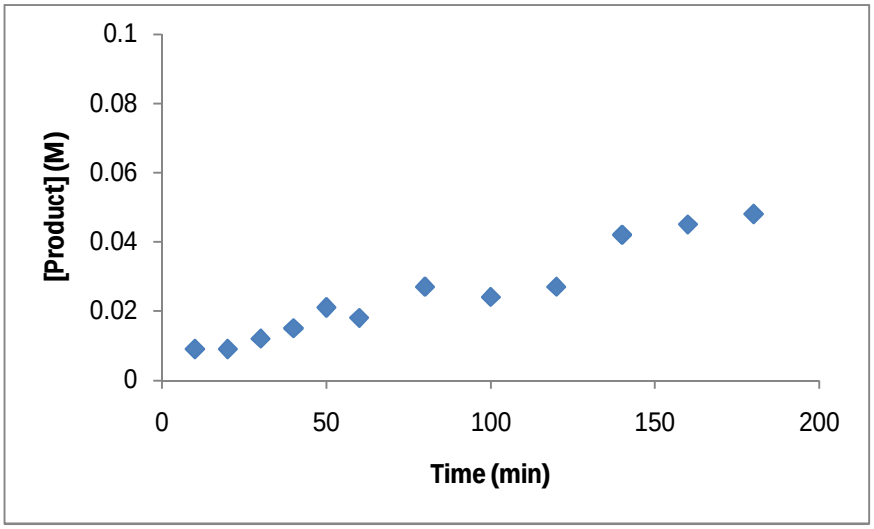

[57] For the full characterization of the product of this reaction, please refer to reference 4a.

Time (min)	NMR Yield (%)	[Product] (M)
10	3	0.009
20	3	0.009
30	4	0.012
40	5	0.015
50	7	0.021
60	6	0.018
80	9	0.027
100	8	0.024
120	9	0.027
140	14	0.042
160	15	0.045
180	16	0.048

Using 4-picoline *N*-oxide

$V_0 = 0.00009$ *M/min*

$k_X/k_H = 0.45$

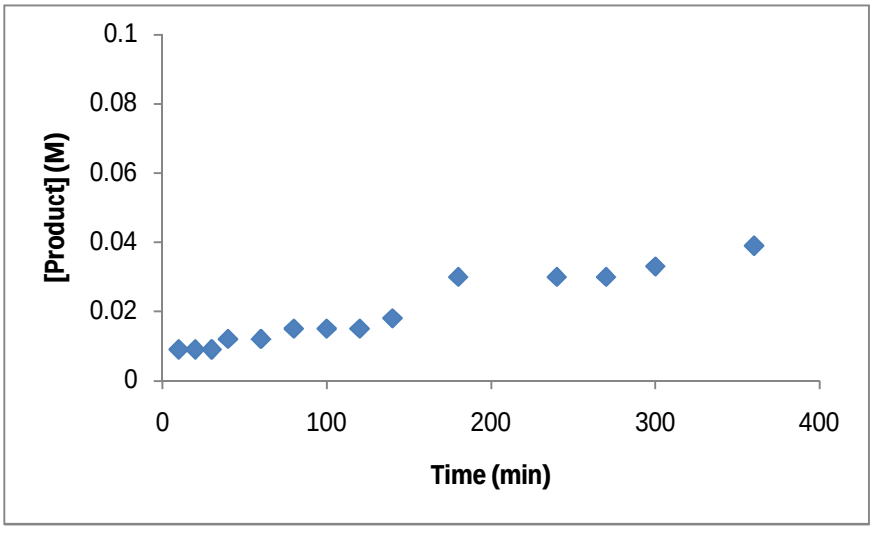

Time (min)	NMR Yield (%)	[Product] (M)
10	3	0.009
20	3	0.009
30	3	0.009
40	4	0.012
60	4	0.012
80	5	0.015
110	5	0.015
120	5	0.015
140	6	0.018
180	10	0.030
240	10	0.030
270	10	0.030
300	11	0.033
360	13	0.039

Using 4-methoxypyridine *N*-oxide

V_0 = 0.0002 M/min

k_X/k_H = 1.00

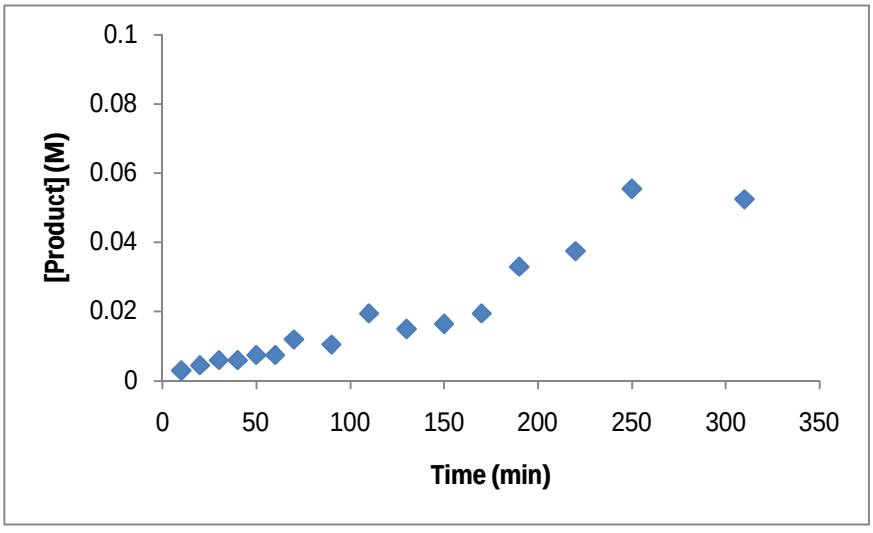

Time (min)	NMR Yield (%)	[Product] (M)
10	1	0.003
20	2	0.0045
30	2	0.006
40	2	0.006
50	3	0.0075
60	3	0.0075
70	4	0.012
90	4	0.0105
110	7	0.0195
130	5	0.015
150	6	0.0165
170	7	0.0195
190	11	0.033
220	13	0.0375
250	19	0.0555
310	18	0.0525

Using 4-(methoxycarbonyl)pyridine *N*-oxide[58]

V_0 = 0.0005 M/min

k_X/k_H = 2.50

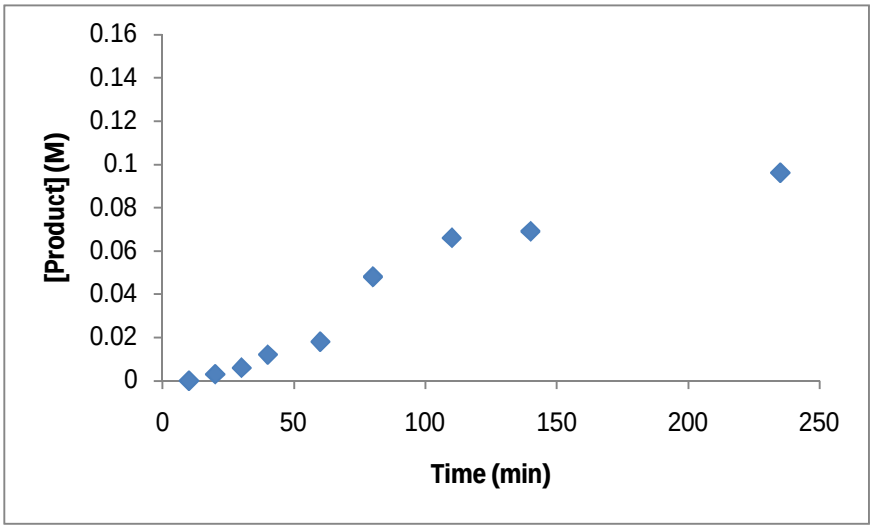

Time (min)	NMR Yield (%)	[Product] (M)
10	0	0
20	1	0.003
30	2	0.006
40	4	0.012
60	6	0.018
80	16	0.048
110	22	0.066
140	23	0.069
235	32	0.096

[58] For the full characterization of the product of this reaction, please refer to reference 4b.

Using 4-nitropyridine *N*-oxide

V_0 = 0.0018 M/min

k_X/k_H = 9.00

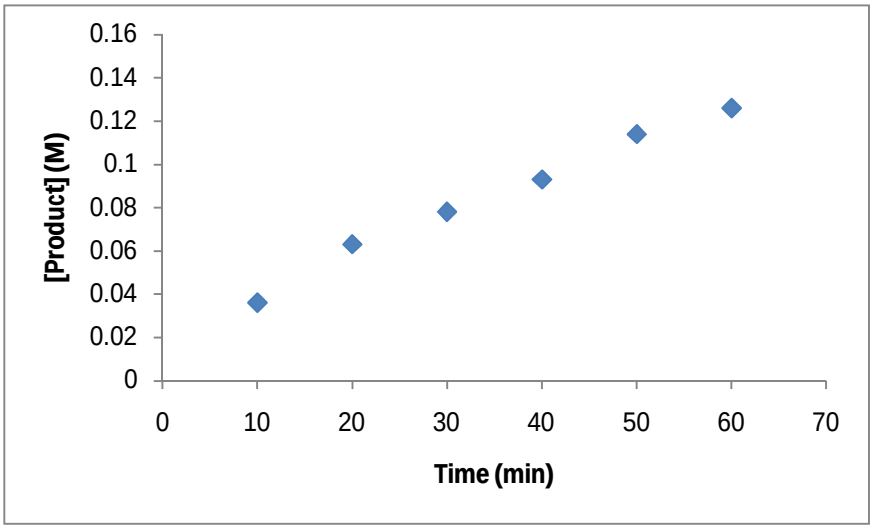

Time (min)	NMR Yield (%)	[Product] (M)
10	12	0.036
20	21	0.063
30	26	0.078
40	31	0.093
50	38	0.114
60	42	0.126

Stoichiometric Reactions Using 1

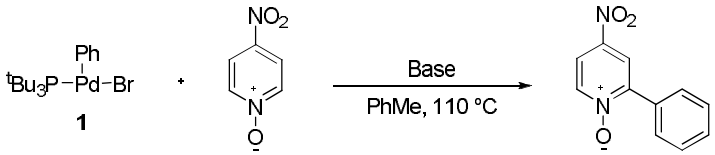

Representative Spectrum

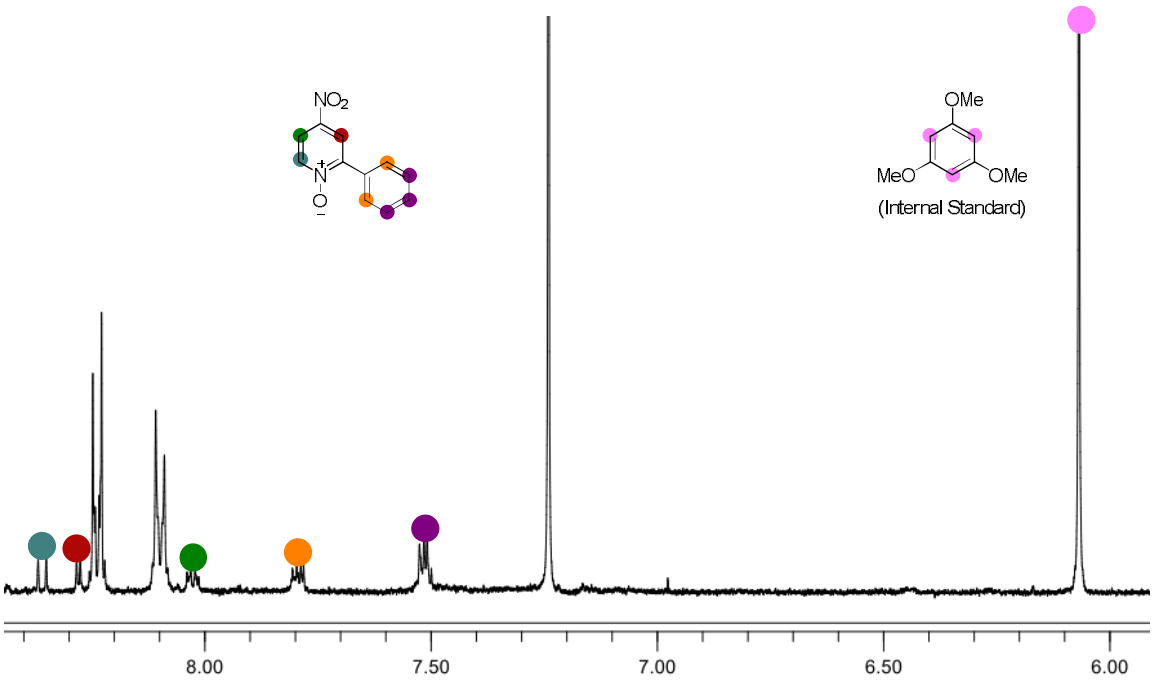

Without Base

4-Nitropyridine *N*-oxide (0.007 g, 0.048 mmol) and trimethoxybenzene (0.004 g, 0.024 mmol) were weighed into a screw-cap vial equipped with a teflon stir bar. The vial was sealed with a cap containing a teflon septum and was then evacuated and refilled with argon (repeat 3 times). The vial was brought into the glovebox where toluene (0.4 mL) was added to the reaction vial and the vial was placed into an aluminum heating block pre-heated to 110 °C with stirring for 20 min. In the glovebox, **1** (0.011 g, 0.024 mmol) was weighed into a screw-cap vial equipped with a stir bar. Toluene (0.1 mL) was added to the vial and the solution was placed on a stirring plate until **1** was

completely dissolved. Using a syringe, the solution of **1** in toluene was added dropwise to the stirring hot solution of 4-nitropyridine *N*-oxide and trimethoxybenzene in toluene. The mixture was heated at 110 °C with stirring for 30 min. An aliquot was taken and concentrated on the vacuum pump and analyzed by NMR for formation of product.

With K_2CO_3

4-Nitropyridine *N*-oxide (0.007 g, 0.048 mmol), K_2CO_3 (0.033 g, 0.24 mmol) and trimethoxybenzene (0.004 g, 0.024 mmol) were weighed into a screw-cap vial equipped with a teflon stir bar. The vial was sealed with a cap containing a teflon septum and was then evacuated and refilled with argon (repeat 3 times). The vial was brought into the glovebox where toluene (0.4 mL) was added to the reaction vial and the vial was placed into an aluminum heating block pre-heated to 110 °C with stirring for 20 min. In the glovebox, **1** (0.011 g, 0.024 mmol) was weighed into a screw-cap vial equipped with a stir bar. Toluene (0.1 mL) was added to the vial and the solution was placed on a stirring plate until **1** was completely dissolved. Using a syringe, the solution of **1** in toluene was added dropwise to the stirring hot solution of 4-nitropyridine *N*-oxide, K_2CO_2 and trimethoxybenzene in toluene. The mixture was heated at 110 °C with stirring for 30 min. An aliquot was taken and concentrated on the vacuum pump and analyzed by NMR for formation of product.

With KOPiv

4-Nitropyridine *N*-oxide (0.007 g, 0.048 mmol), KOPiv (0.034 g, 0.24 mmol) and trimethoxybenzene (0.004 g, 0.024 mmol) were weighed into a screw-cap vial equipped with a teflon stir bar. The vial was sealed with a cap containing a teflon septum and was then evacuated and refilled with argon (repeat 3 times). The vial was brought into the glovebox where toluene (0.4 mL) was added to the reaction vial and the vial was placed into an aluminum heating block pre-heated to 110 °C with stirring for 20 min. In the glovebox, **1** (0.011 g, 0.024 mmol) was weighed into a screw-cap vial equipped with a stir bar. Toluene (0.1 mL) was added to the vial and the solution was placed on a stirring plate until **1** was completely dissolved. Using a syringe, the solution of **1** in toluene was added dropwise to the stirring hot solution of 4-nitropyridine *N*-oxide, KOPiv

and trimethoxybenzene in toluene. The mixture was heated at 110 °C with stirring for 30 min. An aliquot was taken and concentrated on the vacuum pump and analyzed by NMR for formation of product.

With K_2CO_3 and KOPiv

4-Nitropyridine *N*-oxide (0.007 g, 0.048 mmol), K_2CO_3 (0.033 g, 0.24 mmol), KOPiv (0.034 g, 0.24 mmol) and trimethoxybenzene (0.004 g, 0.024 mmol) were weighed into a screw-cap vial equipped with a teflon stir bar. The vial was sealed with a cap containing a teflon septum and was then evacuated and refilled with argon (repeat 3 times). The vial was brought into the glovebox where toluene (0.4 mL) was added to the reaction vial and the vial was placed into an aluminum heating block pre-heated to 110 °C with stirring for 20 min. In the glovebox, **1** (0.011 g, 0.024 mmol) was weighed into a screw-cap vial equipped with a stir bar. Toluene (0.1 mL) was added to the vial and the solution was placed on a stirring plate until **1** was completely dissolved. Using a syringe, the solution of **1** in toluene was added dropwise to the stirring hot solution of 4-nitropyridine *N*-oxide, K_2CO_2, KOPiv and trimethoxybenzene in toluene. The mixture was heated at 110 °C with stirring for 30 min. An aliquot was taken and concentrated on the vacuum pump and analyzed by NMR for formation of product.

Base Effects - Rate Measurements

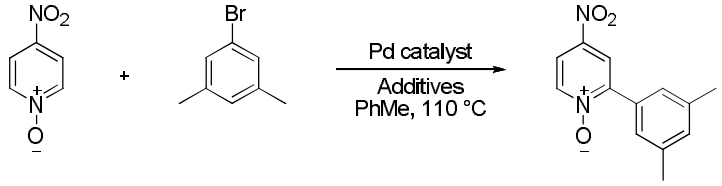

Procedure for a Rate Measurement Using $Pd(P^tBu_3)_2$ and K_2CO_3

4-nitropyridine *N*-oxide (0.153 g, 1.09 mmol), K_2CO_3 (0.151 g, 1.09 mmol), and trimethoxybenzene (0.091 g, 0.54 mmol) as an internal standard were weighed into a two-necked 100 mL flask equipped with a teflon stir bar. The flask was fitted with a reflux condenser and the second neck was sealed with a rubber septum. The reaction

vessel was then evacuated and refilled with argon (repeat 3 times) then brought into a gloxebox where $Pd(P^tBu_3)_2$ (0.014 g, 0.027 mmol) was weighed into the flask. The reaction vessel was then taken out of the glovebox. A solution of 5-bromo-*m*-xylene (0.100 g, 0.54 mmol) in toluene (1.80 mL) was purged with argon (10-15 min) and added to the reaction flask. The flask was placed in an oil bath pre-heated to 110 °C with constant stirring. Aliquots were taken at time intervals as indicated in the data tables below. Upon removal of an aliquot, remaining *N*-oxide precipitated out of solution as a pale-yellow solid. The vial containing the aliquot was concentrated on the vacuum pump and analyzed by NMR for the formation of product.

V_0 = 0.0004 M/min

Time (min)	NMR Yield (%)	[Product] (M)
5	1	0.003
10	2	0.006
15	4	0.012
20	2	0.006
30	7	0.021
40	6	0.018
50	8	0.024
60	9	0.027

Procedure for a Rate Measurement Using $Pd(P^tBu_3)_2$ and KOPiv

4-Nitropyridine *N*-oxide (0.153 g, 1.09 mmol), KOPiv (0.153 g, 1.09 mmol), and trimethoxybenzene (0.091 g, 0.54 mmol) as an internal standard were weighed into a two-necked 100 mL flask equipped with a teflon stir bar. The flask was fitted with a reflux condenser and the second neck was sealed with a rubber septum. The reaction vessel was then evacuated and refilled with argon (repeat 3 times) then brought into a gloxebox where $Pd(P^tBu_3)_2$ (0.014 g, 0.027 mmol) was weighed into the flask. The reaction vessel was then taken out of the glovebox. A solution of 5-bromo-*m*-xylene (0.100 g, 0.54 mmol) in toluene (1.80 mL) was purged with argon (10-15 min) and

added to the reaction flask. The flask was placed in an oil bath pre-heated to 110 °C with constant stirring. Aliquots were taken at time intervals as indicated in the data tables below. Upon removal of an aliquot, remaining *N*-oxide precipitated out of solution as a pale-yellow solid. The vial containing the aliquot was concentrated on the vacuum pump and analyzed by NMR for the formation of product.

V_0 = 0.0003 M/min

Time (min)	NMR Yield (%)	[Product] (M)
5	1	0.003
10	3	0.009
15	5	0.015
20	8	0.024
30	7	0.021
40	11	0.033
50	8	0.024
60	6	0.018

Procedure for a Rate Measurement Using Pd(P^tBu_3)$_2$, K_2CO_3 and PivOH

4-nitropyridine *N*-oxide (0.153 g, 1.09 mmol), K_2CO_3 (0.151 g, 1.09 mmol), PivOH (0.016 g, 0.16 mmol), and trimethoxybenzene (0.091 g, 0.54 mmol) as an internal standard were weighed into a two-necked 100 mL flask equipped with a teflon stir bar. The flask was fitted with a reflux condenser and the second neck was sealed with a rubber septum. The reaction vessel was then evacuated and refilled with argon (repeat 3 times) then brought into a gloxebox where Pd(P^tBu_3)$_2$ (0.014 g, 0.027 mmol) was weighed into the flask. The reaction vessel was then taken out of the glovebox. A solution of 5-bromo-*m*-xylene (0.100 g, 0.54 mmol) in toluene (1.80 mL) was purged with argon (10-15 min) and added to the reaction flask. The flask was placed in an oil bath pre-heated to 110 °C with constant stirring. Aliquots were taken at time intervals as indicated in the data tables below. Upon removal of an aliquot, remaining *N*-oxide

precipitated out of solution as a pale-yellow solid. The vial containing the aliquot was concentrated on the vacuum pump and analyzed by NMR for the formation of product.

V_0 = 0.0025 M/min

Time (min)	NMR Yield (%)	[Product] (M)
5	2	0.006
10	4	0.012
15	6	0.018
20	13	0.039
30	20	0.060
40	32	0.096
50	38	0.114
60	44	0.132

Stoichiometric Reactions using 2

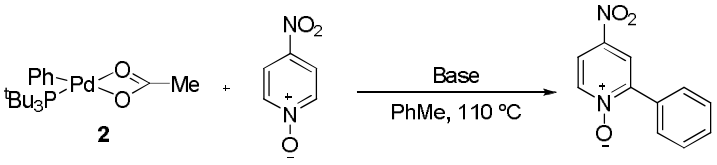

Representative Spectrum

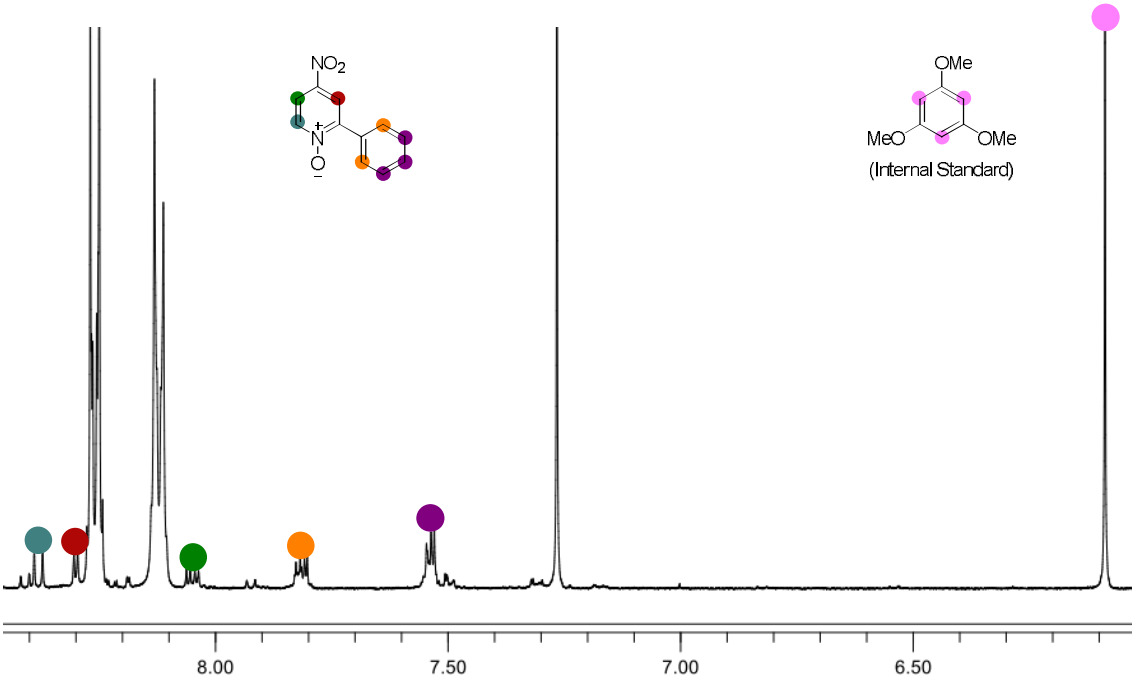

Without K_2CO_3

4-Nitropyridine *N*-oxide (0.189 g, 1.35 mmol) and trimethoxybenzene (0.006 g, 0.034 mmol) were weighed into a screw-cap vial equipped with a teflon stir bar. The vial was sealed with a cap containing a teflon septum and was then evacuated and refilled with argon (repeat 3 times). The vial was brought into the glovebox where toluene (1.5 mL) was added to the reaction vial and the vial was placed into an aluminum heating block pre-heated to 110 °C with stirring for 20 min. In the glovebox, **2** (0.015 g, 0.034 mmol) was weighed into a screw-cap vial equipped with a stir bar. Toluene (0.6 mL) was added to the vial and the solution was placed on a stirring plate until **2** was completely dissolved. Using a syringe, the solution of **2** in toluene was added dropwise to the stirring hot solution of 4-nitropyridine *N*-oxide and trimethoxybenzene in toluene.

The mixture was heated at 110 °C with stirring for 30 min. An aliquot was taken and concentrated on the vacuum pump and analyzed by NMR for formation of product.

With K_2CO_3

4-Nitropyridine *N*-oxide (0.189 g, 1.35 mmol), K_2CO_3 (0.187 g, 1.35 mmol) and trimethoxybenzene (0.006 g, 0.034 mmol) were weighed into a screw-cap vial equipped with a teflon stir bar. The vial was sealed with a cap containing a teflon septum and was then evacuated and refilled with argon (repeat 3 times). The vial was brought into the glovebox where toluene (1.5 mL) was added to the reaction vial and the vial was placed into an aluminum heating block pre-heated to 110 °C with stirring for 20 min. In the glovebox, **2** (0.015 g, 0.034 mmol) was weighed into a screw-cap vial equipped with a stir bar. Toluene (0.6 mL) was added to the vial and the solution was placed on a stirring plate until **2** was completely dissolved. Using a syringe, the solution of **2** in toluene was added dropwise to the stirring hot solution of 4-nitropyridine *N*-oxide, K_2CO_3 and trimethoxybenzene in toluene. The mixture was heated at 110 °C with stirring for 30 min. An aliquot was taken and concentrated on the vacuum pump and analyzed by NMR for formation of product.

Kinetic Experiment Using $Pd(OPiv)_2$

4-Nitropyridine *N*-oxide (0.228 g, 1.63 mmol), K_2CO_3 (0.225 g, 1.63 mmol), $P^tBu_3 \bullet HBF_4$ (0.027 g, 0.12 mmol), $Pd(OPiv)_2$ (0.013 g, 0.041 mmol), and trimethoxybenzene (0.137 g, 0.82 mmol) as an internal standard were weighed into a two-necked 100 mL flask equipped with a teflon stir bar. The flask was fitted with a reflux condenser and the second neck was sealed with a rubber septum. The reaction vessel was then evacuated and refilled with argon (repeat 3 times). A solution of 5-bromo-*m*-xylene (0.150 g, 0.82 mmol) in toluene (2.70 mL) was purged with argon (10-15 min) and added to the reaction flask. The flask was placed in an oil bath pre-heated to 110 °C with constant stirring. Aliquots were taken at 5 to 10 minute time intervals. Upon removal of an aliquot, remaining *N*-oxide precipitated out of solution as a pale-yellow solid. The vial containing the aliquot was concentrated on the vacuum pump and analyzed by NMR for the formation of product.

Time (min)	NMR Yield (%)	[Product] (M)
10	1	0.003
20	1	0.003
25	4	0.012
30	6	0.018
36	9	0.027
41	15	0.045
45	18	0.054
50	21	0.063
61	35	0.105
80	58	0.174
90	69	0.207
100	71	0.213
110	74	0.222

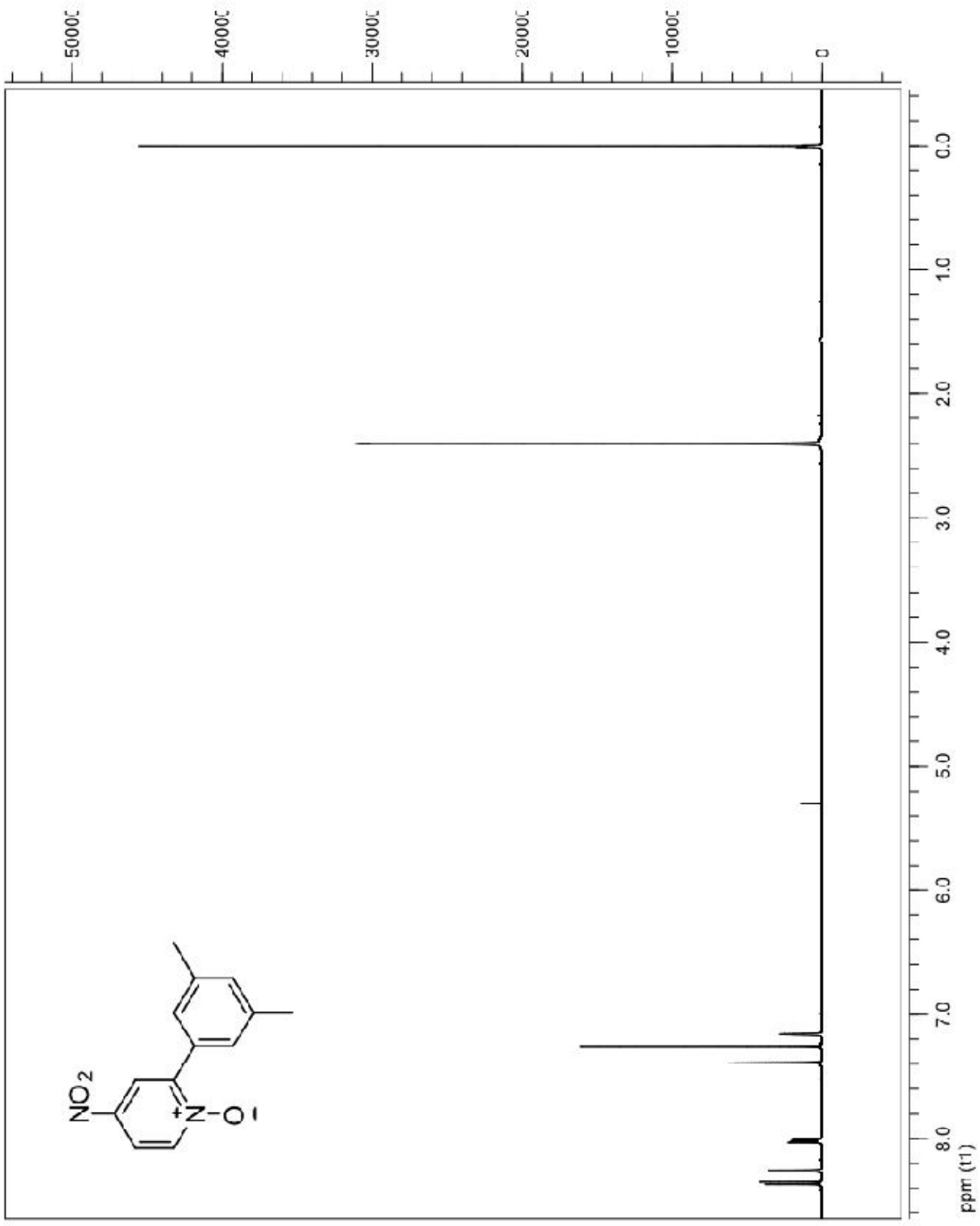
5000
4000
3000
2000
1000
0
8.0
7.0
6.0
5.0
4.0
3.0
2.0
1.0
0.0
ppm (t1)
NO2
+N-O-

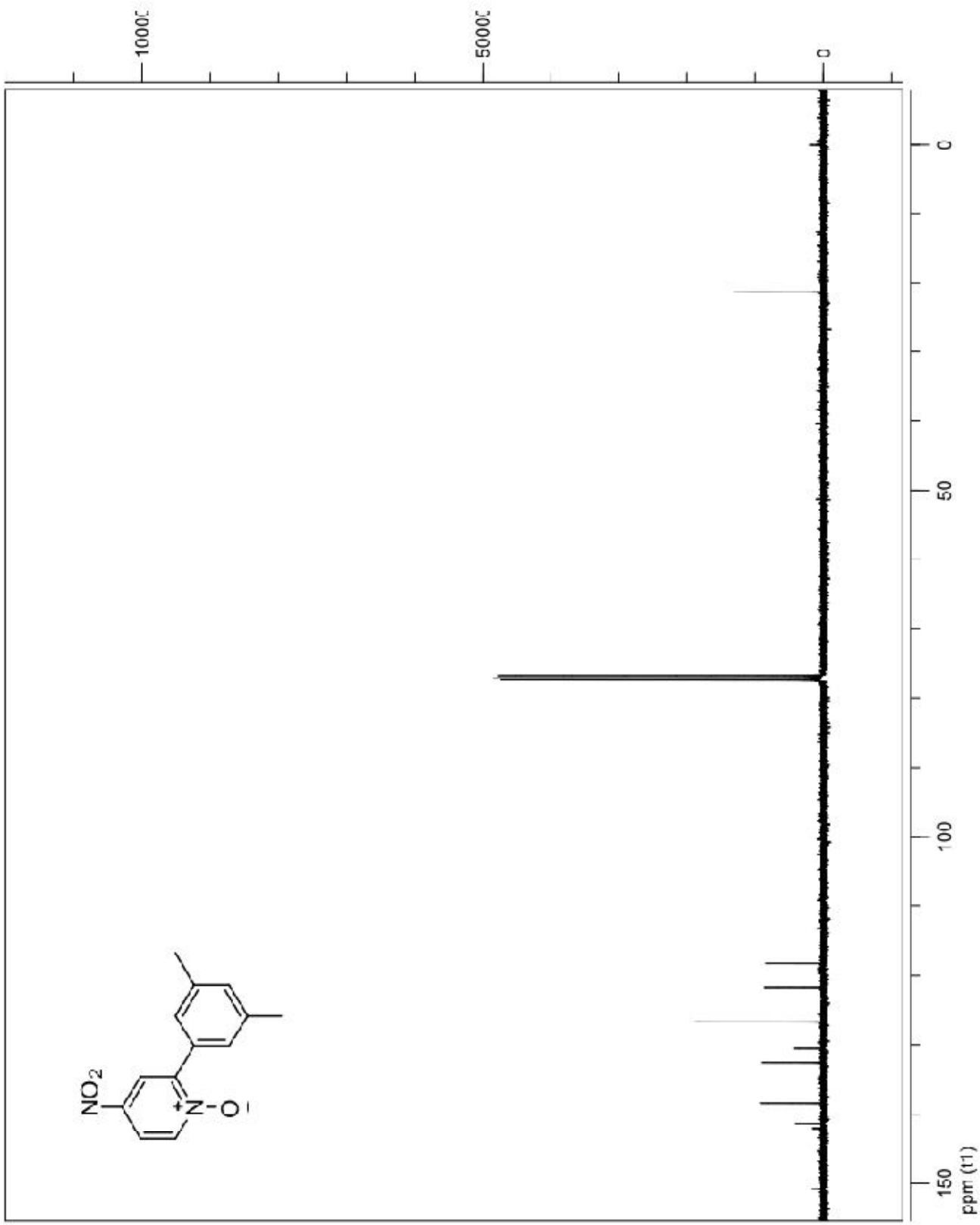
10000
5000
0
0
50
100
150
ppm (t1)
NO2
N
O

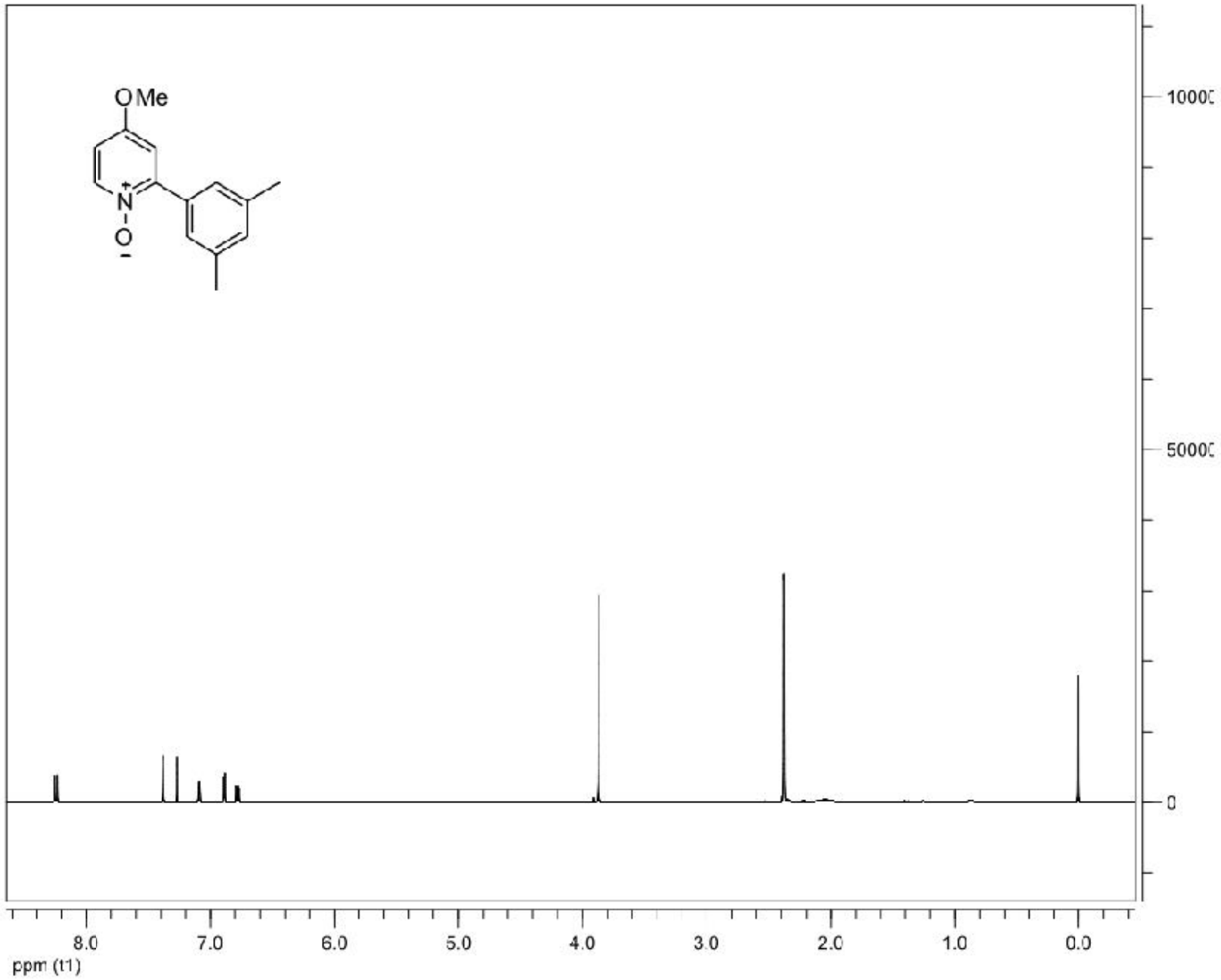
OMe
N
O
10000
50000
0
8.0
7.0
6.0
5.0
4.0
3.0
2.0
1.0
0.0
ppm (t1)

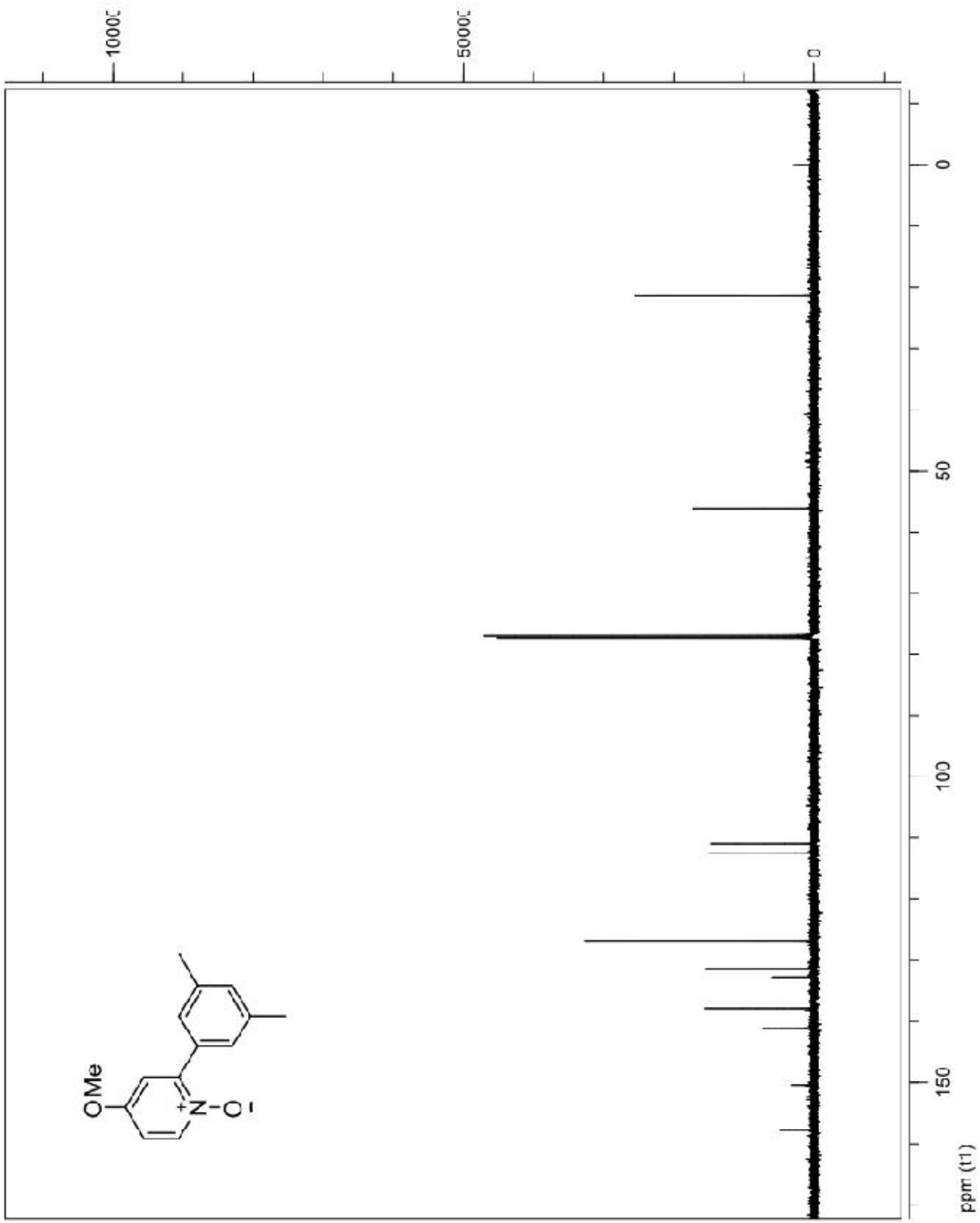
OMe
+N-O
ppm (t1)

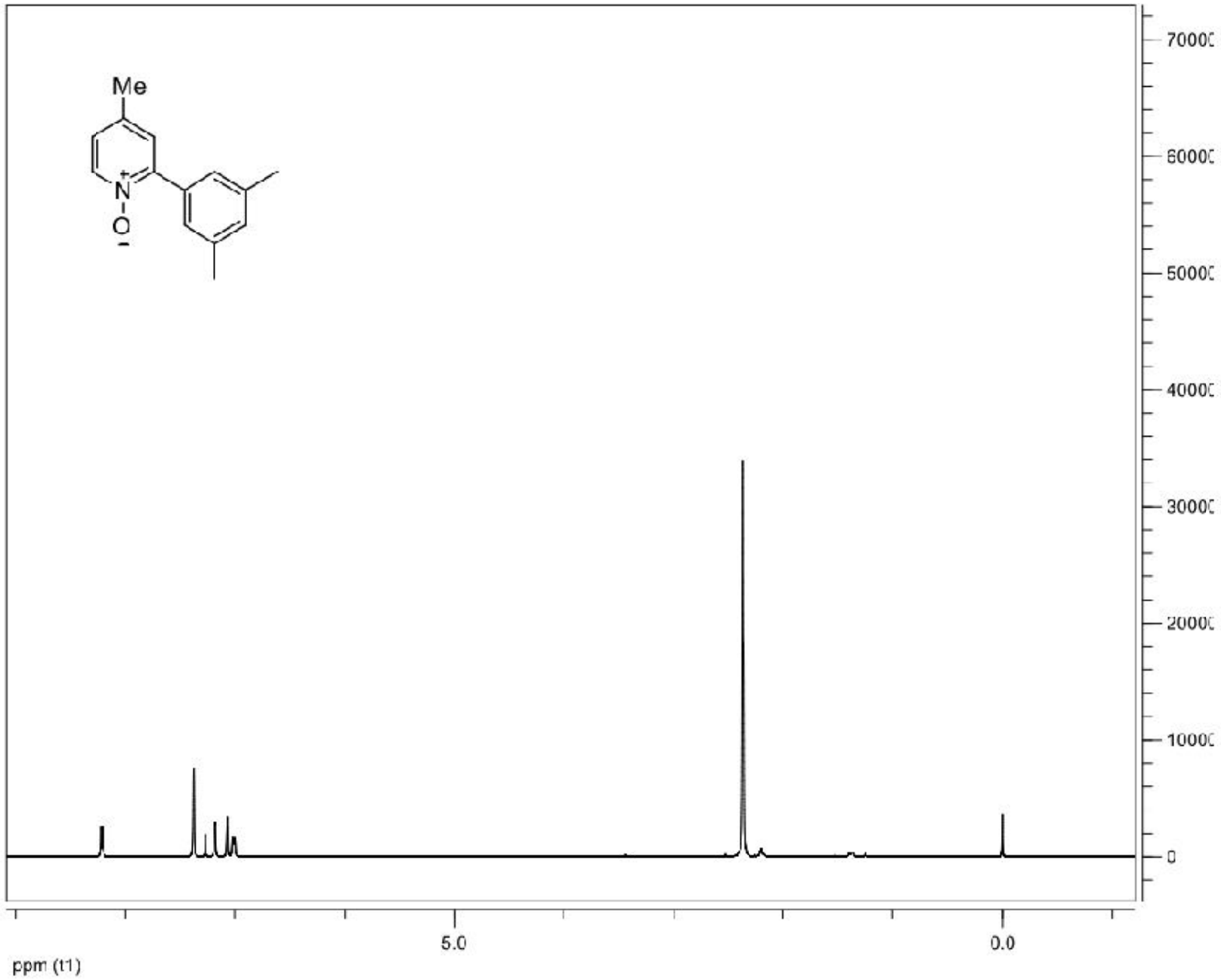
Me
N
O
7000
6000
5000
4000
3000
2000
1000
0
5.0
0.0
ppm (t1)

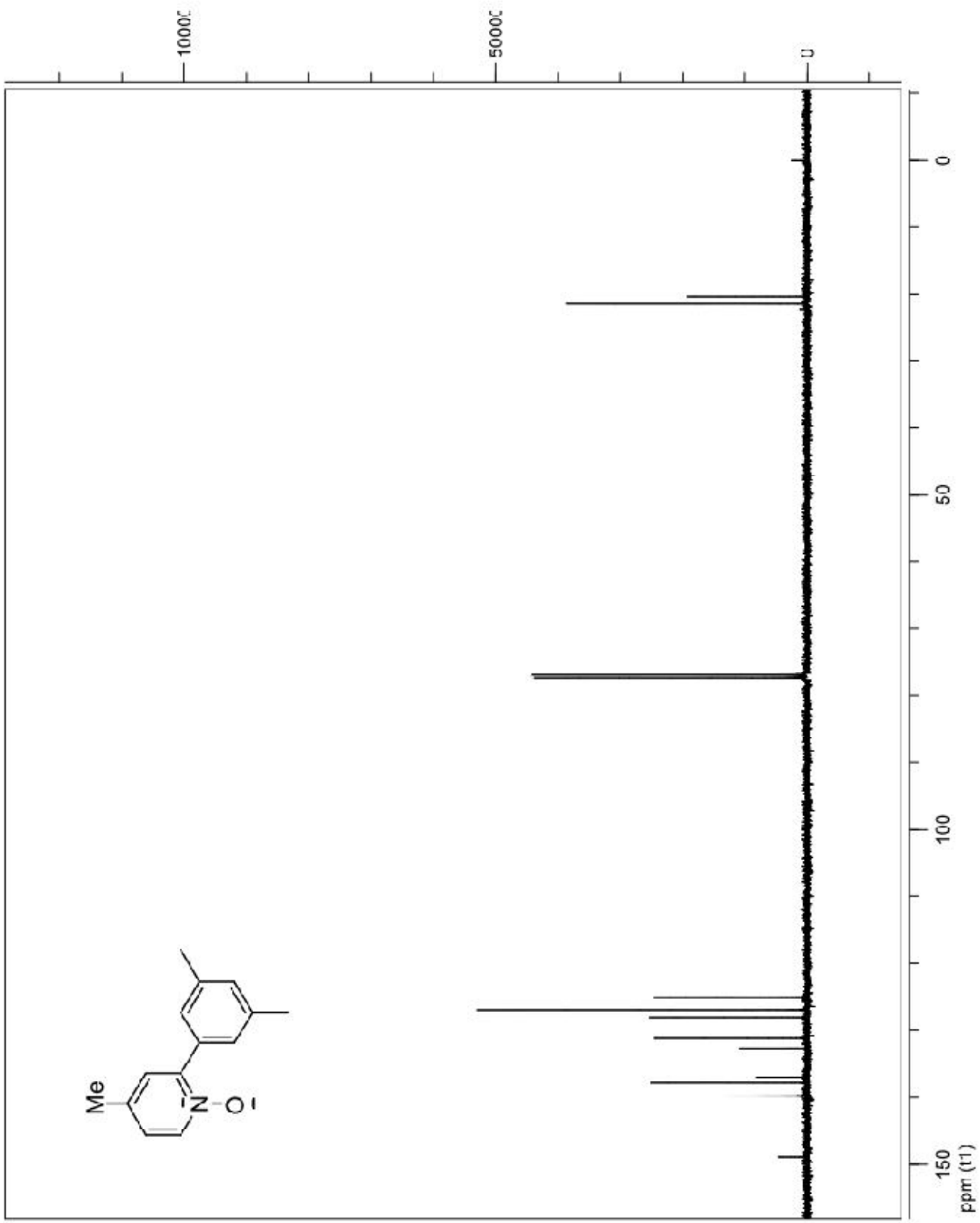
Me
N
O
ppm (t1)

Section Claims

Publications:

1. Sun, H.-Y.; Gorelsky, S. I.; Stuart, D. R.; Campeau, L.-C.; Fagnou, K. "Mechanistic Analysis of Azine *N*-Oxide Direct Arylation: Evidence for a Critical Role of Acetate in the $Pd(OAc)_2$ Pre-Catalyst" *J. Org. Chem.* **2010**, *75*, 8180.

2. Campeau, L.-C.; Stuart, D.R.; Leclerc, J.-P.; Bertrand-Laperle, M.; Villemure, E.; Sun, H.-Y.; Lasserre, S.; Guimond, N.; Lecavallier, M.; Fagnou, K. "Palladium-Catalyzed Direct Arylation of Azine and Azole *N*-Oxides: Reaction Development, Scope, and Applications in Synthesis" *J. Am. Chem. Soc.* **2009**, *131*, 3291.

Poster Presentations:

1. **Ho-Yan Sun***, Keith Fagnou. **2010**. A Mechanistic Evaluation of the C-H bond cleaving step in the Direct Arylation of Pyridine *N*-Oxides. *Keith Fagnou Organic Chemistry Symposium, University of Ottawa.*

2. **Ho-Yan Sun***, Keith Fagnou. **2009**. A Mechanistic Analysis of Azine *N*-Oxide Direct Arylation. *Quebec Ontario Minisymposium in Synthetic and Bioorganic Chemistry, Laval University.*

3. **Ho-Yan Sun***, Keith Fagnou. **2009**. Mechanistic and Kinetic Studies on the Direct Arylation of Pyridine *N*-Oxides. *Spring Organic Synthesis Symposium, University of Ottawa.*

4. **Ho-Yan Sun***, Keith Fagnou. **2009**. Studies on the Mechanism of Direct Arylation of Pyridine *N*-Oxides. *Ottawa-Carleton Chemistry Institute Symposium.*